

POLITECNICO DI TORINO

Master of Science Degree in Information and Communication
Technologies for Smart Societies

Class of Master Degrees in Telecommunication Engineering



An in-depth analysis of future sixth generation networks with integration of aerial platforms

Supervisors

Prof. Michela MEO

Dr. Daniela RENGA

Candidate

Felice SCARPA

A.Y. 2020/2021

*“My brain is only a receiver, in the Universe there is a core
from which we obtain knowledge, strength and inspiration.
I have not penetrated into the secrets of this core,
but I know that it exists.”*

Nikola Tesla

Summary

The spread of new forms of technologies such as the Internet of Things (IoT) and Information and Communication Technology (ICT) will affect the future of the mobile wireless connections. In the society of the future everything and everyone will be interconnected: it is expected that by 2025 the number of connected devices worldwide will rise to 75 billion. This increase translates into rapid growth in mobile traffic, which poses two major problems. First, the new mobile networks require more spectrum and vastly more spectrally efficient technologies. Second, this growth raises doubts about the sustainability of mobile communications. Industrial and academic synergies have begun to conceptualize the next generation of wireless communication systems (i.e., sixth generation, (6G)) to cope with these issues. However, the practical implementation of this new wireless communication system presents some technical challenges. To address some of these issues, 6G research is currently focusing on the development of Non-Terrestrial Networks (NTNs) to promote ubiquitous and high-capacity global connectivity. With NTNs it is envisioned a three-dimensional vertical heterogeneous architecture in which terrestrial infrastructures are complemented by non-terrestrial stations including Unmanned Aerial Vehicles (UAVs), High Altitude Platforms Stations (HAPSs) and satellites.

In this thesis, we consider a portion of a future generation Radio Access Network (RAN), in which we imagine integrating the ground network infrastructure of a densely populated area like the city of Milan (Italy) and its suburbs, with an air network formed by one HAPS. We plan to offer coverage for 16 traffic zones that include urban and suburban areas of the city of Milan, each different from the others in terms of surface extension, typical activities and traffic patterns. From each traffic zone, we consider a sample cluster of base stations (BSs) powered with photovoltaic (PV) panels, equipped with energy storage units, and a connection to the power grid. Our study examines the impact of different strategies, such as Resource on Demand (RoD) and HAPS Offloading strategies, to reduce the cluster energy consumption and improve the Quality of Service (QoS) by adapting the cluster capacity to traffic conditions. Using a detailed simulator, the results show that by applying the RoD and HAPS Offloading strategies at the same time, with

the presence of Renewable Energy (RE) supply both for the ground infrastructure and for the HAPS, significant savings can be obtained in both energetic and economic terms. Moreover the use of Machine Learning (ML) algorithms allow to adapt the network capacity according to the traffic, increasing the QoS.

Acknowledgements

I thank Prof. Michela Meo who allowed me to carry out this wonderful work, advising and following me step by step with an extraordinary positive energy. I also thank my co-supervisor, Dr. Daniela Renga for her competence and patience, dedicating me a lot of time in these months and answering my questions and curiosities with great passion and kindness.

Grazie a mamma e papà, per essere stati sempre al mio fianco e per aver creduto in me.

E infine, grazie a te, Chiara, che sei la persona più bella su questo mondo.

Table of Contents

List of Tables	XI
List of Figures	XIII
Acronyms	XVI
1 Introduction	1
1.1 A hyper-connected future	2
1.2 An overview of existing mobile networks	3
1.3 5G and beyond's main use cases	7
1.4 Some emerging challenges	9
1.5 Towards 6G networks	12
1.5.1 The requirements of 6G	15
1.5.2 Possible candidate technologies	16
1.6 In this thesis: goals and outline	19
2 State-of-the-Art review	20
2.1 An overview on Non-Terrestrial Networks	20
2.1.1 Types of non-terrestrial stations	21
2.1.2 Towards a New Space era	24
2.1.3 Some NTN's architecture proposals	24
2.1.4 Advantages expected from the adoption of NTN's	26
2.2 The development of HAPS networks	26
2.2.1 Which station can be defined as a HAPS?	26
2.2.2 Theoretical characteristics of HAPS	29
2.2.3 The integration of HAPS into VHetNet	31
2.2.4 HAPS as a Super Macro Base Station	34
2.2.5 HAPS implementation regulations	38
2.3 The current situation of HAPs projects	39
2.3.1 An up-to-date review of HAPs projects	39
2.3.2 The technological challenges of HAPs	44

3	Methodology	46
3.1	Basic scenario configuration	46
3.2	Traffic zones	48
3.2.1	Sample clusters	48
3.3	Structure of the BSs	50
3.4	Structure of the HAPS	52
3.5	Definition of strategies for reducing energy consumption	54
3.6	Structure of the simulator	57
3.6.1	Input data	57
3.6.2	Performance indicators	58
4	Results	60
4.1	Sizing Phase	60
4.1.1	Impact of the parameter (PV, B) on energy grid reduction	61
4.1.2	Analysis of the mean energy grid reduction for the selection of the standard configuration of (PV, B)	63
4.1.3	Analysis of the variation of τ and χ parameters	64
4.1.4	Selection of the sample traffic zones	70
4.2	Simulation Phase	72
4.2.1	Analysis of basic scenarios	73
4.2.2	Cost analysis of the basic scenarios	76
4.2.3	Analysis of basic scenarios with other (PV, B) configurations	80
4.2.4	Analysis of the interaction of HAPS beams with traffic zones surfaces	83
4.2.5	Analysis of the strategy for the dynamic choice of τ and χ	87
4.2.6	Analysis of a realistic scenario: interaction between two clusters	97
5	Conclusions	106
	Bibliography	108

List of Tables

2.1	A comparison between the types of non-terrestrial stations	22
3.1	Power model parameters for both BS types	52
3.2	Summary of the simulated scenarios	57
4.1	Energy grid reduction of the three traffic zones for different (PV, B)	64
4.2	Summary of the first configuration of the simulations for the analysis of the variation of τ and χ parameters	64
4.3	Summary of the second configuration of the simulations for the analysis of the variation of τ and χ parameters	65
4.4	Summary of the statistical index for the five sample traffic zones . .	70
4.5	Summary of the energy grid reduction for the five sample traffic zones in the basic scenarios	74
4.6	Summary of the energy grid cost for each traffic zone in the three selected periods	77
4.7	Summary of the configuration of the simulations for the analysis of the interaction of HAPS beams with traffic zones surfaces	84
4.8	Result of adapting the maximum cell capacity using the Adaptive Method algorithm.	86
4.9	Result of the interaction between two cluster in the Business cluster with the RE on Cluster + HAPS Offloading with Dynamic Beam configuration	101
4.10	Result of the interaction between two cluster in the Residential cluster with the RE on Cluster + HAPS Offloading with Dynamic Beam configuration	101
4.11	Result of the interaction between two cluster in the Business cluster with the HAPS Offloading with Dynamic Beam configuration	102
4.12	Result of the interaction between two cluster in the Residential cluster with the HAPS Offloading with Dynamic Beam configuration	102
4.13	Result of the interaction between two cluster in the Business cluster with the HAPS Offloading with Dynamic Beam configuration	104

4.14 Result of the interaction between two cluster in the Rho cluster with the RE on Cluster + HAPS Offloading with Dynamic Beam configuration	104
--	-----

List of Figures

1.1	The timeline of mobile networks	5
1.2	The world coverage map of commercial 5G networks as of 30 September 2020 [11]	6
1.3	The use-cases of 5G and beyond [16]	8
1.4	An example of 5G BS	10
1.5	The E2E network slicing for multiple services based on one physical infrastructure proposed by Huawei® in [21]	11
1.6	A possible road-map for 6G [25]	12
1.7	The three key 6G services proposed by Samsung® in [26]	14
1.8	A comparison of KPIs between 5G and 6G [26]	15
1.9	A sketch of a possible inclusion of NTN components in a 6G network scenario [26]	18
2.1	A NTN typical scenario [35]	21
2.2	A sketch of the distribution of non-terrestrial stations in the airspace with example of beam footprint size	23
2.3	A fully integrated VHetNet envisioned for 6G [42]	25
2.4	The location of non-terrestrial systems in the atmosphere [46]	27
2.5	An example of balloon used as a HAPS [47]	28
2.6	An example of airship used as a HAPS [48]	28
2.7	An example of aerodynamic platform used as a HAPS [49]	29
2.8	CDF resulting from the capacity demand analysis [54]	30
2.9	A sketch on the types of handover of the HAPS networks [42]	33
2.10	A representation of the use cases of HAPS-SMBS networks [64]	35
3.1	A representation of the basic scenario configuration [64]	47
3.2	A representation of the coverage of the urban area of Milan (Italy)	48
3.3	The map of the considered traffic zones over the city of Milan (Italy)	49
3.4	A cluster formed by 1 macro BS and 6 micro BSs powered by (PV,B) and power grid	51
3.5	The coverage surface of the city of Milan and its suburbs	54

4.1	Variation of the energy grid reduction for the 16 traffic zones as the parameter (PV, B) varies	62
4.2	Mean energy grid reduction for each of the 16 traffic zones	63
4.3	Variation of the KPIs as τ and χ parameters vary; Traffic Zone: Rho	65
4.4	Variation of the energy grid reduction as τ and χ parameters vary .	67
4.5	Variation of the capacity demand ratio as τ and χ parameters vary	68
4.6	Variation of the traffic fraction handled by HAPS as τ and χ parameters vary	69
4.7	Traffic time series in the five sample traffic zones	71
4.8	Visualization of the traffic statistics of the five sample areas	72
4.9	Analysis of the energy grid reduction for the basic scenarios	75
4.10	Energy grid price time series	76
4.11	Energy Grid Cost Reduction	78
4.12	Energy Cost Savings	79
4.13	Analysis of the energy grid reduction with different dimensions of (PV, B)	81
4.14	Analysis of the energy grid cost reduction with different dimensions of (PV, B)	82
4.15	Analysis of the interaction of HAPS beams with traffic zones surfaces	85
4.16	Selection of the optimal τ_{demand} values for the Residential cluster over a 72 hour period	88
4.17	Selection of the optimal τ_{price} values for the Residential cluster over a two months period	90
4.18	Selection of the optimal χ values for the Residential cluster over a 72 hours period	92
4.19	Selection of the optimal χ values for the Residential cluster over a 72 hours period - Configuration: HAPS Offloading with Dynamic Beam	93
4.20	Analysis of the strategy for the dynamic choice of τ and χ with the HAPS Offloading with Dynamic Beam strategy applied	95
4.21	Analysis of the strategy for the dynamic choice of τ and χ with the RE on Cluster + HAPS Offloading with Dynamic Beam strategy applied	96
4.22	Schematic of the scenario for the analysis of the interaction between two clusters at the same time	97
4.23	Allocation of HAPS capacity for the two Business and Residential clusters	100
4.24	Allocation of HAPS capacity for the two Business and Rho clusters	103

Acronyms

Symbols

3GPP

Third Generation Partnership Project

5G-NR

5G New Radio

A

AI

Artificial Intelligence

AR

Augmented Reality

AMPS

Advanced Mobile Phone System

B

BS

Base Station

C

CAGR

Compound Annual Growth Rate

CDF

Cumulative Distribution Function

CDMA

Code Division Multiple Access

D

DC

Data Center

E

E2E

End To End

EDGE

Enhanced Data rates for GSM Evolution

F

FSO

Free-Space Optical communication

E

eMBB

Enhanced Mobile Broadband

G

GEO

Geostationary Earth Orbit

GME

Gestore dei Mercati Energetici

GPRS

General Packet Radio Service

GPS

Global Positioning System

GSM

Global System for Mobile Communications

H

Hi-Fi

High-Fidelity

HAP

High Altitude Platform

HAPS

High Altitude Platform Station

HSDPA

High Speed Downlink Packet Access

HSPA

High Speed Packet Access

HSUPA

High Speed Uplink Packet Access

I

ICAO

International Civil Aviation Organization

ICT

Information and Communication Technology

IoT

Internet of Things

IT

Information Technology

ITU

International Telecommunication Union

ITU-R

International Telecommunication Union - Radiocommunication Sector

K

KPI

Key Performance Indicator

L**LEO**

Low Earth Orbit

LTE

Long Term Evolution

M**ML**

Machine Learning

MEO

Medium Earth Orbit

MIMO

Multiple-Input and Multiple-Output

M-MIMO

Massive-Multiple-Input and Multiple-Output

MMS

Multimedia Messaging Service

mMTC

Massive Machine Type Communications

mmWave

millimeter Wave

MNO

Mobile Network Operator

M2M

Machine To Machine

N

NFV

Network Function Virtualization

NRT

Non-Real Time

NTN

Non-Terrestrial Network

O**OFDM**

Orthogonal Frequency-Division Multiplexing

P**PV**

Photovoltaic

Q**QoS**

Quality of Service

R**RAN**

Radio Access Network

RE

Renewable Energy

RoD

Resource on Demand

RT

Real Time

S**SDN**

Software-Defined Networking

SINR

Signal-to-Interference-plus-Noise Ratio

SMBS

Super Macro Base Station

SNR

Signal-to-Noise Ratio

T**TDMA**

Time Division Multiple Access

U**UMTS**

Universal Mobile Telecommunications System

UAV

Unmanned Aerial Vehicles

URLLC

Ultra Reliable Low Latency Communications

USD

United States Dollar

V**VHetNet**

Vertical Heterogeneous Network

VR

Virtual Reality

W**WAP**

Wireless Application Protocol

Wi-Fi

Wireless-Fidelity

X

XR

Extended Reality

Chapter 1

Introduction

This Chapter is about the mobile wireless connections of the present and how the development and spread of new forms of technologies such as the Internet of Things (IoT) and Information and Communication Technology (ICT) will affect the future.

Section 1.1 introduces a perspective on the global growth of wireless connectivity and how this trend associated with the theme of urbanization has led to the development of the concept of smart society.

Section 1.2 gives an overview of the development of mobile cellular network technologies, starting from the so-called pre-cellular or 0G systems up to today's 5G.

Section 1.3 describes the three main use cases for the capabilities of 5G technologies defined by the International Telecommunication Union - Radiocommunication Sector (ITU-R).

Section 1.4 discusses some emerging challenges of 5G, starting from the increase in bandwidth demand and consequent demand for more spectrum, passing through the problem of the proliferation of Base Stations (BSs) and up to the difficulties of the physical network infrastructure.

Section 1.5 introduces the concept of sixth generation networks, discussing which emerging trends and services have led industrial and academic to talk about next generation wireless communication systems. Then some of the core requirements of 6G are discussed, and finally some of the candidate technologies with a particular focus on Non-Terrestrial Networks (NTNs).

Finally, Section 1.6 explains the objective of this thesis work and how the rest of the thesis is organized.

1.1 A hyper-connected future

The global wireless connectivity market is estimated to grow from USD 69.00 billion in 2020 to USD 141.10 billion by 2025, at a Compound Annual Growth Rate (CAGR) of 15.4% [1]: this growth in the global market is closely related to the spread of the IoT and ICT as basic technologies of the modern world. The IoT is a growing network of objects that communicate between themselves and other internet-enabled devices over the Internet [2]. Nowadays, the interconnection of devices embedded in everyday objects is essential to obtain information from the devices, connect with others and share data quickly through mobile devices and other electronic devices [3]. This information is transmitted, received and processed through ICT methods: today, ICT is deeply intertwined with almost every aspect of economic and social activities, and it continues to hold the promise of tremendous innovation and growth opportunities going forward if the right enabling conditions are put in place [4].

The concept of global growth of wireless connectivity has a parallel connection with the concept of urbanization, which is the gradual shift in residence of the human population from rural to urban areas. The urbanization combined with the overall growth of the world's population could add another 2.5 billion people to urban areas by 2050, with an overall projection of about 68% of the world population [5]. This global trend has inevitable environmental and social consequences. To address the many challenges that urban population growth poses and to achieve global sustainable development goals, smart city initiatives have often been cited as one of the best strategies [6].

According to the European Commission definition, a smart city is a city that adopts technological solutions to improve the management and efficiency of the urban environment. The smart city concept is part of the broader smart society principle: smart societies will make a more intelligent use of ICT to transform cities and improve the quality of life of their inhabitants, to produce and distribute energy more efficiently, to solve fundamental health, environmental, and transport challenges. Therefore, smart societies have strong potential to improve the quality of life and they are no longer a futuristic promise but a reality. Several governments have started ambitious smart city projects around the world to address some of the challenges brought about by the rapidly evolving digital world and the fast growth of urbanization [7].

Currently, the smart city concept has leveraged mostly wired and wireless conventional networks. However, the development of future smart cities is increasingly being geared toward the provision of smart services. To implement the smartness in a smart city, IoT technologies, ICT solutions and their corresponding service delivery models, and various underlying wireless access technologies, should all be seamlessly integrated [8].

Under these assumptions, in the society of the future everything and everyone will be interconnected: based on the trends of the IoT, it is expected that by 2025 the number of connected devices worldwide will rise to 75 billion [9]. The growing number of connected "things" defines the problem of increasing data traffic: the term massive IoT perfectly describes the huge amount of IoT sensors and devices that will communicate with each other. In this scenario, the network solution capable of connecting millions of devices must ensure scalability and versatility, offering high capacity and efficiency, providing advanced functions to facilitate the expansion of new use cases.

1.2 An overview of existing mobile networks

Commercial wireless communications service began in 1979 and the release rate for a new communications technology is one per decade. Prior to 1979, wireless communications services were reserved for professional services only, and systems using this technology are retroactively defined as pre-cellular systems or zero generation (0G) systems.

In 1979, the first cellular system in the world became operational by Nippon Telephone and Telegraph in Tokyo, Japan. First generation (1G) cellular devices were analog and used Advanced Mobile Phone System (AMPS) technology, first launched in the United States and which used separate frequencies for each conversation. The AMPS system was assigned a bandwidth of 40 MHz in the 800-900 MHz frequency range and all systems offered handover and roaming capabilities, but cellular networks were unable to interoperate between countries.

In the early 1990s, with the transition from analogue to digital technology, there was talk of second generation (2G) cellular networks. 2G systems used digital mobile access technology such as Time Division Multiple Access (TDMA) and Code Division Multiple Access (CDMA). Briefly, TDMA divides signal in time slots while CDMA allocates each user a special code to communicate over a multiplex physical channel. The most common 2G technology was the TDMA-based Global System for Mobile Communications (GSM): it makes international roaming very

common between mobile phone operators, enabling subscribers to use their phones in many parts of the world. Two technologies to enhance the second generation of cellular networks were General Packet Radio Service (GPRS) and Enhanced Data rates for GSM Evolution (EDGE). Through GPRS there has been a shift from circuit to packet switching to increase the supported data rates: through traditional circuit switching, data transfer was billed per minute of connection time, regardless of whether the user was actually using capacity or was in a data transfer switch state typically was charged per megabyte of traffic transferred. This has allowed the spread of services such as access to Wireless Application Protocol (WAP), Multimedia Messaging Service (MMS) and for Internet communication services such as e-mail and access to the web. EDGE technology was an extended version of GSM which has enabled clear and fast transmission of data and information as an extension compatible with previous versions of GSM. For this, its use in next-generation cellular networks was preferred over GSM due to its flexibility in carrying packet-switched data and circuit-switched data.

With an ever-increasing demand to remove the distinction between fixed and mobile networks in order to access the Internet from anywhere, the development of third generation (3G) cellular networks was necessary. The first commercial 3G networks were introduced in mid-2001 [10]: they used wideband-CDMA technology also called Universal Mobile Telecommunications System (UMTS), based on the GSM network. UMTS was based on the ITU which formulated a plan to implement the global frequency band in the 2000 MHz range, which will support a single ubiquitous wireless communication standard for all countries of the world but unlike EDGE, UMTS requires new BSs and new frequency allocations. 3G technologies enable network operators to offer users a wider range of more advanced services like wide area wireless voice telephony, video calls, broadband wireless data, mobile television, Global Positioning System (GPS) and video conferencing, while achieving greater network capacity through improved spectral efficiency. Reinforcement technologies were also developed for 3G cellular networks, among which High Speed Packet Access (HSPA) was particularly relevant. HSPA means the union of two mobile protocols: (i) High Speed Packet Downlink Access (HSDPA), which is a wideband-CDMA downlink packet data service with data transmission up to 8-10 Mbps and 20 Mbps for Multiple-Input and Multiple-Output (MIMO) systems over a bandwidth of 5 MHz in wideband-CDMA downlink; and (ii) High Speed Packet Uplink Access (HSUPA), which is a complementary service to HSDPA that has improved advanced person-to-person data applications with higher and symmetrical data rates, such as mobile email and real-time person-to-person games. With 3G we moved from voice-centric systems to data-centric systems, defining the entry into the new era of smartphones.

The fourth generation (4G) of cellular networks was first released in 2009 in Oslo and Stockholm. The technology behind 4G is not a simple upgrade of the CDMA present in 3G, as it is based on Orthogonal Frequency-Division Multiplexing (OFDM) mobile access which is a single-band receiver with the advantages of reducing or eliminating the interference between the signals, improving the spectrum utilization and realizing low cost. The feature of 4G is that its communication speed is much faster than that of 3G with a data rate up to 1 Gbps for stationary users and a data rate up to 150 Mbps for moving users. It's based on Long Term Evolution (LTE), which is a standard for wireless broadband communication for mobile devices and data terminals, based on the GSM/EDGE and UMTS/HSPA technologies. Unlike previous cellular networks, 4G technologies have introduced other spectra and frequency bands, namely those around 600 MHz, 700 MHz, 1.7 GHz, 2.1 GHz, 2.3 GHz and 2.5 GHz, with a bandwidth between 1.25 MHz and 20 MHz. 4G technology can offer support for interactive multimedia, voice, video streaming, the Internet and other broadband services. According to the GSMA™ Global Mobile Trends 2021 Report [11], by 2025, 4G will account for 57% of the global mobile customer base, by far the largest share. Smartphone and 4G adoption are rising in many high growth emerging markets. For example, in India, the world's second most populous country, smartphone penetration is now approximately 70%, with 85% of these smartphones running on 4G networks. This trend will continue over the next five years as smartphone prices fall and there is an increase in availability of local content to make the internet more relevant to users.

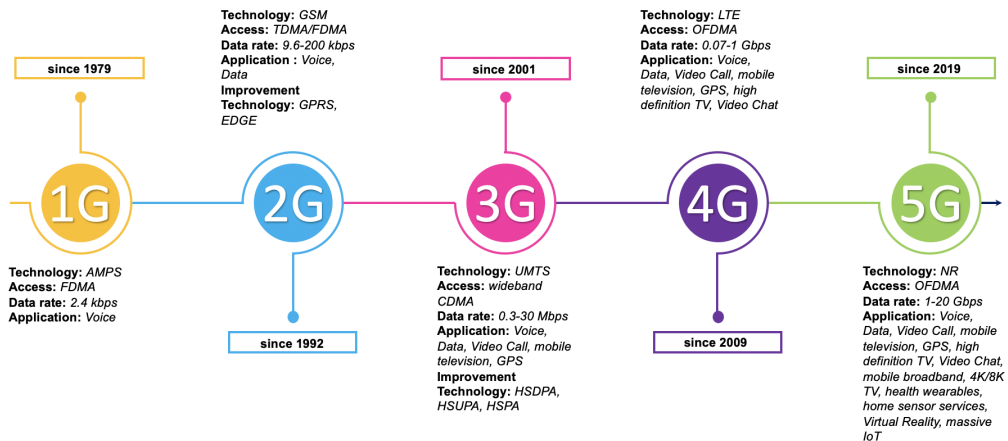


Figure 1.1: The timeline of mobile networks

Despite the forecast of a consistent penetration of 4G technology in the world population, fifth generation (5G) mobile networks have started to be implemented as early as 2019, as can be seen from Figure 1.1. This because the existing 4G network was primarily designed to enhance mobile data services, however it still has numerous limitations, including poor support for concurrent connections, high power consumption, and too high a price per bit. 5G is able to unleash the potential of the IoT and become a driving force for the smart city, addressing and overcoming these problems. Moreover, the transition from 4G to 5G will serve both consumers and multiple industries: with global mobile data traffic expected to grow eight times by the end of 2024 [12], there is a need for a more efficient technology, higher data rates and spectrum utilization. New applications such as 4K/8K video streaming, virtual and augmented reality and emerging industrial use cases will also require higher bandwidth, greater capacity, security, and lower latency.

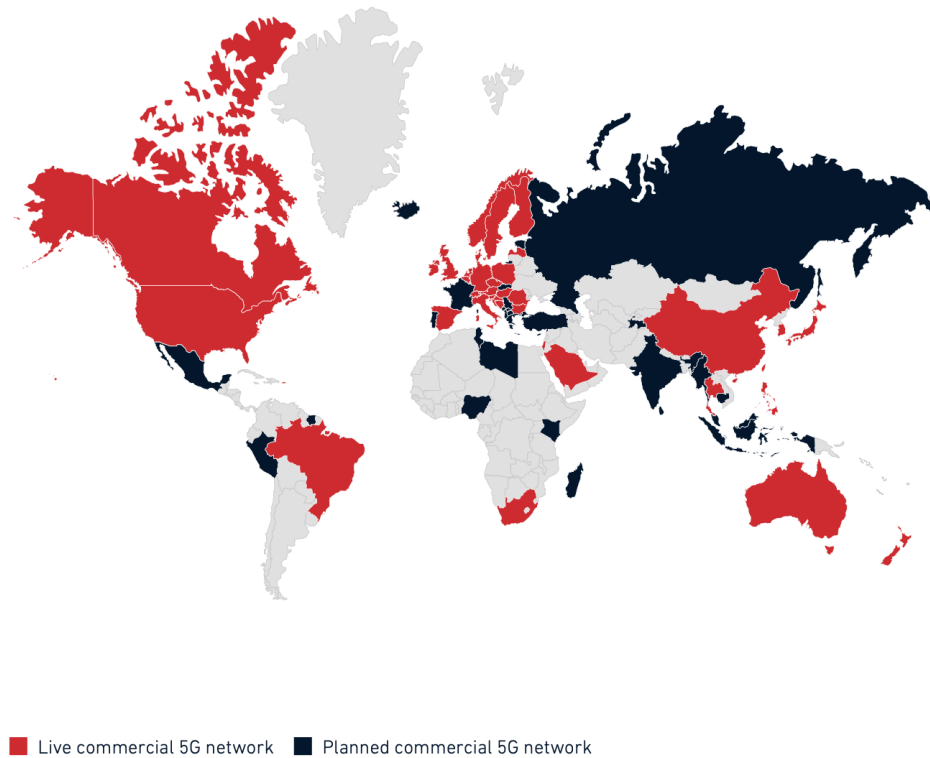


Figure 1.2: The world coverage map of commercial 5G networks as of 30 September 2020 [11]

5G technology operates over a wide frequency range of the radio spectrum, offering a wider range than previous cellular networks. 5G needs spectrum across low, mid and high spectrum bands to deliver widespread coverage and support a wide range of use cases [13]. By low bands we mean the spectrum below the frequency of 1 GHz: Sub-1 bands support widespread coverage, even indoors, in urban, suburban and rural areas. Mid-bands are also called Sub-6 bands because they operate at frequencies below 6 GHz and offer a good mix of coverage and capacity benefits. The Sub-1 and Sub-6 spectra are incredibly important, because these low-frequency radio waves can travel long distances and penetrate walls and obstacles: this means that carriers can implement much larger networks without having to build a vast number of BSs. Finally, there's millimeter Wave (mmWave), which refers to the ultra-high-frequency radio waves, between 30Ghz and 300Ghz, that are used to supercharge 5G connections and deliver download speeds of multiple gigabits per second.

It is important to point out that these frequency bands have been defined by the Third Generation Partnership Project (3GPP) as frequency bands for the 5G New Radio (5G-NR) air interface, based on guidance from both the ITU and regional regulators. In a nutshell, the 5G-NR is a new radio frequency portion of the circuit between the mobile device and the active BS being developed for 5G designed to significantly improve the performance, flexibility, scalability and efficiency of current mobile networks, and to get the most out of the available spectrum, be that licensed, shared or unlicensed, across a wide variety of spectrum bands [14]. Thus, it is clear that to ensure good coverage, high data rate, and low latency, 5G deployment requires the use of both lower frequency and higher frequency. For this reason, as reported in [15], considering that the existing 4G networks will be in service for the near/medium future, 5G-NR distributed at lower frequencies must coexist well with LTE in the same frequency band.

Taking up again what is reported in [11], despite the global pandemic and associated economic constraints, new 5G networks continue to be deployed. As can be seen from Figure 1.2, as of 30 September 2020 there were 113 operators with a 5G network in 48 countries. These operators together represented 40% of the global mobile subscriber base, presenting a large addressable audience and settlement is expected with a stable rate of 8 new 5G networks per month.

1.3 5G and beyond's main use cases

The ITU-R has defined three major use cases for the capabilities of 5G technologies and beyond [16]: (i) Enhanced Mobile Broadband (eMBB); (ii) Ultra Reliable Low Latency Communications (uRLLC); and (iii) Massive Machine Type Communications (mMTC).

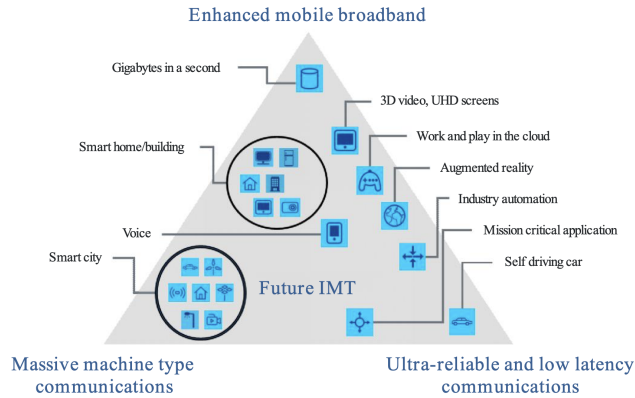


Figure 1.3: The use-cases of 5G and beyond [16]

Firstly, eMBB addresses human-centered use cases for accessing multimedia content, services and data. In a future vision, this scenario will include new application areas and requirements in addition to existing mobile broadband applications for improved performance and a smoother user experience. It covers a range of cases, including large area coverage and hotspots: for the large area coverage case, you want seamless coverage and medium to high mobility, with a user data speed significantly improved over existing data rates; while, for the case of hotspots, i.e. for an area with a high density of users, a very high traffic capacity is required, while the mobility requirement is low and the user's data speed is higher than that of the coverage of an extended area.

Furthermore, uRLLC refers to using the network for mission critical applications that require uninterrupted and robust data exchange: some examples include wireless control of industrial manufacturing or production processes, remote medical surgery, distribution automation in a smart grid, transportation safety, etc. This use case has stringent requirements for capabilities such as throughput, latency and availability.

Finally, mMTC is characterized by a very large number of connected devices typically transmitting a relatively low volume of non-delay-sensitive data. So, this technology aims to provide connectivity to a huge number of devices such as sensors that typically transmit and receive only small amount of data sporadically. An mMTC network is designed to be latency-tolerant, efficient for small data blocks to be transmitted or received, and to be sent on low bandwidth pipes. The main performance requirement for a mMTC network service is to support a high connection density, of up to 1 million devices per square km, which is 10 times the maximum amount possible with 4G LTE.

These three use cases are intended to be the top three application performance indicators for 5G and beyond, so future technologies need to be envisaged to cover these indicators.

1.4 Some emerging challenges

The Cisco[®] Annual Internet Report (2018–2023) [17], reports that 5G devices and connections will be over 10 percent of global mobile devices and connections by 2023 and the fastest growing mobile device category is Machine To Machine (M2M) followed by smartphones. The mobile M2M category - which is directly connected to the growth of the IoT - is projected to grow at a 30% CAGR from 2018 to 2023, while smartphones will grow at a 7% CAGR within the same period. Focusing on global network performances, the average mobile network connection speed will be 43.9 Mbps by 2023 and 5G speeds will be 13 times higher than the average mobile connection by 2023, reaching an average speed of 575 Mbps. Altogether, over 70% of the global population will have mobile connectivity by 2023 which means a significant increase in bandwidth demand that requires the need for optimized bandwidth management.

Moreover, the increased capacity and data rates due to 5G require more spectrum and vastly more spectrally efficient technologies, beyond what used in 3G and 4G systems [18]. Surely, some additional spectrum derives from the mmWave band, which poses some difficulties due to the intrinsic characteristics of the propagation of millimeter waves: these radio waves propagate over much shorter distances than those of the Sub-1 and Sub-6 bands. Hence, the coverage of a specific area requires a large number of BSs which increase the complexity of the infrastructure as well as the need to install radio equipment on road services such as poles, traffic lights etc.

The installation of new 5G BSs throughout the territory is also necessary to support all those services offered by this technology. One of the problems arising from the proliferation of 5G BSs stems from the common understanding among the population that such installations could lead to an uncontrolled increase in radio frequency pollution. Although, many works in the literature (e.g., [19]) have shown no scientific evidence of health effects triggered by radio wave exposure of BSs working below the maximum limits, the public debate on the installation of new 5G BSs makes the bureaucratic process for their establishment difficult. Hence, spectrum is a scarce and very valuable resource, and there is fierce competition for spectrum at all levels of government, from regional to international. Just as the radio spectrum is divided into frequency bands allocated for different services, each band can only be used by services that can coexist without creating

mutual interference.



Figure 1.4: An example of 5G BS

Another challenge arises from the connection links between the BS and the backhaul of a 5G network, which rely on wireless and optical fiber technologies. This is the result of using the same physical network infrastructure to provide customized services for each of the use cases reported in Section 1.3. One key technology required to accomplish these demands under the same infrastructure is the network slicing, which is a concept that virtually separates the infrastructure into many parallel slices that are isolated from each other to prevent congestion and to prevent faults in one slice from affecting the others [20]. In this context, we refer to the part of the communication system that implements the radio access between the end-user device and the backhaul as Radio Access Network (RAN), which can support Real Time (RT) and Non-Real Time (NRT) functions. As the 5G network architecture aims to flexibly and efficiently meet diversified mobile service requirements, with (Software-Defined Networking) SDN and (Network Function Virtualization) NFV supporting the underlying physical infrastructure, 5G cloudifies access, transport and backhauls: this cloud adoption enables so-called End To End (E2E) network slicing [21]. An example of E2E network slicing for multiple services based on one physical infrastructure proposed by Huawei[®] is shown in Figure 1.5.

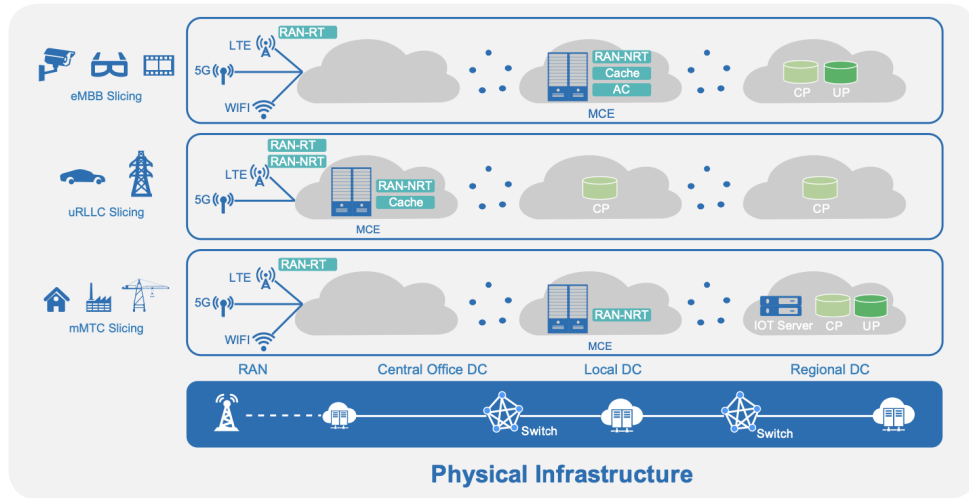


Figure 1.5: The E2E network slicing for multiple services based on one physical infrastructure proposed by Huawei[®] in [21]

As illustrated in the preceding figure, the physical infrastructure of the network architecture consists of sites which support multiple modes (such as 5G, LTE and Wi-Fi) and a three-layer cloud CD that consists of computing and storage resources. In accordance with the requirements of eMBB, uRLLC, and mMTC, these use cases are supported independently on a single physical infrastructure and network slices that operate as logical arrangements and are separated as individual structures. Despite this promising solution, considerable work is required for implementing fiber services and ensuring availability of wireless backhaul solutions with sufficient capacity.

Moreover, no single solution addresses the needs of all use cases: the hugely varying system requirements mean many solutions will be required. Case-by-case system optimization will be needed and compatibility across different use cases must be redefined. The current 5G network is not yet capable of meeting all the demanding design needs of existing and emerging requirements, such as ultra-high reliability, ultra-low latency, ultra-secure networks [22]. Motivated by this, prospects for future physical layers and wireless systems: in addition to the terrestrial networks, also infrastructures based on satellite and aerial platforms will be needed to support the coverage and capacity requirements.

Finally, one of the most important problems deriving from the advent of 5G is given by the considerable increase in energy consumption which is followed by an increase in energy costs. This topic is under the magnifying glass of the networking

research community, since the energy consumption of telecommunications networks has a remarkable growth rate, about 12% per year [23]. This growth is closely related to the proliferation of 5G BSs: numerous papers have studied methods for reducing the consumption of BSs through the use of Renewable Energy (RE) or resource management strategies such as Resource on Demand (RoD) strategies, which use sleep modes on BSs in periods of low traffic, or other types of strategies with the aim of supporting sustainability and reducing costs.

1.5 Towards 6G networks

To support the competitive advantage of wireless networks, industrial and academic synergies have begun to conceptualize the next generation of wireless communication systems (i.e., sixth generation, (6G)) aimed at laying the foundation for layering the communication needs of 2030s [24]. Moreover, the recent upsurge of diversified mobile applications, especially those supported by Artificial Intelligence (AI) technology, is spurring heated discussions on the future evolution of wireless communications. Furthermore, in addition to the growth of AI, today's exponential growth of other advanced technologies such as robotics and automation will usher in unprecedented paradigm shifts in the wireless communication. For these reasons, in contrast to previous generations, 6G will be transformative and will revolutionize the wireless evolution from connecting humans to connecting various things until connecting intelligence, with even more stringent requirements. Inspired by these trends, in [25] the authors attempt to conceptualize a road-map for 6G, which is based on the strategic plans of various standard bodies and is also projected based on the 5G status. The possible overview of the road-map is depicted in Figure 1.6.

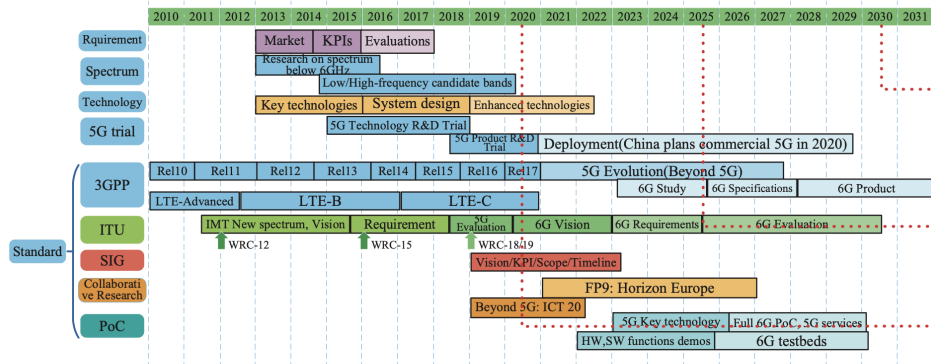


Figure 1.6: A possible road-map for 6G [25]

Following the aforementioned circumstances, Samsung[®]'s 6G vision white paper [26] proposes four major megatrends advancing toward 6G: (i) connected machines; (ii) use of AI for the wireless communication; (iii) openness of mobile communications; and (iv) increased contribution for achieving social goals.

Regarding connected machines (such as vehicles, robots, drones, displays, appliances, smart sensors, etc.), the number of connected devices is expected to reach 500 billion by 2030, about 59 times larger than the expected population at that time. It is also expected that devices such as Augmented Reality (AR) glasses, Virtual Reality (VR) headsets and hologram projectors will be available in the mass market. Even though in the development of 5G, machines and devices have been considered in defining the requirements and technologies to be developed, new 6G technologies must be developed specifically to connect billions of devices and must be oriented towards the requirements of the devices rather than the requirements of humans. This is because machines are considered extenders of the sensory abilities of the human being: the abilities of machines do not have the physical constraints that the perception abilities of humans have.

AI is expected to be a cornerstone for wireless communications applications: it can improve performance of handover operation, optimize BS location determination, reduce network energy consumption or predict, detect and enable self-healing of network anomalies. The main problem is due to the limit of what is achievable today, as the use of AI in communication networks was not considered in previous versions of wireless communication systems such as 5G. For this, it is necessary to consider AI as a fundamental concept in the development of future technologies, in order to guarantee the improvement of the entire network in terms of performance, cost and ability to provide various services.

Regarding the possibility of having open source software that implements network functions, today open RAN is a hot topic in mobile telecommunications, as it aims to create a multi-vendor RAN solution that allows separation between hardware and software with open interfaces and virtualization, software hosting that monitors and updates networks in the cloud. The promised benefits include supply chain diversity, flexibility of solutions and new capabilities that lead to more competition and further innovation. Therefore, the openness of mobile communications is a key trend for the development of new mobile communication technologies.

Finally, the development of technologies that allow connection to an increasing number of people, especially in those areas without network coverage, is a highly appreciated element by governments and international organizations. In this delicate period due to the pandemic, 5G has made it possible to enable remote teaching, allowing the possibility of improving educational equality. Despite the help of 5G, regional and social disparities are still present and widespread. Hyper-connectivity and ultimate experience delivered by 6G mobile communications will improve and enable access to required information, resources (both virtual and physical),

and social services without constraints of time and physical location, reducing differences in regional and social infrastructure and economic opportunities and thereby provide alternatives to rural exodus, mass urbanization and its attendant problems.

Obviously, the three proposed use-cases for 5G, i.e., eMBB, uRLLC and mMTC described in Section 1.3, are still valid for 6G and will continue to be improved and updated. Due to advances in communications as well as other technologies, new 6G services will emerge and they will be introduced through hyper-connectivity involving humans and everything. Again in [26], the authors propose three key 6G services as depicted in Figure 1.7: (i) truly immersive Extended Reality (XR); (ii) hologram mobile Hi-Fi; and (iii) digital replica.

XR has attracted great attention and opened new horizons in various fields and it is expected that the market sizes for VR and AR will grow exponentially by 2030. One critical obstacle between the potential and reality of XR is hardware: current mobile devices lack sufficient stand-alone computing capability; this challenge can be overcome by offloading computing to more powerful devices or servers. Another challenge is sufficient wireless capacity: in order to provide truly immersive AR, the density should be largely improved and it will require 0.44 Gbps.

Moreover, it is expected that mobile devices will be able to render media for 3D hologram displays: in order to provide hologram display as a part of real time services, extremely high data rate transmission, hundreds of times greater than current 5G system, will be essential. In this context, to reduce the magnitude of data communication required for hologram displays and realize it in the 6G era, AI can be leveraged.

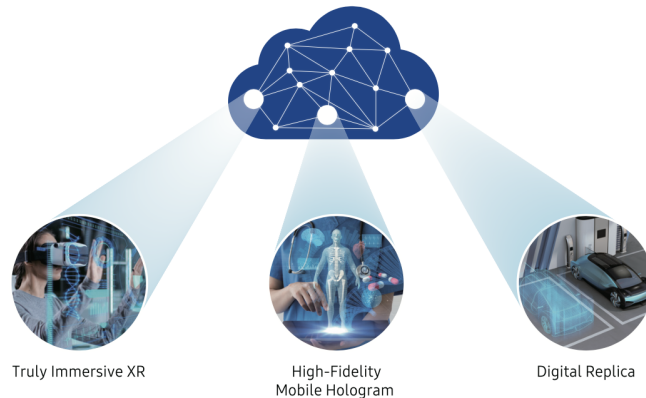


Figure 1.7: The three key 6G services proposed by Samsung[®] in [26]

Finally, with the help of advanced sensors, AI, and communication technologies, it will be possible to replicate physical entities, including people, devices, objects, systems, and even places, in a virtual world, without temporal or spatial constraints. The technical challenges are significant: only to be able for duplicating a 1 m x 1 m area, 0.8 Tbps throughput with a periodic synchronization of 100 ms and a compression ratio of 1/300, is required.

1.5.1 The requirements of 6G

The new services in 6G era proposed in Section 1.5 require a large amount of real-time data, a hyper-fast data rate and very low latency. The solution for these requirements can not relying only on improvement of the communication link performance, because there are two main problems: (i) the growth of the computational capacity of the devices has a lower rate than the computational capacity required by the services; and (ii) the battery life of mobile devices is not optimal with respect to the demand for services, especially multimedia ones.

For this reason, it is necessary to define new performance-oriented requirements. An example of Key Performance Indicators (KPIs) enhancement in the transition from 5G to 6G is shown in Figure 1.8.

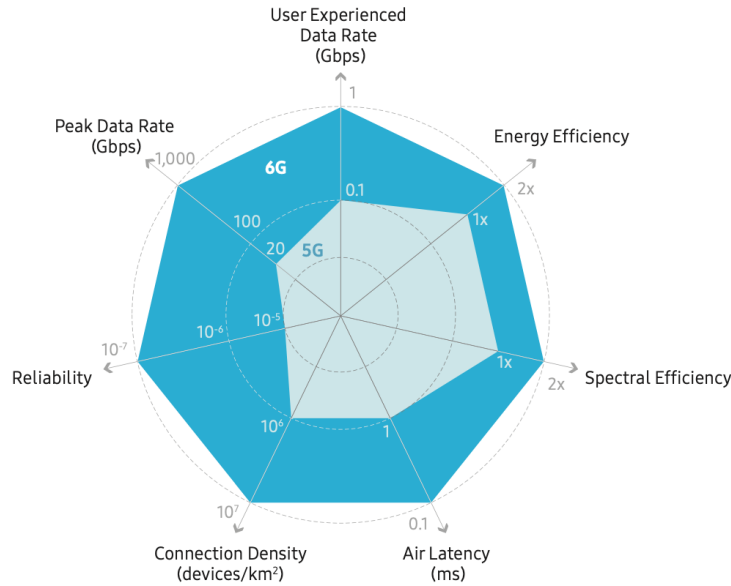


Figure 1.8: A comparison of KPIs between 5G and 6G [26]

Only by considering the eMBB use case is it evident how its function imposes high peak data rates: while 5G was designed to reach a peak data rate of 20 Gbps, the development of new standards and protocols for 6G services (e.g., vehicular networks) aspires to deliver a peak data rate of 1000 Gbps [27]. Moreover, the user experienced data rate requirements are increasing since the birth of wireless communications: as shown in Figure 1.1, 1G had data rates of a few kbps, which further increased up to few hundreds of Mbps in 5G and it is expected to reach 1 Gbps with 6G technologies.

Since the next-generation wireless communication system will consist of massive self-organizing and self-healing robots, high computation power will be required. Therefore, the need for energy will be increasing with the increase in intelligent robots: in such a scenario, an energy-efficient and scalable intelligent network design will be required [28]. Furthermore, considering the growing concern about environmental sustainability, the energy consumption of 6G networks should be minimized, improving the energy efficiency by at least two times.

Another characteristic of the future wireless network is that it will comprise of smart factories, smart hospitals, schools, universities, and autonomous robots. This will require a highly spectral efficient network having high computing power: the spectral efficiency of 6G networks is supposed to be 2 times higher than of 5G.

Then, to provide the ultimate experience of delay-sensitive real-time applications, latency-related performance needs to significantly improve. Performance targets include air latency less than 100 μ s, E2E latency less than 1 ms and extremely low delay jitter in the order of microseconds. Low latency is directly connected to extremely-high reliability: smart cities will need to be connected to airplanes, ships, bullet trains, and Unmanned Aerial Vehicles (UAVs) and some of the critical applications which include health care, defense sector, monitoring, and surveillance will require ultra-reliability and low delay. For this reasons, in 6G reliability will improve by 100 times compared to 5G so that the error rate is 10^{-7} .

A final KPI is the connection density in terms of devices per square kilometer: the explosive growth in the number of connected machines will require 6G to support about 10^7 devices per square kilometer [16], which is ten times larger than the connection density requirement of 5G. This requirement is directly connected to the mMTC use-case and it's the domain where IoT comes in.

1.5.2 Possible candidate technologies

As early as March 2019, the US Federal Communications Commission adopted new rules to encourage the development of new communication technologies and accelerate the deployment of new services in the spectrum above 95 GHz [29]. In particular, to enable innovators and entrepreneurs to access this spectrum more easily, the Spectrum Horizons First Report and Order has created a new category

of experimental licenses for the use of frequencies between 95 GHz and 3 THz. In the same period, 3GPP published a technical report on requirements studies for NR systems above 52.6 GHz. To date, the latest version of this report was published in March 2021 [30], underlining how the trend of mobile communications tends towards use of terahertz bands in future wireless systems. Surely, the availability of wideband spectrum is the main driver for terahertz communications since one of the main challenge for the new mobile communication networks is given by the scarcity of available bandwidth as described in Section 1.4. However, the practical implementation of radio communications in the terahertz band presents some technical challenges especially in the physical level.

In [26], the authors underline four main challenges:

- (i) severe path loss and atmospheric absorption, due to the high frequencies¹;
- (ii) radio frequency front-end, photonics and data conversion, due to a lack of existing efficient devices, which can generate and detect signals in these frequencies;
- (iii) antenna, lens, and beamforming architecture, because as a consequence of the severe free-space path-loss, massive antenna arrays are necessary to compensate for the path loss;
- (iv) new waveforms, signals, channels, and protocols, because it is necessary to explore alternative waveforms to support GHz-wide channels and to develop proper design of signals, channels, and protocols, which are effective yet of low complexity for terahertz operation.

In addition to the challenges listed above, it is important to report a lack in the structure of the network topology: although terahertz technologies are promising despite some difficulties, until now cellular BSs have typically been deployed with fixed locations and connected by fixed networks. With such static network topology and wireline backhaul and fronthaul, it is difficult and costly to establish additional BSs to accommodate an increase of data traffic or to fill holes in coverage. Moreover, existing cellular infrastructures show vulnerability to natural disasters:

¹Since the free-space path loss (FSPL) is the attenuation of radio energy between the feedpoints of two antennas, it increases with the square of distance d between the antennas because the radio waves spread out by the inverse square law and decreases with the square of the wavelength λ of the radio waves. Considering that the frequency of a radio wave f is equal to the speed of light c divided by the wavelength λ , the path loss can also be written in terms of frequency by using the Friis formula:

$$FSPL = \left(\frac{4\pi df}{c} \right)^2$$

It is easy to see how increasing the frequency f leads to an increase in free-space path loss.

connectivity outages during natural disasters, in particular, may slow down or impede appropriate reaction, create significant damage to business and property, and even loss of lives [31].

To address these issues, 6G research is currently focusing on the development of Non-Terrestrial Networks (NTNs) to promote ubiquitous and high-capacity global connectivity [32]. 6G envisions a three-dimensional vertical heterogeneous architecture in which terrestrial infrastructures are complemented by non-terrestrial stations including UAVs, High Altitude Platforms (HAPs) and satellites [33]. The use of NTN components might be useful to provide coverage even in locations where there is no terrestrial network, as illustrated in Figure 1.9.

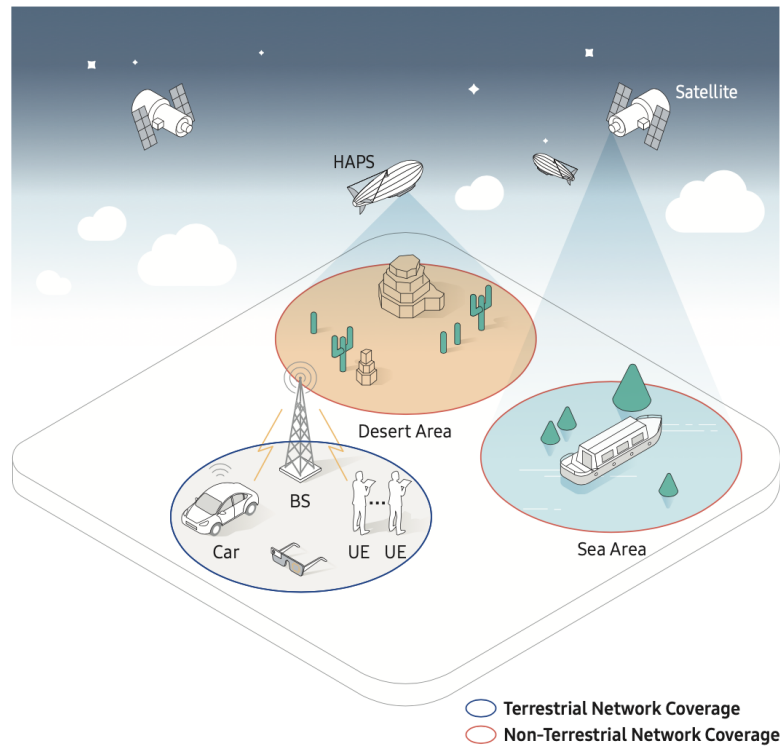


Figure 1.9: A sketch of a possible inclusion of NTN components in a 6G network scenario [26]

Moreover, since the architecture of 6G communication network should be developed so that it can resolve the issues arising from the limited computation capability of mobile devices, a possible way to achieve this is to offload computation tasks to more powerful devices or servers installed on these mobile aerial platforms.

In conclusion, realization of NTN technology necessitates consideration of new

aspects absent from terrestrial networks, including support of moving cells, large cell sizes, long propagation delays, large Doppler shift due to the high speed of NTN components, and large path loss. Additional aspects may arise and need to be considered, since the mobile industry is at the initial stage for developing technologies to support NTN. As NTN components become widely deployed, investigation of technologies will proceed, to improve the overall performance of communications involving NTN components and to provide tight integration of NTN components in overall operation of mobile communication systems.

1.6 In this thesis: goals and outline

This thesis work aims to analyze a new generation of mobile networks that integrate aerial platforms (e.g., airships) in order to: (i) reduce the energy consumption, by moving loads when the energy is expensive or scarce, and responding to the smart grid; and (ii) improve the Quality of Service (QoS), by lowering traffic peaks, and adapting the cluster capacity to traffic conditions. In this environment, we envision that the aerial platforms can complement the terrestrial backhaul in dense regions with high peak traffic demands, thus achieving load balancing.

The rest of this work thesis is organized as follows. Chapter 2 presents an updated review of the documents and ongoing work on the integration of mobile networks and aerial platforms. Chapter 3 discusses the methodology implemented for the development of the simulations carried out, with particular attention to what and how certain choices were made, in order to be able to evaluate the reliability and validity of this research. In Chapter 4, a series of experiments are performed and the experimental results are thoroughly analyzed. Finally, in Chapter 5 we conclude the paper with a short summary and discuss possible future work.

Chapter 2

State-of-the-Art review

In this Chapter a review is carried out on the updates in the literature regarding NTN and with particular interest in aerial platforms capable of creating HAP stations (HAPSs) networks.

Section 2.1 introduces a view on the development of a NTN with a focus on the types of non-terrestrial stations involved in this its architecture, which is consequently treated and analyzed.

Section 2.2 gives information about the HAPSs that are used as intermediate layer of the NTN architecture and describes some of their intrinsic characteristics. Moreover, a focus on the generation and implementation of the HAPS network is carried out, with explanation of some important use cases.

Finally, Section 2.3 discusses some existing HAPSs projects in the world and what are the main challenges encountered in their development.

2.1 An overview on Non-Terrestrial Networks

The development of NTN systems as an effective solution to complement terrestrial networks in providing services over uncovered or under-served geographical areas [34]. In [35], 3GPP defines an NTN as a network, or segment of networks using radio frequency resources on board a satellite, or UAV platforms, or HAPs, which we refer to as non-terrestrial stations.

A typical scenario of a NTN providing access to a terrestrial terminal (e.g., a user equipment) is depicted in Figure 2.1.

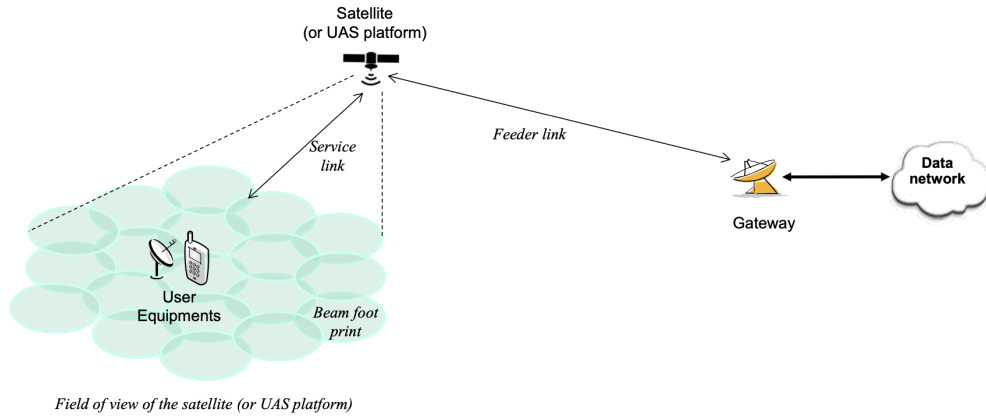


Figure 2.1: A NTN typical scenario [35]

As you can see from Figure 2.1, NTN features: (i) a terrestrial terminal that could be a user equipment; (ii) a non-terrestrial station, which could operate similarly to a terrestrial BS; (iii) a service link between the terrestrial terminal and the non-terrestrial station; and (iv) a gateway that connects the non-terrestrial access network to the core network through a feeder link.

2.1.1 Types of non-terrestrial stations

According to the type of the non-terrestrial station involved, a NTN may have different deployment options. In [34], the authors group non-terrestrial stations in two main categories that typically depend on the altitude: (i) spaceborne stations, which are typically satellites orbit at an altitude over 200 km; and (ii) airborne stations, which are typically UAVs or HAPs orbit at low altitudes up to 50 km.

Satellites are spaceborne stations which could be classified according to altitude range, orbit and beam footprint¹ size. Geostationary Earth Orbit (GEO) satellites orbit on the Earth's equatorial plane at an altitude of about 35800 km. Since they are placed at such long distance, they experience large signal propagation delay and attenuation. Nevertheless, they can cover large geographical areas with a beam footprint size up to 3500 km and are continuously visible from terrestrial terminals. Traditionally, GEO satellites have been used primarily for satellite

¹Satellites or aerial vehicles typically generate several beams over a given area. The footprint of the beams are typically elliptical shape [36].

communications as they avoid rapid movement between the terminals and the satellite transceiver and allow for a large beam footprint size using a single satellite. To enable efficient reuse of frequencies and high-speed broadband rates in the coverage area, multibeam satellite systems have been developed. However, new, more ambitious types of constellations are currently being developed, motivated by advanced communication technologies and cheaper launch costs [37]. Following this trend, Medium Earth Orbit (MEO) and Low Earth Orbit (LEO) satellites have been developed, which orbit at lower altitudes than GEO satellites, as can be seen from Table 2.1. Although they provide better signal strength and shorter propagation delay than GEO satellites, MEO and LEO satellites have a circular orbit around the Earth and are therefore non-stationary. For this reason, they must operate within a constellation of satellites in order to ensure continuity of service. In LEO satellites, in particular, the adoption of the Gallium Nitride technologies [38] was a major breakthrough in the improvement of satellite technology, because these technologies allow the development of nano- and pico-satellites contributing to the creation of small LEO satellites mega-constellations. However, nowadays the use of products with Gallium Nitride technologies is reserved for military applications, because mass-market 5G devices use silicon wafers: it is expected that the adoption of this technology also for commercial networks will be achieved with the adoption of 6G [34]. Since the LEO mega-constellations have the ability to offer high throughput and low latency broadband services, many of the most important companies in the world employed in the technological innovation sector (eg, SpaceX, Amazon, etc.) have announced their intent to activate NTN through the use of LEO satellites, in order to offer satellite Internet access. Among the projects under development, the one that most of all seems to be ready to be activated is the Starlink constellation of SpaceX: as of July 2021, 1470 LEO satellites have been deployed with the aim of reaching a final constellation close to 12000 LEO satellites [39].

Table 2.1: A comparison between the types of non-terrestrial stations

Station Type	Altitude Range	Orbit	Beam Footprint Size
GEO satellite	about 35.800 km	Fixed position	200-3500 km
MEO satellite	2000-35000 km	Circular	100-1000 km
LEO satellite	200-2000 km	Circular	100-1000 km
HAP	20-50 km	Quasi-stationary position	60-500 km
UAV	Few hundred meters	Quasi-stationary position	5-200 km

Among the airborne stations we find HAPs and UAVs. As can be seen from Table 2.1, HAPs can operate in the stratosphere at an altitude of about 20 km. The advantage of using HAPs is due to their quick deployment and the ability to have a beam footprint size of up to 500km. These stations have begun to be considered to support flexible deployment and cheaper wireless services compared to the prohibitive costs of services offered by terrestrial infrastructure. Given that networks created using HAPS are the main topic of this thesis work, an in-depth study of them will be dealt with in Section 2.2. As far as UAVs are concerned, such devices can create stations at low altitudes in the order of hundreds of meters. Thanks to their flexibility, they can create a broadband wireless connection on a large scale in disaster situations or for events of short duration. Another use of UAVs is as relay nodes for mobile land devices. Although they can offer on-demand services with a high energy saving compared to an always-on fixed land infrastructure, UAVs need a large energy storage because they are devices that need propulsion to maintain and support movement. For this reason, they are devices that can create non-terrestrial stations for situations that do not require long usage times as they have high power management constraints.

In the sketch in Figure 2.2, it is possible to observe an example of the distribution of non-terrestrial stations in the airspace.

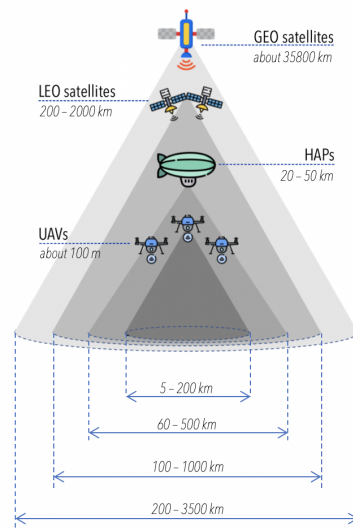


Figure 2.2: A sketch of the distribution of non-terrestrial stations in the airspace with example of beam footprint size

2.1.2 Towards a New Space era

With the development of the concept of NTN, we are going into the direction of a New Space era. In [37], the authors state that this concept implies a new mentality towards air space which originates from three main aspects: (i) space privatization; (ii) component miniaturization; and (iii) new services based on space data. Space privatization refers to the manufacturing and the launching of non-terrestrial systems by private companies, in contrast to the traditional institutional approach. Then, component miniaturization allowed easy access to space by launching multiple systems - especially satellites - into a single launcher. Finally, the concept of new services based on space data is inspired by the fact that New Space creates new opportunities in terms of collecting data from ground sensors directly via non-terrestrial systems.

Furthermore, as mentioned in Section 1.5.2, existing cellular infrastructures express vulnerabilities in harsh environments, such as unserved or crowded areas or zones devastated by natural disasters: therefore, the use of non-terrestrial stations in the airspace has a significant impact on the improvement of the offer of on-demand coverage with a reduction of installation costs. However, the New Space concept is not limited to the activation of NTN only for the cases mentioned: the use of these new types of networks can guarantee services such as trunking, backhauling, high-speed mobility and high-throughput in urban areas with existing ground network infrastructure.

2.1.3 Some NTN architecture proposals

In the literature various researches have proposed novel network architectures for NTN. For instance, in [40] the authors propose a novel network architecture for an integrated nanosatellite-5G system operating in the mmWave domain, while in [33] the authors envision a three-dimensional vertical heterogeneous architecture in which terrestrial infrastructures are complemented by non-terrestrial stations including UAVs, HAPs and satellites. Moreover, in [41] the UAVs were considered to provide ubiquitous connectivity in public safety scenarios or in remote areas. However, there are still several questions to be answered for proper network design. The papers presented typically focus on autonomous non-terrestrial stations architectures, but a multi-layer network, in which heterogeneous non-terrestrial stations cooperate at different altitudes in an integrated way, has not yet been formalized. Thanks to the technological advance of the non-terrestrial systems, intermediate layers of communications systems between terrestrial and traditional satellite segments have emerged. In fact, the advent of systems like UAVs, HAPs and LEO satellites enables a novel multi-layer architecture with multiple inter-layer

links capable to overcome the most challenging scenarios.

An example of a three-layer network architecture called Vertical Heterogeneous Network (VHetNet) depicted in Figure 2.3, is discussed in [42]: the three layers are composed of the satellites space network, the aerial network and the terrestrial network. In this context, UAVs combined with HAPSs and satellites, can operate together to support more robust information broadcasting compared to a standalone deployment by adding redundancy against single point of failure in the path [31]. By the scope of this thesis work, an in-depth study on the use of HAPS layers as intermediate level of the proposed VHetNet will be discussed in Section 2.2.3.

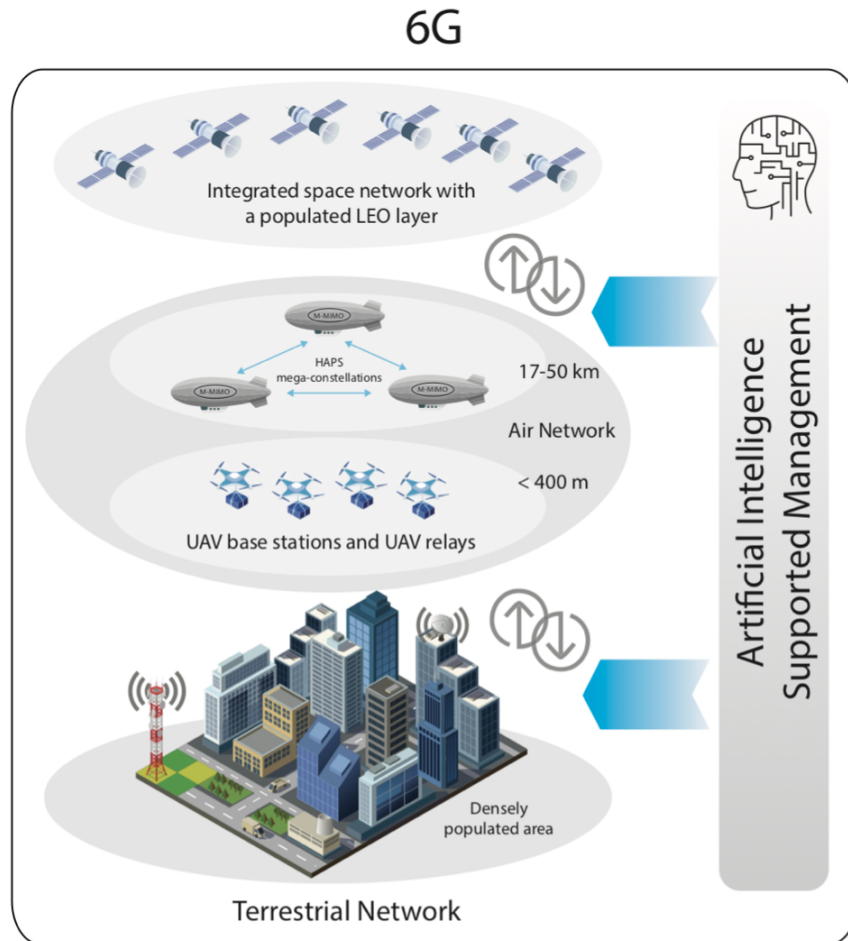


Figure 2.3: A fully integrated VHetNet envisioned for 6G [42]

2.1.4 Advantages expected from the adoption of NTN

In [43], 3GPP defines three main advantages deriving from the adoption of NTN: (i) enhanced network reliability, by ensuring service continuity, in cases where it cannot be offered by a single or a combination of terrestrial networks, which is especially true in case of moving platforms (e.g., car, train, airplane etc.) and mission-critical communications; (ii) service ubiquity in unserved (e.g., desert, oceans, forest etc.) or underserved areas (e.g., urban areas), where a terrestrial network does not exist or it is too impractical/cost-ineffective to reach; and (iii) service scalability due to the efficiency of the satellites in multicasting or broadcasting over a very wide area, offloading the terrestrial network, by broadcasting popular content to the edge of the network or directly to the users.

2.2 The development of HAPS networks

As discussed in Section 2.1.3, HAPS is an essential component for the integration and implementation of VHetNets. These types of tiered hierarchical networks consisting of non-terrestrial flying stations are a promising solution for providing extended coverage and enhanced security in future communications. In this architecture, multiple types of flying layers cooperate to improve the space-to-ground link reliability and capacity [44]. In particular, HAPS can serve both UAVs and ground users from a high altitude and act as relay nodes from satellites when needed. Although the conventional target of HAPS is to bring broad coverage to remote areas or in disaster recovery cases, it is envisioned that HAPS can act as a Super Macro BS (SMBS) to provide connectivity in a multitude of applications.

2.2.1 Which station can be defined as a HAPS?

According to Article 1.66A of the ITU's ITU Radio Regulations [45], a HAPS is a station located on an object at an altitude of 20 to 50 km and at a specified, nominal, fixed point relative to the Earth. Therefore a HAPS is a network node that operates in the stratosphere - see Figure 2.4 - at an altitude around 20 km and due to the unique properties of the stratosphere, a HAPS can stay at quasi-stationary position, providing significant benefits to the ubiquitous connectivity goal [42].

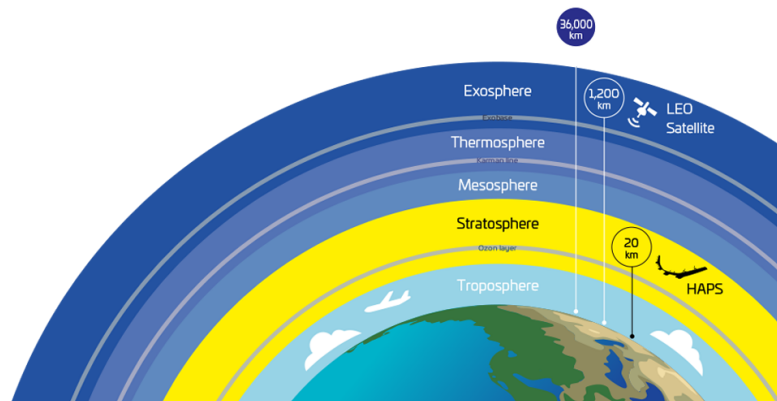


Figure 2.4: The location of non-terrestrial systems in the atmosphere [46]

HAPs are mainly UAV platforms, such as balloons, RE-powered aircraft or airships, which can be divided into two macro-categories: (i) aerostatic platforms; and (ii) aerodynamic platforms.

The term aerostatic platforms refers to those platforms that are lighter than air such as balloons and airships, which lift gas in an envelope to provide buoyancy to float in the air and therefore they are not very robust to winds and turbulent conditions.

More specifically, the balloons do not have a propulsion system and can operate at an altitude between 2 and 20 km. For very low altitudes it is possible to think of using tethered balloons, in order to increase the robustness to winds and turbulence, compromising the coverage area. Their payload is around 20 kg which makes them unsuitable for applications from 5G and beyond and they have an operating time of up to several months. An example of balloon used as a HAPS is shown in Figure 2.6.

Airships, on the other hand, have a propulsion system and can operate stably in the stratosphere at an altitude of 20 km. Given the large surface area available and the absence of clouds, they have the ability to generate a large amount of energy using large solar cells. This allows them to be suitable for a longer-term scenario up to several years. Moreover, they have a large payload capacity of up to 450 kg, making them suitable for 6G applications. An example of airship used as a HAPS is shown in Figure 2.6.



Figure 2.5: An example of balloon used as a HAPS [47]



Figure 2.6: An example of airship used as a HAPS [48]

The term aerodynamic platforms refers to those platforms that are heavier than air, which float by exploiting dynamic forces created by the movement of the air through electric motors and propellers, and therefore they are more robust to winds and turbulent conditions than aerostatic platforms. These platforms move forward and circle the area intended for coverage in order to maintain a quasi-stationary position. For this, they need adjustments in antenna pointing and communication beams. They usually have smaller dimensions than aerostatic platforms and therefore have a limited payload capacity. Their small size, however, translates into reduced deployment costs, greater flexibility in take-off/landing and easier mobility control, which makes them more suitable for short-term use such as disasters and emergency situations. An example of aerodynamic platform used as

a HAPS is shown in Figure 2.7.



Figure 2.7: An example of aerodynamic platform used as a HAPS [49]

2.2.2 Theoretical characteristics of HAPS

Latency

According to [42], the relatively low altitude of HAPS systems corresponds to a round trip delay of 0.13 to 0.33 ms which makes them a good option for low latency such as URLLC applications. Hence, the HAPS constellation-based communication system can overcome the inherent high-latency problem of the satellite networks. Moreover, it is expected a high downlink Signal-to-Noise Ratio (SNR), a favorable link budget, and low path loss which allows to use a user equipment without the need of specialized ground stations.

Operation time

As mentioned in Section 2.2.1, thanks to the presence of solar-powered RE it is expected a long-term utilization up to several months or even years. However, there may be a turnover to always guarantee the network architecture: this situation does not appear to be problematic given the low launch costs and risks, and the ease with which it is possible to return the platforms to Earth without releasing debris into the atmosphere as is the case with satellites. Although the choice of energy source was considered as a fundamental issue in HAPS, solar power coupled with energy storage has been regarded as the primary means of providing energy for HAPS since they have large surfaces suitable to accommodate solar panel films [50].

Beam footprint

According to ITU recommendations [51], a HAPS should have a wide footprint of about 500 km in radius. Even though almost all HAPS projects have much smaller coverage areas around 100 km, a network of few multiple HAPSs can extend the coverage to serve a whole country. For example, while a 18 HAPSs system is estimated to be sufficient to cover Greece including all islands [52], a constellation of 16 HAPSs is considered to cover Japan [53].

Capacity Demand

The ITU in its report [54], provides the results of HAPS broadband applications spectrum needs with an in-depth capacity demand analysis. The study used a geospatial simulation-based approach for a selection of 32 countries, and is based on the following assumptions: (i) 50 km radius coverage and 33 users/km², with a number of users rounded to 250 000; (ii) a target availability level set to 99.5%; (iii) a target connectivity level set to 30 GB; (iv) a end user throughput requirement set to 2.5 Mbps; (v) a data volume of 30 GB per month per user; (vi) a busy hour ratio of 1.55; and (vii) an utilisation rate of 60%. The analysis concluded that the maximum capacity of HAPS is 60 Gbps, while analyzing the Cumulative Distribution Functions (CDF) of the HAPS throughput and the number of users, it has been shown that the 90th conservative percentile of HAPS will provide coverage for 130 000 users with a capacity of 30 Gbps. The resulting CDFs are depicted in Figure 2.8.

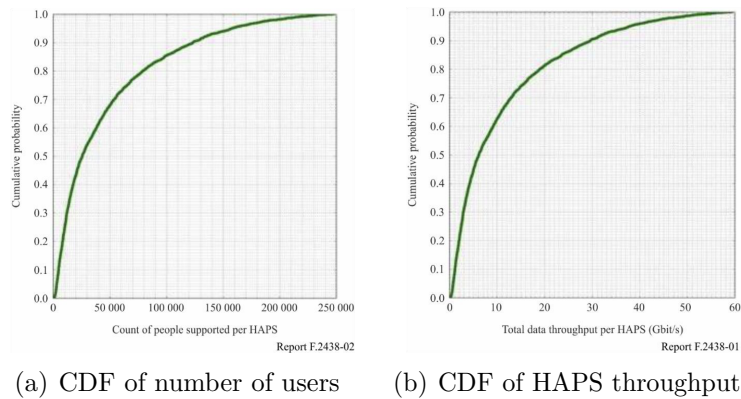


Figure 2.8: CDF resulting from the capacity demand analysis [54]

Energy consumption

HAPS energy is consumed by: (i) the flight control system; and (ii) the communications payload system. The energy consumed by the flight control system includes the consumption for stability and propulsion power and the consumption caused by HAPS altitude and course control. Furthermore, the type of platform and its characteristics, such as weight and dimensions, affect the energy consumption of the flight system, as greater weights and dimensions increase consumption. Second, the energy consumed by the communications payload system depends on the type of communications payload and communications techniques. In general, since more active components and calculation processes are included in the payload, heavier loads are required and higher energy consumption is expected.

Energy sources

There are three types of energy sources that have been used for HAPS operations: (i) conventional energy sources; (ii) energy beams; and (iii) solar energy [42]. Among conventional energy sources we find fuel tanks and electrical batteries: HAPS supplied by conventional energy sources have a very short flight duration of about 48 hours and require frequent landing for refueling [55], so their use is suitable for a temporary solution or an emergency situation. Alternatively, energy beams from the ground can be used to supply the HAPS energy system: due to the high power irradiation risks by both microwave-powered and laser-powered platforms, they are not regarded as safe solutions [55]. Finally, solar energy is a RE source and is the main energy source considered by most HAPS projects. Solar energy is appropriate for HAPS due to two basic reasons; (i) HAPSs are operated above the clouds, where the natural solar energy is abundant there; and (ii) HAPSs are typically huge platforms that can have large solar panels to generate large amounts of energy.

2.2.3 The integration of HAPS into VHetNet

As explained in Section 2.1.3 and keeping in mind the architecture of a VHetNet like the one in Figure 2.3, it was shown that HAPSs have the ability to complement satellite networks by providing communication services on a regional scale. The two major methods of cooperation between satellites and HAPSs are backhauling and trunking [56].

Through backhauling, the downlink communication is split into two steps: (i) a first hop between the satellite and the HAPS, which is prone to the use of high bandwidth optical links, as it suffers little atmospheric effects; and (ii) a second hop between the HAPS and ground, which having a much shorter path than the satellite height, improves the link budget enabling smaller antennas or wider bandwidth.

Instead, through trunking, HAPSs have a trade-off between regional coverage and reduced signal degradation, making them a low-cost solution for broadcast services: the user can connect directly to HAPS in its coverage area and connect to satellites for communications between different coverage areas.

The proposed framework has three complementary communication segments: (i) satellites-HAPSs; (ii) HAPSs-UAVs; and (iii) HAPSs-ground.

In the satellite-HAPSs segment, the HAPS layer enables long-distance communications between satellites, ensuring speed, reliability and efficiency. This type of communication channel bypasses the need to install a large number of ground stations [57]. Furthermore, it can also function as a distributed DC with the aim of recording the orbit of satellites, monitoring their status and avoiding collisions, that is, recording essential information to preserve the functionality of the mega-constellations of the satellites. On the other hand, satellites help the HAPS layer in improving the handover² performance.

Hence, in the HAPSs-UAVs segment, the HAPS layer is tasked with managing the mobility of UAVs by providing intelligent edges³, offloading heavy loads, and assisting large-scale monitoring and detection, in order to ensure uRLLC and eMBB communications.

Finally, in the HAPSs-ground segment, the HAPS layer provides a fast Internet access and wireless communication services, such as IoT and distributed Machine Learning (ML), to urban, suburban, and remote areas, reducing the reliance on the terrestrial and satellite networks.

In exposing their vision of the possible architecture of a VHetNet, in [42] the authors focus their study on the role of the HAPS layer on three main concepts: (i) handover management; (ii) network management; and (iii) role of AI.

Handover management

Unlike the handover algorithms for terrestrial networks, in which the BSs are stationary, in the HAPS networks the stratospheric atmosphere and the mechanical

²Handover (also called handoff) is the process by which an active user equipment, in its active state, changes its point of attachment to the network, or when such a change is attempted [58]. When a user equipment moves out of one BS coverage to the next, the communication will be handed over from the first BS to the next without discernible disruption to the user equipment's call or data session.

³Intelligent edge refers to the analysis of data and development of solutions at the site where the data is generated. By doing this, intelligent edge reduces latency, costs, and security risks, thus making the associated business more efficient. The three major categories of intelligent edge are operational technology edges, IoT edges, and IT edges [59].

design of the aerial platforms make the state quasi-stationary. These exceptions cause changes in the size and location of the HAPS footprint⁴, leading to instability of communication links and increasing the likelihood of handover. Therefore, in HAPS networks the handover can be inter-HAPS or intra-HAPS (i.e. inter-cell): the first is caused by the passage from an area covered by one HAPS to another covered by another, the latter can be caused by the movement of a user from one cell to the next one or by the instability of the platform position [60]. A sketch on the types of handover of the HAPS networks is shown in Figure 2.9.

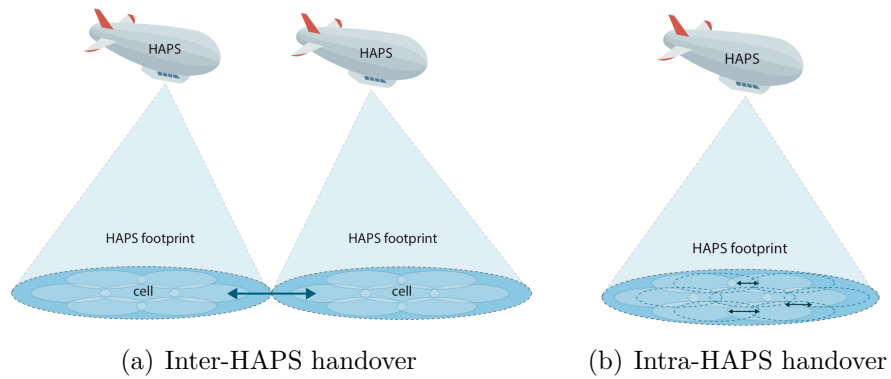


Figure 2.9: A sketch on the types of handover of the HAPS networks [42]

Since HAPS networks are expected to provide coverage for network connected entities moving at high speed, handover management solutions must work with delay-sensitive applications. Authors in [42] propose intelligent and self-adaptive handover solutions, with the use of dynamic beamforming techniques in order to reduce the handover frequency given the high number of users expected.

Network management

As HAPS networks are expected to consist of a multitude of aerial platforms, it is necessary to undertake a network management capable of coordinating and making these platforms work together. Therefore, HAPS control and coordination systems need to develop a good level of autonomy to make intelligent decisions in a collaborative way. Authors in [61] studied the implementation of coordination systems between semi-autonomous HAPs through the use of ML techniques: it was found that swarm intelligence-based approaches may be more efficient and reliable

⁴The HAPS footprint refers to the coverage area on Earth by the entire HAPS, intended as the sum of the coverage cells provided by each beam.

but with less optimal coverage results; while reinforcement learning algorithms will achieve better coverage peaks but at the risk of occasional dips. Other solutions that include network control and management softwarization, such as SDN [62] and NFV [63], have been introduced in the literature.

It is envisioned that in future HAPS networks, through softwarization combined with intelligent algorithms, the network control and management functions are going to be distributed and automated to best meet the multi-dimensional service requirements.

Role of AI

Since HAPS can be equipped with computational devices, enabling computations in air without congesting the communication links towards the terrestrial DCs, and HAPS can support computational offloading for some delay sensitive applications, it is clear how AI plays a fundamental role for HAPS networks and, conversely, HAPS networks are AI enablers. In fact, thanks to the possibility of offering a large coverage area due to their aerial position, HAPSs collect an enormous amount of data that are the engine for ML algorithms and for data analysis.

Moreover, as explained in the previous section, it is expected that HAPS systems will consist of several HAPS of different types and characteristics: it is evident that there is a high need to introduce automation in HAPS systems through exploiting the power of AI algorithms.

2.2.4 HAPS as a Super Macro Base Station

From the previous discussion, it is clear that the HAPS layer has the characteristics of providing enhancements for the development and enabling of essential functionalities for future applications of both terrestrial and satellite communications. Given recent advances in research on the subject, the potential applications of a HAPS can be much broader than conventional ones reserved for areas unserved or underserved. A futuristic view on the fields of application of HAPS predicts that in the 2030s these new networks will be able to provide large-scale communications, offload computing, caching, data acquisition, and processing in densely populated areas.

In [64], the authors envision HAPS as a SMBS⁵ (HAPS-SMBS) as another type of BS in the multi-tier VHetNet architecture to be deployed particularly in dense urban areas in line with the smart city paradigm, motivated by the urgency of

⁵The BS is referred to as Super Macro BS because of its large coverage area, enhanced capacity with multiple-MIMO, and the provision of supporting distinct features, such as data acquisition, computing, caching, and processing.

increasing traffic volume in complex urban scenarios as well as the problems of deploying terrestrial BSs and LEO satellites constellations. This means that unlike conventional HAPS, which targets broad coverage for remote areas or disaster recovery, next-generation HAPS-SMBS will have the necessary capabilities to address the high capacity, low latency, and computing requirements especially for highly populated metropolitan areas.

The utility of HAPS-SMBS development is defined by defining seven use cases: (i) for delivering IoT services; (ii) for backhauling small and isolated BSs; (iii) for covering unpredictable user events; (iv) as an aerial DC; (v) for defeating coverage holes; (vi) for supporting and managing aerial networks; and (vii) for supporting Intelligent Transportation Systems.

A representation of the use cases of HAPS-SMBS networks is depicted in Figure 2.10.

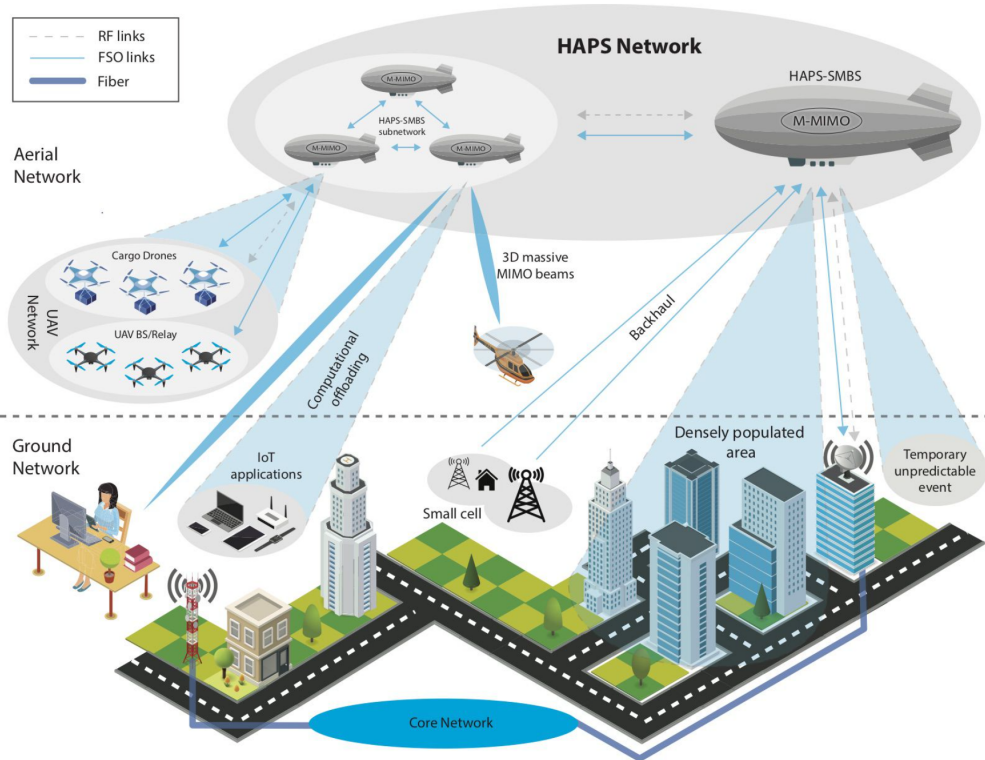


Figure 2.10: A representation of the use cases of HAPS-SMBS networks [64]

HAPS-SMBS for delivering IoT services

With the ever-increasing growth of the IoT, the current infrastructure and so far considered methods of designing wireless access architecture will become incapable of supporting the high demand of wireless systems and services. So, the wide footprint of HAPS systems is ideal for providing larger coverage to a high number of IoT devices, making HAPS-SMBS an attractive solution to complement terrestrial networks to collect data from IoT devices and provide reliable uplink connections with them.

HAPS-SMBS for backhauling small and isolated BSs

Small cell BSs' fiber optic communications backhauling concept has been fully utilized for 5G, but cannot be used in an ordinary way given the difficulties and high costs. A cost-effective solution is given by the combination of mmWave bands' wider channel bandwidths and MIMO digital beamforming [65]. Despite this, the latest advances in research into HAPS systems and Free-Space Optical communication⁶ (FSO), have motivated the backhauling of small cell outdoor via FSO and HAPS-SMBS: the results of [67] show that data rates in the multi Gbps ranges can be obtained in clear weather conditions and that rain is the main cause of communication degradation. For this reason, the authors propose to use FSO when weather conditions are clear or foggy, and to switch to radio frequency communication during rainy conditions.

HAPS-SMBS for covering unpredictable user events

Unexpected and temporary events such as thunderstorms can lead to network congestion, especially in crowded cities. In these circumstances, the proposed HAPS-SMBS architecture can provide additional coverage via additional spot beams in order to support instant capacity requests in densely populated areas.

HAPS-SMBS as an aerial DC

HAPS-SMBS will enable aerial DCs providing a backup computational facility, when and where the ground infrastructure fails to function, or to support agile computational offloading, moving computations at the network edge near the end user as the user terminals do not have sufficient computational power.

⁶FSO is an optical communication technology in which data is transmitted by propagation of light in free space allowing optical connectivity. There is no requirement of the optical fiber cable. Working of FSO is similar to optical fiber cable networks but the only difference is that the optical beams are sent through free air instead of optical fiber cable cores that is glass fiber [66].

HAPS-SMBS for defeating coverage holes

Coverage holes are encountered when the terrestrial user equipments in an area experience insufficient Signal-to-Interference-plus-Noise Ratio⁷ (SINR) from a terrestrial BS to run a high data rate application due to the blockage of physical obstructions [68]. Since these blockage effects become more severe for mmWave cellular networks, a HAPS-SBMS can supplement the existing terrestrial networks, steering a beam to the targeted direction. Through their physical advantages, HAPS-SMBS can perform 3D beamforming that enables the creation of separate spot beams in the three-dimensional space at the same time for different users.

HAPS-SMBS for supporting and managing aerial networks

HAPS-SMBS can be equipped with processors capable of providing support for other air elements in the network with limited computational resources. Furthermore, such processors may be able to execute complex ML algorithms using as input all the data collected from large portions of the air network, in order to dynamically learn the state of the network, resources and topology and then control and manage them intelligently.

Moreover, these processors can be essential to manage the swarm of cargo drones that will likely disrupt the retail industry in the near future.

Another use may be to adopt HAPS-SMBS as an interface to provide seamless communication to LEO satellites, because having a larger footprint than terrestrial gateways it can cover more LEO satellites at the same time.

HAPS-SMBS for supporting Intelligent Transportation Systems

Intelligent Transportation Systems (ITS) together with the advent of autonomous and connected vehicles are two paradigms that will forcefully enter everyday life. Although these paradigms are still very much studied topics by academics and industries, there is still no single communication network solution capable of supporting data traffic requirements. Huge data fusion and processing are key requirements for such applications, but vehicles are unable to process this data in

⁷The definition of SINR is usually defined for a particular receiver (or user). In particular, for a receiver located at some point x in space (usually, on the plane), then its corresponding SINR given by

$$SINR(x) = \frac{P}{I + N}$$

where P is the power of the incoming signal of interest, I is the interference power of the other (interfering) signals in the network, and N is some noise term, which may be a constant or random. The SINR is often expressed in decibels or dB.

a very short time given their limited capabilities. For this, HAPS-SMBS can be an effective solution, as data from vehicles can be offloaded and processed in the cloud. However, a problem could arise from the high mobility of vehicles, which would interrupt offloading due to frequent handover. Fortunately, a HAPS-SMBS offers coverage over a large area, which would eliminate frequent handovers and offer a broad view of the vehicle fleet, which is an essential element in coordinating vehicle-to-everything communications.

The potential of using the HAPS-SMBS system in ITS has been explicitly stated in the case of platooning of cars or trucks. As stated in [69], platooning of cars or trucks is one of the most relevant applications of autonomous driving, since it has the potential to greatly improve efficiency in road utilization and fuel consumption. These methods for jointly driving and coordinating a group of vehicles traveling together on the same route have the aim of making the use of the road network more efficient and less congested and optimizing consumption. Although traditional network architectures for vehicle platooning are distributed, i.e. the computational capacity is shifted aboard the vehicle fleet in order to ensure direct vehicle-to-vehicle communications, through the development of Multi-access Edge Computing (MEC) there is a tendency to shift the computational load to centralized structures, for example by exploiting the BSs and implementing a centralized platoon controller. From this point of view, the use of HAPS-SMBS would guarantee both a greater exploitation of the centralized computational capacity and a more extensive visibility given by a larger footprint than that of a BS, allowing greater control over the moving platoons in that certain area and a reduction in handover problems.

2.2.5 HAPS implementation regulations

In the recent deployments, HAPSs have been frequently deployed at 17 or 18 km above the ground [70]. Countries determine the maximum altitude of controlled airspaces, and a typical value is 20 km [71].

The regulations referring to HAPSs are divided into two aspects: (i) aspects related to aviation, managed by the International Civil Aviation Organization (ICAO); and (ii) aspects related to the spectrum, managed by the ITU.

Regarding aviation regulations, although the regulations are still in progress, the ICAO establishes a clear difference between aerostatic and aerodynamic platforms, particularly in relation to RT management. Therefore, the regulations are implemented in accordance with the specifications of the developed project and with the rules of the national civil authorities of each country. Therefore, it is essential to develop a set of regulations on an international scale for a large-scale deployment of HAPS.

Regarding spectrum regulation as reported in recently published reports by ITU [72, 73, 74], it is concluded that a bandwidth of 396 MHz to 2969 MHz is needed for

the ground to HAPS links. A bandwidth of 324 MHz to 1505 MHz is determined as necessary for the HAPS to ground links. At World Radiocommunication Conference 2019, it is agreed to append the 31 - 31.3 GHz, 38 - 39.5 GHz bands for the HAPS usage, in addition to the already dedicated 47.2 47.5 GHz and 47.9 48.2 GHz bands for worldwide usage. These bands will be used in addition to the previously dedicated International Mobile Telecommunications bands in the 2 GHz and the 6 GHz bands.

2.3 The current situation of HAPs projects

Between the 1990s and the 2000s many projects were developed to explore the potential of the application of HAPs for both the telecommunications field and remote sensing [70]. However, among the projects developed in those years, only very few have had continuity. Instead, in recent times there has been a renewed interest in the development of new projects more focused on the field of telecommunications, but with some projects that focus on the development of platforms for varying applications [75].

2.3.1 An up-to-date review of HAPs projects

The first flights into the stratosphere were made in the 1930s, using pressurized aluminum capsules attached to a large hydrogen balloon manned by pioneers such as the Swiss physicist Auguste Piccard [76]. The first experimental project specifically linked to a HAP dates back to 1969 when the US Navy supported the Raven company in the construction of the High Platform II. It was an unmanned airship that was intended to analyze the feasibility of such platforms for high-altitude reconnaissance. The platform had a length of 25 m, a weight of 62 kg, an electric propulsion powered by a propeller and a power of 300 W provided by solar cells. The test trip was carried out in 1970: the duration was about an hour and a half and the airship reached an altitude of about 21 km.

In the last 20 years, many research and development projects on HAPs have been carried out, but the majority were unsuccessful as they were initiated by small or medium-sized enterprises or by start-ups. Furthermore, since 2000, the number of publications dealing with HAP has significantly increased. In [70], the authors supported a bibliometric analysis, showing that in the world, excluding China, 850 publications were written in 2015 alone, compared to 600 in 2010. It is expected that the market on HAPs will continue to grow at an annual rate of 8.7% by 2023 [77].

In recent years there have been significant developments in the design and structure of the platforms, in addition to developments in the efficiency of the

solar cells of the energy system, in the antenna system, in wireless communication techniques, in applications and also in business models. An up-to-date review of the HAPs projects is listed below.

SHARP

The idea for SHARP [78] was first conceived in 1980 and it was approved in 1982 by the Canadian Department of Communications. The SHARP concept envisages the use of pilotless airplanes as aerodynamic platforms for relaying telecommunication signals, providing surveillance and monitoring services. The airplanes would circle slowly for many months at an operating altitude of 21 kilometres and relay signals within a diameter of 600 kilometres. Microwave power would be transmitted from a large ground antenna system to a circling airplane and the power beam would be accurately focused onto the airplane. On October 7, 1987 the first public demonstration occurred in the presence of the Minister of Communications and the press. This flight was recognized as being the first of its kind by the Fédération Aéronautique Internationale and it demonstrated successful communication for one hour flight duration.

ERAST

The United States ERAST Program was initiated in 1994 and conducted by NASA in conjunction with industry, and it aimed to develop and demonstrate technologies that enable an aircraft at high altitude to perform long-duration missions for environmental monitoring. AeroVironment produced a family of three unmanned solar energy aerodynamic platforms: (i) Pathfinder; (ii) Centurion; and (iii) Helios. These platforms reached altitude records with the Pathfinder (21.48 km, 1997) and Helios (29.52 km, 2001) [79], while in 2002, Pathfinder Plus demonstrated the communication of high-definition TV signals, 3G mobile voice, video and data, and high-speed internet connectivity. Due to a high demand for unanswered funds, the ERAST Program was closed in 2004.

Japan's Stratospheric Platform and SkyNet

Studies of Japan's Stratospheric Platform Program started in 1998 with the objective to develop a system based on a large, unmanned, solar powered stratospheric airship that could maintain a geostationary position at about 20 km altitude and conduct a long duration mission to deliver a variety of telecommunications and Earth observation services via the SkyNet telecommunication infrastructure [80]. Two different sub-scale test vehicles were flown in 2003 and 2004: an unpowered balloon made a single flight in 2003, reaching an altitude of 16 km, and a low altitude

airship made eight flights in 2004. After failing to get financial support to develop the first full-scale airship, the program was terminated in 2005.

CAPANINA

The European Union CAPANINA project ran between 2003 and 2006 with the main goal to develop low-cost HAPs capable of providing coverage to users including users travelling at speeds up to 300 km/h using an optical backhaul. The project was coordinated by the United Kingdom's University of York. The test to validate communication links between the RF and the FSO communication system was done on August 31, 2005: the balloon, flew at 22-26 km altitude, covering an area of 60 km radius, and the systems worked well and the customers were satisfied with the test results, which showed the equipment's ability to operate at high altitudes [81].

X-station

X-station is a HAP developed since 2005 by the Swiss company StartXX. The X-Station's first business application was to be an airship platform for delivering 3G/4G wireless communications and digital broadcasting services. At its operating altitude of 21 km, the X-Station would have a service area about 1,000 km in diameter for delivering different communication technologies such as TV and radio, broadcast, mobile telephony, VoIP, remote sensing, and local GPS. It uses solar energy and batteries, supports 100 kg payload for up to one-year flight duration [82].

Elevate

Elevate is a balloon developed since 2009 by the Spanish company Zero 2 Infinity [83]. It is a transportation service to lift payloads in the stratosphere for testing and validation of new technologies. The vehicle can carry up to 100 kg for about 24 hours flight endurance.

Loon

Project Loon, from Google, started in 2012 and has the objective to create a network of stratospheric balloons to provide Internet access in remote area and to connect people everywhere using a network of HAPSs. The flight altitude is about 20 km, lasting up to 100 days, using energy from solar panels. The idea is to launch a constellation of several balloons, forming a ring at determinate latitude. Several tests have been conducted with the release of dozens of balloons, in places like New Zealand, Australia and northeastern Brazil. In February 2016, following

an agreement with the government of Sri Lanka, Google started tests to provide Internet access services in the country using the Project Loon balloons, in a joint work with local operating companies. Another important event in 2016, in Puerto Rico, was the test of an autolauncher crane specially built for the project, enabling the launch of a balloon in just 30 minutes [84].

Zephyr S

In 2013, Astrium, currently Airbus Defence and Space, purchased the Zephyr Project from QinetiQ. Airbus is developing the Zephyr S version (single-tail), formerly Zephyr 8, keeping the payload in 5 kg, but with greater autonomy by the use of new solar cells and batteries and structural weight reduction. It is the world's leading solar-electric stratospheric UAV, with a wingspan of 25m and weighs less than 75kg. In February 2016, Airbus received from the United Kingdom's Ministry of Defence a request for the production and operation of 2 Zephyr S: this is the first contract in the world for providing an operational HAP. Zephyr's maiden flight in 2018 exceeded performance expectations, confirming the significant potential that the platform design offers. With evolutionary development in the Zephyr DNA, work is underway to offer incremental enhancements to Zephyr-S tailored to customer payload and geographical performance requirements [85].

Aquila

The Aquila UAV, developed from 2014 by Facebook, is a flying wing with a wingspan of 42 m and a total weight of about 400 kg. The aircraft has four propellers driven by electric motors, with power supplied by solar cells during the day and rechargeable batteries at night. The Aquila will fly between 18 and 27 km altitude, for a period of 3 months. It will be taken to the stratosphere by a helium balloon. It is expected the use of a laser connection to form a high-speed communications network. In case of obstruction by clouds, a radio connection will be used with some reduction in data rate [86]. More test flights have been conducted to retrieve as much data as possible, but in June 2018 Facebook decided to stop its program to work with partners like Airbus on HAPS connectivity and their technologies like flight control and high-density batteries [87].

Stratobus

The Stratobus project is led by the Franco-Italian firm Thales Alenia Space and it started in 2016. The Stratobus is a stratospheric, autonomous, solar-powered, non-rigid airship intended for use as a pseudo satellite at a geostationary position at 20 km altitude where it can perform a variety of functions, including Intelligence Surveillance and Reconnaissance (ISR), communications, environmental monitoring

and navigation [88]. A key point that makes Stratobus airships particularly interesting in the field of NTN, is that they are designed to communicate with ground stations, satellites in orbit and other Stratobus airships to form an extended airborne network. For this reason, its technical characteristics have been taken into consideration for modeling the simulated HAPS in this thesis work and some further considerations are made in Section xx.

Hawk30

Since 2017 HAPSMobile, which is a subsidiary of the Japanese SoftBank holding planning to operate HAPS networks, is developing the Hawk30 solar-powered unmanned aircraft for stratospheric telecommunications. The Hawk30 design is a development of the NASA Pathfinder and NASA Helios high-altitude, long-endurance unmanned aircraft built by AeroVironment for NASA. Its objective is to provide 4G LTE and 5G direct to devices over a 200 km diameter area, and 40 aircraft could cover the entire Japanese archipelago. It should be interoperable with terrestrial cell towers to expand their coverage and as a proxy for the SoftBank-backed OneWeb satellite constellation, when it is not suited for providing links directly to devices. On 21-22 September 2020, the HAPSMobile Hawk30 (rebranded as Sunlider) flew 20 hours from Spaceport America, and reached an altitude of 19.1 km on its fifth demonstration flight. It tested the long-distance LTE communications developed with Loon for standard LTE smartphones and wireless broadband communications [89].

PHASA-35

PHASA-35 is a UAV developed by United Kingdom's BAE Systems in collaboration with Prismatic. Designed as a cheaper alternative to satellites, the aircraft can be used for surveillance, border control, communications and disaster relief with a potential ability to stay airborne for up to 12 months. Developed in less than two years, the aircraft carried out its first flight in February 2020 and further trials are currently ongoing. In January 2021, BAE Systems announced plans to carry out a flight demonstration in the United States after acknowledging strong growing interest in the aircraft from across the U.S. Department of Defense and federal agency customer base [90].

Skydweller

In November 2019, the Italian company Leonardo S.p.A. announced that it has invested in Skydweller Aero Inc., a US/Spanish start-up specializing in solar-powered remotely piloted aircraft [91]. The initiative will lead to the development and use of the Skydweller drone, the first remotely piloted solar-powered aircraft capable

of carrying large loads with unlimited persistence in flight. Compared to existing systems, Skydweller combines unique characteristics of persistence and range with the flexibility typical of an airplane. It will be able to operate from air bases located all over the world, covering unlimited distances in areas characterized by any environmental condition. This innovative platform will be used for purposes ranging from land and sea surveillance to environmental and infrastructure monitoring, from geo-information services to telecommunications and precision navigation. The system can be rapidly deployed to provide communications to support operators in emergency and disaster situations. In April 2021, a successful flight demonstration was carried out, with particular focus on the aircraft's initial control, actuation and sensor systems, following rigorous software design, installation and ground testing [92].

2.3.2 The technological challenges of HAPs

The design of an aircraft that must operate in the stratosphere like a HAP imposes some technological challenges such as: (i) lightweight structures; (ii) energy generation and storage; (iii) thermal management; and (iv) operations at low altitudes. Regarding the structure, it should be emphasized that at an altitude of about 20 km the air is thin, with a density of about 7% of that above sea level. For this reason, in the case of aerostatic structures, typically lighter than air, the envelope material must have low weight characteristics, high strength, high ability to withstand damage, low permeability to lifting gas, maintain flexibility at low temperature and low degradation with UV radiation and ozone [93]. Also for aerodynamic platforms, lightweight structures are essential: a typical wing structure of a HAP airplane consists of tubular spar and ribs using composite material (carbon fiber), rigid foam leading edge and plastic film skin [79]. The weight of various components of a HAP airplane is distributed along the wingspan to reduce the structural stress on the wing. These optimized structures for high-altitude flights have the disadvantage of fragility at gust conditions found at lower altitudes.

Energy generation and storage also present numerous challenges: like all aircraft, HAPs require a power source for the propulsion system and the supply of electricity to their systems and payload. The most commonly adopted solution for very long life HAP is, during the day, solar energy converted into electrical energy by photovoltaic (PV) cells, and part of this electrical energy is used to charge a storage system. Although with promising advantages, it was one of the greatest technological challenges: to date there are no standardized consumption models applicable even in the simulation phase.

Thermal management and operation at low altitudes are two minor challenges than the previous two. Thermal management research should be intensified since the temperature influence can be in aerostatic lifting force or internal pressure, in the

case of super-pressure airships. While, an important point in the HAPs operation at low altitude, especially in phases of launch and recovery, is the choice of weather windows where the weather conditions are appropriate.

Chapter 3

Methodology

In this Chapter the methods used to carry out the simulations of this thesis work are discussed, with particular attention to what and how certain choices were made, in order to be able to evaluate the reliability and validity of this research.

Section 3.1 introduces the basic configuration of the simulated scenario, in order to give some information related to the composition of the scenario itself and motivate why some choices have been made with the aim of reaching the goal.

Section 3.2 provides information on the mobile traffic zones considered in the city of Milan and suburbs, with particular focus on the sample clusters considered.

Section 3.3 describes the structure of the terrestrial BSs, while Section 3.4 discusses the choices made for simulation of the HAPS object.

Section 3.5 explains the definition of the strategies used in order to reduce the cluster energy consumption, providing some examples of the used pseudo-algorithms. Furthermore, the different simulated scenarios are defined in detail.

Finally, Section 3.6 defines how the simulator is structured, which tools and material were used, and how the data were collected and analyzed.

3.1 Basic scenario configuration

In this thesis work a portion of a future generation RAN is analyzed, in which we imagine to integrate the ground network infrastructure of a densely populated area with an air network formed by one HAPS, which performs as a HAPS-SMBS. A representation of this scenario is represented in Figure 3.1.

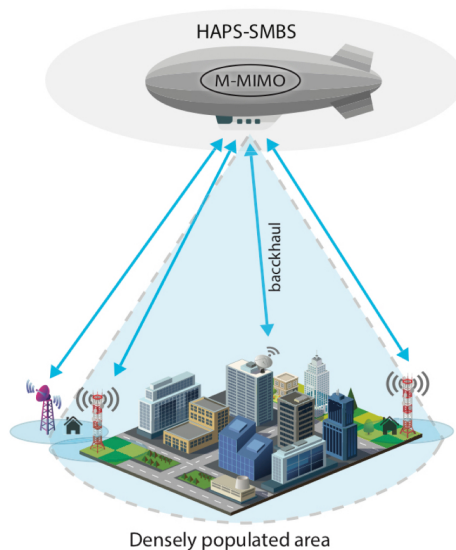


Figure 3.1: A representation of the basic scenario configuration [64]

We envisioned to offer coverage for 16 traffic zones of the city of Milan (Italy) through the use of a single HAPS equipped with Massive-MIMO¹ (M-MIMO) technology, i.e. capable of offering a coverage beam for each of the traffic zones. Furthermore, each traffic zone (or service area) consisted of a cluster comprising a macro BS which defines a cell within the entire service area, and 6 micro BSs which define small cells which provide additional capacity to the inside the coverage area of the macro cell, when the traffic demand is close to the peak.

In order to achieve the goal of reducing the energy consumption of the ground infrastructure by adapting the network capacity to the traffic demand, different reduction strategies have been used. Therefore it was observed if and how the use of an aerial support structure is actually useful to increase the power saving without affecting the QoS.

In the following sections, the data relating to the configuration of the simulated objects and the energy reduction strategies used are analyzed in detail.

¹M-MIMO is a type of technology applied to wireless communications in which base stations are equipped with a large number of antenna elements to increase energy and spectral efficiency. M-MIMO systems typically feature tens, hundreds, or even thousands of antennas in a single antenna array. Other technologies, such as beamforming and space multiplexing, allow M-MIMO to be one of the key technologies for current 5G NR systems and future communication systems [94].

3.2 Traffic zones

The considered scenario foresees the presence of a HAPS placed at an altitude of 20 km from the ground and able to provide coverage over a large area, e.g. with a diameter greater than 40 km, by means of a number of smaller cells between 40 and 100 with a radius of between 2 and 3 km. In light of these considerations, it was hypothesized to cover a high-density urban area such as the city of Milan (Italy), through 10 beams or even more considering the suburbs as well. A scheme of the assumed urban area is shown in Figure 3.2.

More specifically, 16 traffic zones that include urban and suburban areas of the city of Milan were considered: the traffic data used in this work were provided by a large Italian Mobile Network Operator (MNO). These data report the hourly traffic volume of the BSs contained in a sample cluster for each of the 16 traffic zones, for a total duration of approximately 2 months. These areas were selected for being different in terms of surface extension, typical activities and traffic patterns, in order to have a quite representative vision of the various zones that coexist in a urban area. For the sake of simplicity, it was hypothesized to offer a distinct coverage cell from the HAPS for each of the 16 zones, in order to have a one-to-one correspondence between cell and traffic zone.



Figure 3.2: A representation of the coverage of the urban area of Milan (Italy)

3.2.1 Sample clusters

A traffic zone comprises 12 clusters made up of 1 macro BS and 6 micro BSs, i.e. each cluster contains 7 cells. In this work, it was decided to consider a sample cluster for each of the 16 traffic areas, thus having a total number of 112 cells (and

therefore BSs) distributed in 16 clusters representative of their traffic area. To get an idea of the distribution and size of the sample clusters over the city of Milan, it was decided to trace the grid of the BS cells on the map. This result was obtained starting from the EPSG:4326² coordinates of the cell vertices and plotting these vertices on Google Maps using the Python gmpplot library [95].

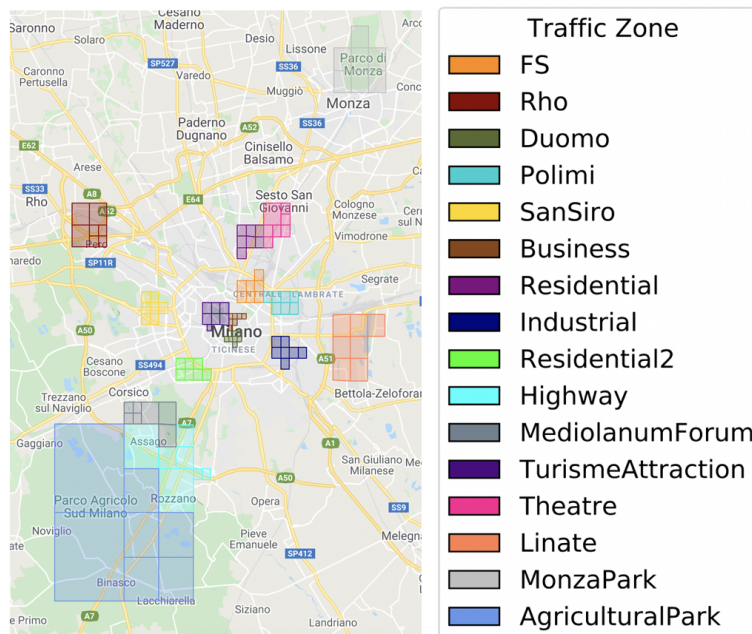


Figure 3.3: The map of the considered traffic zones over the city of Milan (Italy)

As can be seen from Figure 3.3, the distribution of traffic areas is wide, allowing the analysis of the city of Milan and its suburbs. In addition, the traffic zones are very different from each other. In the business area (brown) and industrial area (dark-blue) traffic peaks are observed in the central (or working) hours of the day, while in the residential area (purple and light-green) traffic increases during the evening as it follows the typical behavior of people in their daily life. Other areas such as San Siro (yellow), in which there is a famous football field, Rho (dark red), in which there is an area that hosts major events, Theatre (magenta) and

²European Petroleum Survey Group (EPSG) Geodetic Parameter Dataset (also EPSG registry) is a public registry of geodetic datums, spatial reference systems, Earth ellipsoids, coordinate transformations and related units of measurement. Each entity is assigned an EPSG code between 1024 and 32767. With EPSG:4326 it is intended the WGS84, which is the latitude/longitude coordinate system based on the Earth’s center of mass, used by the GPS among others.

Mediolanum Forum (dark-grey) have traffic activities that depend on the possibility that events are held or not, so the traffic is bursty and variable. The Duomo di Milano (dark-green) and Tourism Attraction (violet) are tourist areas, with high traffic throughout the day. The FS (orange) area hosts the Milano Centrale train station while the Linate (light-coral) area hosts the Milano Linate airport, therefore they are characterized by high activity levels as they are very crowded areas. The Politecnico di Milano (dark-cyan) area hosts a large campus with several students, especially during working hours. Finally, Highway (cyan), Monza Park (light-grey) and Agricultural Park (cerulean) are traffic areas in which the traffic is not very intense given the small number of people present inside them.

The previous overview of traffic zones was useful to understand how in the area considered there are different classes of traffic data with different QoS constraints, linked to the requirements of speed, latency and computing capacity, where by traffic data classes we mean data deriving from mobile, vehicular or massive IoT communications.

3.3 Structure of the BSs

Each cluster is made up of 1 macro BS and 6 micro BSs: the macro BS defines the cell for the entire service area, while the micro BSs offer additional capacity. The cluster is powered by a series of PV panels³ and an energy accumulator, i.e. a series of batteries: the cluster uses the RE generated by the PV panels and in the event that the energy produced is greater than the energy required by the BSs, the difference in energy is stored in the batteries; conversely, if the BSs require more energy than that supplied by the PV panels, the difference in energy is taken from the batteries. In the simulator, the series of PV panels and the series of batteries are treated as single elements having the task of powering the 7 BSs of the cluster. In the rest of this thesis work, the pair formed by the PV panel (PV) and the battery (B) will be abbreviated with the writing (PV,B), which represents the RE part. Furthermore, if the energy generated by the PV panel and that stored in the battery is not sufficient to power the BSs, the difference in energy is taken from the public electricity grid. It follows that one of the main objectives of this work was to minimize the consumption of energy taken from the grid, in order to obtain

³PV panels absorb and convert shortwave solar irradiance into DC electricity to charge batteries and operate BSs. A 1-kWp PV panel typically has a 5 m² area, and the lifetime of a typical PV panel may exceed 25 years [96]. The power generated by a PV panel can be influenced by several factors, such as the DC rating of the PV panel, the tilt angle of the PV panel, and the geographic location or solar irradiation profile of the site at which the panel is located [97]

a reduction in the cost of energy. The cluster is schematized in Figure 3.4.

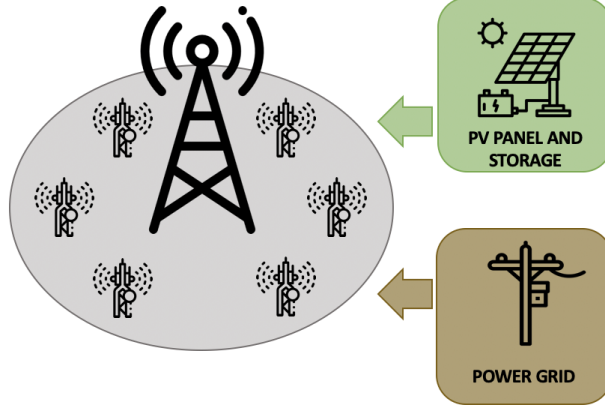


Figure 3.4: A cluster formed by 1 macro BS and 6 micro BSs powered by (PV,B) and power grid

In this work, assuming a PV panel efficiency equal to 16%, a 1-kWp PV panel requires an occupancy area of 5 m² [98]. Lead-acid batteries with a size of 20 kWh were considered for energy storage. A maximum Depth of Discharge of 70% was considered in this study and losses of 15% in energy efficiency due to the charging and discharging process were considered.

We used consumption models for BSs taking as a reference what the authors suggested in [99]. The proposed linear model is made explicit by the formula:

$$P_{in} = N_{trx} \cdot (P_0 + \Delta_p P_{max} \rho), \quad 0 \leq \rho \leq 1 \quad (3.1)$$

The model in 3.1 expresses how the trend of the input power (P_{in}) necessary for the operations of the BSs, linearly depends on the number of transceiver (N_{trx}), on the power consumption when the RF power is zero (P_0), the gradient of the load dependent power consumption (Δ_{in}), the maximum RF output power at maximum load (P_{max}) and the traffic load (ρ^4). More in detail, the power model parameters for both BS types are summarized in Table 3.1.

⁴It should be emphasized that the traffic load turns out to be

$$\rho = \frac{P_{out}}{P_{max}}$$

where P_{out} is the relative RF output power.

Table 3.1: Power model parameters for both BS types

BS Type	N_{trx}	$P_{max}[\mathbf{W}]$	$P_0[\mathbf{W}]$	Δ_p
Macro	6	20	130.0	4.7
Micro	2	6.3	56.0	2.6

Finally, we have assumed a maximum bitrate for each of the BSs (both macro and micro) equal to 150 Mbps: the reason why this value has been assumed will be explained later in Section 3.4.

3.4 Structure of the HAPS

In the simulator, we envisioned the presence of a single HAPS (i.e. an airship) able to cover all 16 traffic zones through the use of M-MIMO technology. As for the ground infrastructure, HAPS was also powered by a series of PV panels and a series of batteries. In this case, however, since there is no specific energy consumption model for an aerial platform in the literature and considering the huge surface available on the HAPS to host PV panels, we hypothesized that the RE is always available in sufficient quantity on HAPS and the only limit is the HAPS band capacity.

Regarding the HAPS band capacity, we assumed that the HAPS coverage radius is equal to 50 km, from which a total area covered by the HAPS of about 7850 km², and that the total HAPS capacity was equal to 30 Gbps. Based on the ITU report [54], in order to provide continuous coverage, we assumed a very high number of cells, equal to 256 cells. Therefore, each cell can cover an area of about 30 km²⁵ with a single cell capacity of about 117 Mbps⁶. However, we assumed to have a lower number of cells with higher capacity each.

⁵Since the total surface is $S_{tot}=7850$ km² and the number of cells is $N_{cell}=256$, we have the surface covered by one single cell

$$S_{cell} = \frac{S_{tot}}{N_{cell}} \approx 30 \text{ km}^2$$

⁶Since the total HAPS capacity is $C_{tot}=35$ Gbps and the number of cells is $N_{cells}=256$, we have the single cell capacity

$$C_{cell} = \frac{C_{tot}}{N_{cells}} \approx 137 \text{ Mbps}$$

The capacity is provided for each cell by one or more HAPS beams, that are properly directed to cover the area served by each cell. Each cell provides coverage over an area having a surface of about 30 km². Therefore, as it is possible to observe in Figure 3.5, knowing that the surface covered by the city of Milan and its suburbs is approximately equal to 560 km², the number of cells useful to cover Milan and its suburbs is equal to 19 ⁷.

Finally, each of the 19 BS cells in Milan and its suburbs could contain about 12 clusters of 1 macro BS and 6 micro BSs each, and, in case of uniform distribution of capacity, each cell can provide 1.8 Gbps ⁸ in the covered traffic zone. Therefore, the available bandwidth per cluster is equal to 150 Mbps ⁹. This value corresponds to the actual maximum capacity of each BSs (both macro and micro).

⁷Since the total surface of Milan and its suburbs is $S_{tot}=560$ km² and the surface covered by one single cell is $S_{cell}=30$ km², we have the number of cells useful to cover Milan and its suburbs

$$N_{cell} = \frac{S_{tot}}{S_{cell}} \approx 19$$

⁸Since the total HAPS capacity is $C_{tot}=35$ Gbps and the number of cells is $N_{cells}=19$, we have the single cell capacity covering one traffic zone

$$C_{cell} = \frac{C_{tot}}{N_{cells}} \approx 1.8 \text{ Gbps}$$

⁹Since the single cell capacity is $C_{cell}=1.8$ Gbps and the number of clusters in one zone is $N_{clusters}=12$, we have the cell capacity covering one cluster

$$C_{cluster} = \frac{C_{cell}}{N_{clusters}} = 150 \text{ Mbps}$$

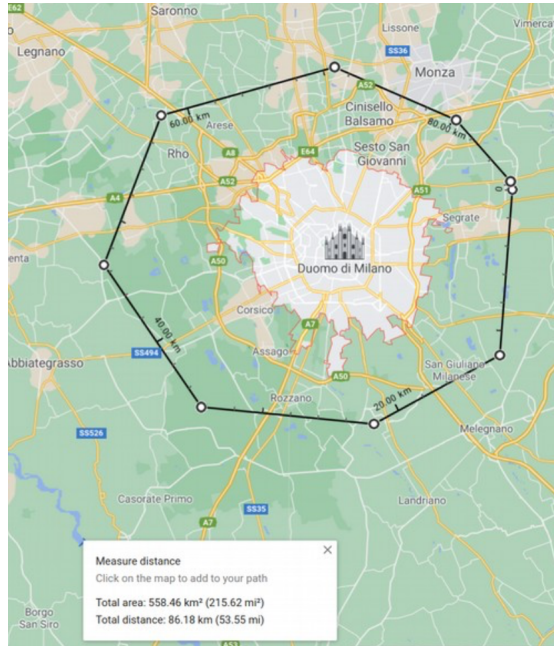


Figure 3.5: The coverage surface of the city of Milan and its suburbs

3.5 Definition of strategies for reducing energy consumption

In order to reduce energy consumption, preferring the use of RE rather than exploiting the energy deriving from the grid, we have considered two strategies: (i) Resource on Demand (RoD); and (ii) HAPS Offloading.

The RoD strategies allow to dynamically adapt the available radio resources according to the real instantaneous traffic demand of the network [100], limiting the presence of redundant radio resources for considerable times, hence adapting the network energy consumption the actual volume variations. In our case study, the RoD strategy is applied by turning off unnecessary micro BSs when the load deriving from user requests is low. More in detail, the RoD strategy applied in this thesis is proposed in [101]: in case of low traffic (i.e., lower than a threshold), one or more micro BSs are turned off, and their traffic is moved to the macro BS, as long as the macro BS has enough capacity to handle the traffic. The load threshold (ρ_{min}) is set equal to 0.37, according to what suggested in [101].

In practice, the RoD strategy can be summarized through the following pseudocode.

Algorithm 1 : RoD strategy

```

1: for  $t = 1, T$  do                                ▷ for each time step
2:   for  $\mu = 1, m$  do                                ▷ for each micro BS
3:     if  $\lambda_\mu^t < \rho_{min} \cdot C$  and  $C_M^t + \lambda_\mu^t \leq C$  then
4:        $\lambda_\mu^t \leftarrow 0$                                 ▷ turn off the micro BS
5:        $C_M^t \leftarrow C_M^t + \lambda_\mu^t$                 ▷ move traffic to the BS macro
6:     end if
7:   end for
8: end for

```

The following notations have been used in the pseudocode: λ_μ^t indicates the traffic managed by the micro BS μ at time step t , C_M^t indicates the currently capacity used by the macro BS up to time step t , and C indicates the maximum capacity of the macro BS.

The HAPS Offloading strategy is the aerial counterpart of the RoD strategy: since the main topic of this thesis concerns the analysis of future communication networks with the implementation of aerial platforms, when this strategy is selected, we have chosen to assign a priority to HAPS for the offloading of mobile traffic, even if the macro BS still has some capacity available. Using this strategy we offload some traffic from the micro BSs to the HAPS, depending on QoS requirements based on traffic types. For instance, we can move high bandwidth demanding traffic in order to avoid congestion in the terrestrial network and make it available for critical communications, or we can shift popular content, since the HAPS has huge coverage and it can store contents, to limit duplicates in multiple locations still having a reasonable delay. It is useful to underline that in this thesis no distinction was made on the type of traffic data, but we have chosen to transfer all the traffic that can be transferred to the HAPS.

If the HAPS cell capacity is saturated, the remaining traffic can be shifted to the micro BS, as long as the RoD conditions for traffic offloading are respected.

When the HAPS Offloading strategy is applied, two different behaviour modes of the beams were analyzed: (i) constant beam; and (ii) dynamic beam. In the case of constant beam, the capacity provided by the HAPS beam (or beams) within each cell is fixed a priori at the start of the simulation and remains so for the entire simulated period. Conversely, in the case of dynamic beam, the capacity of the beams varies dynamically over time: it is reduced by a given fraction (χ) if the traffic is below a certain threshold (τ), in order to adapt the beam capacity to traffic conditions. In the latter case, an analysis was carried out to select the optimal

values of the reduction fraction of the maximum beam capacity and threshold: the results will be shown in the next chapter. These two modes of beam behavior were analyzed in order to gain insight into if and how the application of energy reduction strategies affects QoS.

In practice, the dynamic beam algorithm can be summarized through the following pseudocode.

Algorithm 2 : Dynamic beam

```

1: for  $t = 1, T$  do                                ▷ for each time step
2:    $\Lambda^t \leftarrow \lambda_M^t$ 
3:   for  $\mu = 1, m$  do                                ▷ for each micro BS
4:      $\Lambda^t \leftarrow \Lambda^t + \lambda_\mu^t$ 
5:   end for
6:   if  $\Lambda^t \leq \tau \cdot C_c$  then
7:      $C_b^t \leftarrow \chi \cdot C_b^t$                     ▷ reduce the max beam capacity
8:   end if
9: end for

```

The following notations have been used in the pseudocode: Λ^t indicates the traffic managed by the cluster at time step t , λ_M^t and λ_μ^t indicate the traffic managed by the macro BS and the micro BS μ at time step t respectively, C_c indicates the maximum capacity of the cluster, and C_b^t indicates the capacity of the HAPS cell at time step t .

In all the performed simulations, we have chosen to always assume that the RoD strategy for ground BSs is applied, with the aim of evaluating how the HAPS Offloading strategy, if applied, affects the energy behavior and QoS of the analyzed clusters. Furthermore, unlike what happens for HAPS, where we assumed to have RE always present and available in sufficient quantity, for the ground network infrastructure we decided to simulate two complementary scenarios, that were with or without RE supply. If the RE supply on the ground was not taken into consideration, the cluster was powered only through the power grid and therefore we had $(PV, B) = (0,0)$. Vice versa, with the presence of RE supply on the ground, the cluster was powered both by the green energy pair (PV, B) and by the power grid, i.e. the cluster had a scheme equal to the one presented previously in Figure 3.4. In the latter case, a detailed analysis of the effect of different dimensions of (PV, B) will be dealt with in the next chapter.

Therefore, four different scenarios have been considered: (i) NO RE scenario, in which only the RoD strategy was considered applied without the presence of ground RE supply; (ii) RE on Cluster scenario, in which only the RoD strategy with the presence of ground RE supply was considered; (iii) HAPS Offloading scenario, in which both RoD and HAPS Offloading strategies was considered, without the

presence of ground RE supply; and (iv) RE on Cluster + HAPS Offloading scenario, in which both RoD and HAPS Offloading strategies was considered, with the presence of ground RE supply. The four simulated scenarios are summarized in Table 3.2.

Table 3.2: Summary of the simulated scenarios

Scenario	Strategy		
	RoD	HAPS Offloading	Ground RE
NO RE	Yes	No	No
RE on Cluster	Yes	No	Yes
HAPS Offloading	Yes	Yes	No
RE on Cluster+ HAPS Offloading	Yes	Yes	Yes

3.6 Structure of the simulator

In order to investigate the potential benefits of using an aerial platform to move the traffic load from the BS to the ground in order to reduce energy consumption and improve services, we recreated the working environment through a simulator written in Python. The main structure of the simulator consists of a loop which, for each of the sample clusters of the 16 traffic zones, updates the conditions of the single cluster for each time step, based on the amount of traffic handled by each of the 7 BSs in the cluster, in that specific moment.

The time horizon of the time loop is 1463 hours, with a granularity of 1 hour, i.e. each time-step is 1 hour. More specifically, 60 days and 23 hours are analyzed, i.e. 8 weeks from Sunday to Saturday, 4 days from Sunday to Wednesday and 23 hours on Thursday.

3.6.1 Input data

In our study we used mobile traffic data provided by a large Italian MNO: they report the hourly traffic volume for each of the 112 BSs considered, in the city of Milan and suburbs, for a duration of 1463 hours in 2015. More precisely, the period considered runs from 00.00 on 1st March 2015 to 11.00 pm on 30th April 2015.

Moreover, to correctly map the position of the considered cell within the city of Milan or its suburbs, the information was obtained from text files which contained the data relating to the sample cluster considered for that specific cell. After having carried out a pre-processing of this information, it was possible to obtain the data relating to the coordinates of the vertices of the cells belonging to the traffic areas

and their relative surface.

After that, in order to have realistic data on the production of RE energy on the ground for the city of Milan, we used the database on the website of the PVWatts calculator [102], which offers the possibility of downloading a CSV file that contains the information of the parameters relating to hourly energy production.

Finally, to understand the economic impact deriving from the energy savings of the cluster, we used data on the price of energy taken from the website of the Italian Gestore dei Mercati Energetici (GME¹⁰) [103]. From GME it is possible to find various databases with historical data relating to the market of the day ahead, from 2004 onwards. We have chosen to consider three time periods: (i) spring 2015; (ii) winter 2021; and (iii) spring 2021. The first period was considered because it was equal to the period of the traffic data, while the others to see the price differences five years apart and in two different periods of the year.

3.6.2 Performance indicators

For each of the simulated scenarios, a CSV file was generated containing, among the others, the following three KPIs: (i) energy grid reduction; (ii) capacity demand ratio; and (iii) traffic fraction handled by HAPS.

The energy grid reduction of the cluster, is a KPI that allows us to understand the energy savings of a given cluster. More specifically, the energy grid reduction is calculated as the ratio between two factors a and b, where: (a) is the difference between the reference consumption of the cluster, i.e. the consumption that the cluster would have considering the RoD strategy not applied and the BSs powered only by energy taken from the grid, and the actual consumption of the cluster, considering certain strategies applied; and (b) is the reference consumption of the cluster. It is measured both as a percentage of energy savings and as an absolute energy value (i.e., in Wh).

The capacity demand ratio allows to evaluate the relationship between the total capacity offered to the users in the cluster area (including capacity, provided by both BS and HAPS) and the total real traffic demand. It is a KPI that gives an idea of how oversized the service is and if there are any untapped capabilities that

¹⁰GME is the company responsible in Italy for the organization and management of the electricity market, as well as for ensuring the economic management of adequate availability of the power reserve.

could improve the QoS.

The traffic fraction handled by HAPS gives information regarding the amount of traffic that is handled by the HAPS when the HAPS Offloading strategy is applied. This KPI is very useful to understand how much traffic is sent on HAPS in order to analyze the effects that this load shift brings in terms of energy consumption and QoS.

Other performance indicators will be evaluated in the next chapter, as they relate to simulations of particular cases.

Chapter 4

Results

This Chapter discusses the results obtained from the simulations performed. It is emphasized that the work environment has been simulated through a program written in Python language, that has been further deployed as part of the thesis work. The Chapter was structured in such a way as to clearly differentiate the two phases of our work.

Section 4.1 describes the results obtained during the first phase of the simulation, that is the parameter setting phase and the selection of basic configurations.

Finally, Section 4.2 shows the results obtained during the simulation phase, commenting and critically comparing the values of the KPIs obtained in the various scenarios modeled.

4.1 Sizing Phase

In this section, we compare the results obtained for the choice of the optimal values of the parameters that will be used in the subsequent simulation phase. The parameters analyzed were: (i) the size of the PV panels and of the battery (PV, B), in the case of presence of RE on the ground; and (ii) the threshold (τ) and the reduction fraction of the maximum HAPS cell capacity (χ), in the case of application of the HAPS Offloading strategy with Dynamic Beam. Furthermore, we carried out an analysis of the traffic patterns of the 16 traffic zones, in order to select 5 significant traffic zones, i.e. those zones with traffic statistics different from each other and on which the simulations were carried out.

4.1.1 Impact of the parameter (PV, B) on energy grid reduction

We now investigate the impact of the variation of the parameter (PV, B) on the energy grid reduction, taken as percentage of energy savings. In this analysis, only the scenarios in which the RE is present on the ground have been taken into consideration, namely: (i) RE on Cluster; (ii) RE on Cluster + HAPS Offloading with Constant Beam; and (iii) RE on Cluster + HAPS Offloading with Dynamic Beam. The range of variation of the parameter (PV, B) chosen was between (1, 1) [kWp, kWh] and (9, 9) [kWp, kWh], as it allows to observe the dynamics of the energy grid reduction behavior and allows to have a good trade-off between costs and autonomy of the system, as studied in [104]. To better catch the impact of the variation of the parameter (PV, B), the energy grid reduction was calculated on all 16 traffic zones.

From the three graphs in Figure 4.1, that report the grid energy reduction versus several different system sizes, in different traffic area and under various scenarios, it is possible to notice how each of the 16 traffic zones reacts differently to the variation of (PV, B)¹: this behavior is due to the fact that each of the traffic zones has a different traffic load and that the aerial extension of the zones is very different from each other, for example it goes from an extension of 69.14 km² of Agricultural Park to 0.56 km² of Duomo. Therefore, it is understandable how large dimensions of (PV, B) have a more relevant impact on the energy grid reduction of areas not very extensive. Then, with reference to a traffic area, it is noted that starting from a size of the PV panel set at 4 kWp, keeping the size of the PV panel fixed, there is an exponential increase in energy grid reduction as the size of battery B increases. This trend is positive, because it allows us to use larger battery sizes while keeping the size of the PV panel fixed, which has a considerable cost. Furthermore, it is possible to exploit this property in central urban environments (e.g., the Duomo area in the center of Milan) where the space available for the installation of PV panels is limited. Moreover, this behavior is at the basis of the reasoning according to which the application of the HAPS Offloading strategy in addition to the RoD strategy with RE on the ground improves energy savings. Let's take again the Duomo traffic zone as an example, which, as already defined, is a central urban area with a low surface area but with a high amount of traffic throughout the day, as it is frequented by many tourists. We have that by setting the dimensions of (PV, B) equal to (3 kWp, 4 kWh), which are realistic dimensions for this zone, the effect of adding

¹It is useful to remember that the power supplied by the PV panels is measured in kWp while the battery B capacity is measured in kWh.

the HAPS Offloading strategy is evident: we pass from an energy grid reduction of 47% in the RE on Cluster scenario to an energy grid reduction of 62% in the RE on Cluster + HAPS Offloading scenario with Dynamic Beam and 67% with Constant Beam. We therefore have an increase of up to +43% of the energy grid reduction in the case of both strategies applied, compared to the RE on Cluster alone.

This result leads us to conclude that in those areas that have limited space, it is possible to keep the dimensions of the PV panels relatively low, trying to increase the size of the batteries. Furthermore, the use of HAPS greatly improves energy savings and is an interesting solution not only for remote areas without ground infrastructure, but also for central urban areas with high traffic density but with little space available.

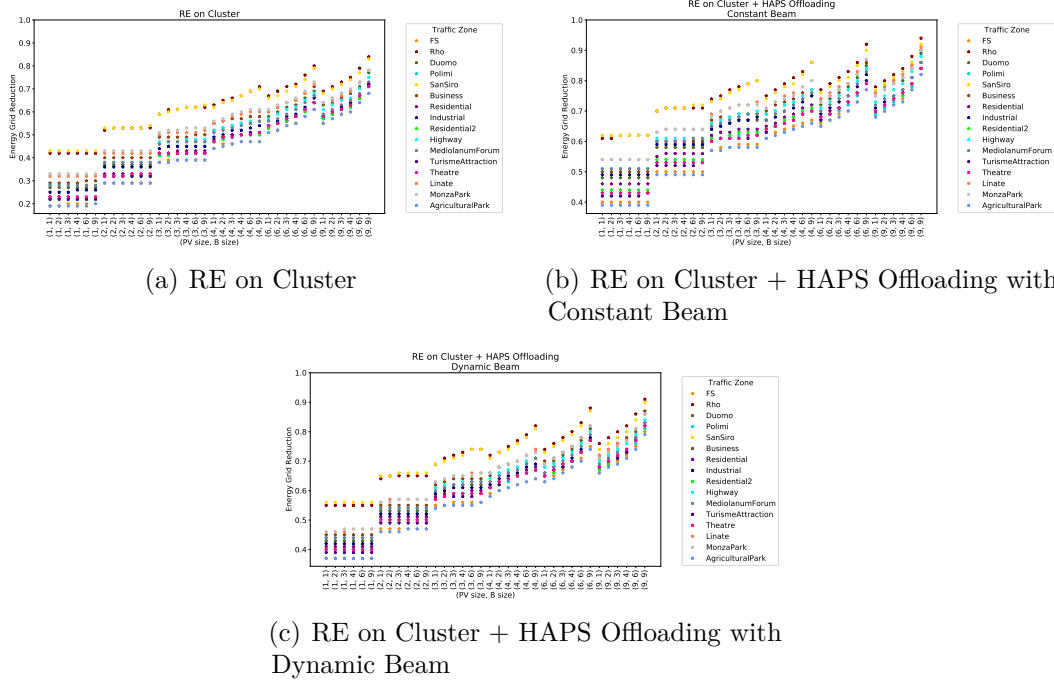


Figure 4.1: Variation of the energy grid reduction for the 16 traffic zones as the parameter (PV, B) varies

4.1.2 Analysis of the mean energy grid reduction for the selection of the standard configuration of (PV, B)

To limit the number of simulations, we chose to determine a standard size configuration of (PV, B) to be used in the subsequent analysis on the τ and χ parameters. Therefore, considering the RE on Cluster + HAPS Offloading with Dynamic Beam scenario, we calculated the energy grid reduction for each of the 16 traffic zones as the average of the energy grid reduction values obtained in the previous analysis and shown in Figure 4.1(c).

Looking at Figure 4.2, we have chosen three representative traffic zones, based on the mean energy grid reduction values: (i) Rho, because it has the highest mean energy grid reduction (i.e., 72%); (ii) Agricultural Park, because it has the lowest mean energy grid reduction (i.e., 56%); and (iii) Mediolanum Forum, because it has an average mean energy grid reduction (i.e., 62%). These three zones were considered as representative traffic zones also for the subsequent analysis of the τ and χ parameters.

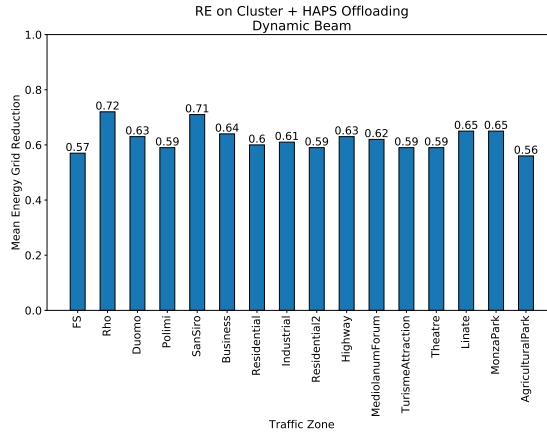


Figure 4.2: Mean energy grid reduction for each of the 16 traffic zones

Then, we collected the measurements of five different values of (PV, B) for the three representative traffic zones. The summary of this collection is presented in Table 4.1. Observing these results, we chose the 3 kWp dimensions for the PV panels and 4 kWh for the battery B, as the standard configuration for the subsequent simulations. This choice was made because the energy grid reduction values in the case of (PV, B) = (3, 4) [kWp,kWh] are close to the mean energy grid reduction value for the 3 representative zones.

Table 4.1: Energy grid reduction of the three traffic zones for different (PV, B)

Traffic Zone	(PV [kWp], B [kWh])				
	(2,3)	(3,4)	(4,3)	(6,6)	(9,6)
Rho	65%	73%	75%	83%	86%
Agricultural Park	46%	56%	61%	70%	74%
Mediolanum Forum	54%	62%	66%	75%	78%

4.1.3 Analysis of the variation of τ and χ parameters

We now analyze the impact of the variation of the threshold on the traffic load (τ) and the reduction fraction of the maximum HAPS cell capacity (χ) when the RE on Cluster + HAPS Offloading strategy with Dynamic Beam is applied. We measure this impact over the three KPIs explained in Section 3.6.2, i.e., energy grid reduction, capacity demand ratio, and traffic fraction handled by HAPS. Firstly, we decide to vary τ between the following discrete values: [0.1, 0.25, 0.37, 0.5, 0.75, 0.87, 1]; and to vary χ between the following discrete values: [0.25, 0.5, 0.75].

The summary of the first configuration of the simulations is presented in Table 4.2.

Table 4.2: Summary of the first configuration of the simulations for the analysis of the variation of τ and χ parameters

Scenario Beam Algorithm (PV, B)	RE on Cluster + HAPS Offloading Dynamic (3, 4)
τ	[0.1, 0.25, 0.37, 0.5, 0.75, 0.87, 1]
χ	[0.25, 0.5, 0.75]

Simulations were launched for the three representative traffic zones, for a total of 21 simulations. For simplicity, we have decided to report only the plots of the variation of the three KPIs with respect to the variation of the threshold τ and for each of the fractions χ , only for the traffic area of Rho. As can be seen from the plots of Figure 4.3, the variations in KPIs are zero or however negligible for τ values greater than 0.37. For this reason we have chosen to narrow the range of variation of τ between the following discrete values: [0.05, 0.1, 0.15, 0.2, 0.25, 0.3, 0.37].

The summary of the second configuration of the simulations is presented in Table 4.3.

Table 4.3: Summary of the second configuration of the simulations for the analysis of the variation of τ and χ parameters

Scenario Beam Algorithm (PV, B)	RE on Cluster + HAPS Offloading Dynamic (3, 4)
τ	[0.05, 0.1, 0.15, 0.2, 0.25, 0.3, 0.37]
χ	[0.25, 0.5, 0.75]

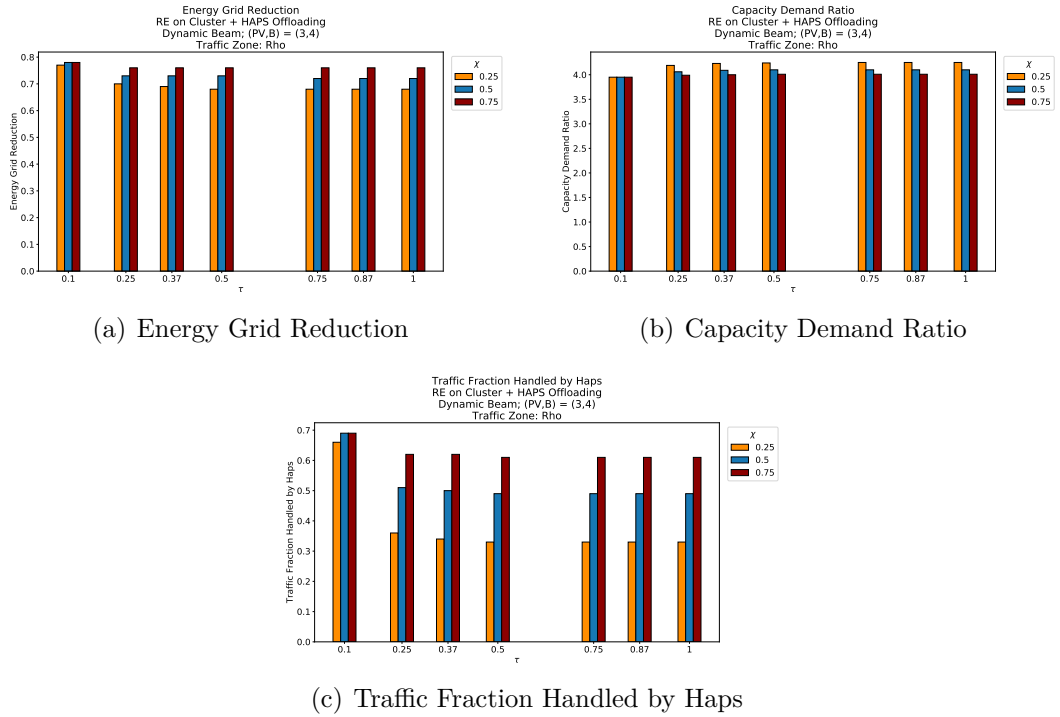


Figure 4.3: Variation of the KPIs as τ and χ parameters vary; Traffic Zone: Rho

The results of the variation of the three KPIs for each of the three representative traffic zones are plotted in Figures 4.4, 4.5, and 4.6.

From the plots in Figure 4.4, it can be seen that the energy grid reduction decreases as τ increases and, with the same τ , increases as χ increases, in each of the three representative traffic zones. This behavior is completely compatible with what we expected, because as the τ value increases there is more probability that

the HAPS cell is reduced and therefore a greater probability that the traffic is managed by the BSs on the ground, leading to an increase in energy taken from the grid.

Then, from the plots in Figure 4.5, it can be seen that the capacity demand ratio increases as the τ increases and, with the same τ , decreases as the χ increases, in each of the three representative traffic zones. This decrease corresponds to a greater expenditure in terms of energy taken from the grid, due to the fact that the traffic is more managed by the BSs on the ground.

Finally, from the plots in Figure 4.6, it can be seen the traffic fraction handled by HAPS decreases as the τ increases and, with the same τ , increases as the χ increases, in each of the three representative traffic zones. In this case, an increase in τ leads to a reduction in the traffic handled by the HAPS, because it is more likely that the HAPS cell capacity will be reduced. Furthermore, in this situation the difference in capacity managed by the HAPS is considerable as χ varies, given a certain τ : this variation is even more accentuated for high values of τ , because it is very likely that the traffic is less than the maximum for a high τ .

Observing these results, we have chosen to set standard values of τ and χ equal to 0.15 and 0.5 respectively. This choice was made because these values allow us to keep the capacity demand ratio below 4.0, thus guaranteeing a high QoS, and the traffic fraction handled by HAPS and the energy grid reduction are high.

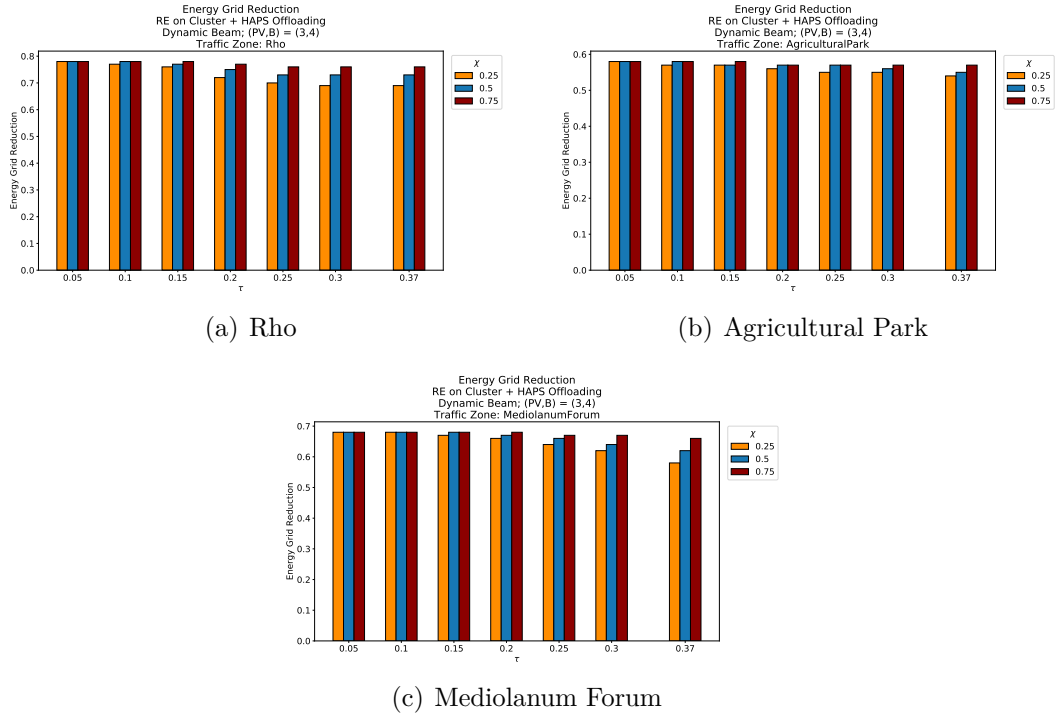


Figure 4.4: Variation of the energy grid reduction as τ and χ parameters vary

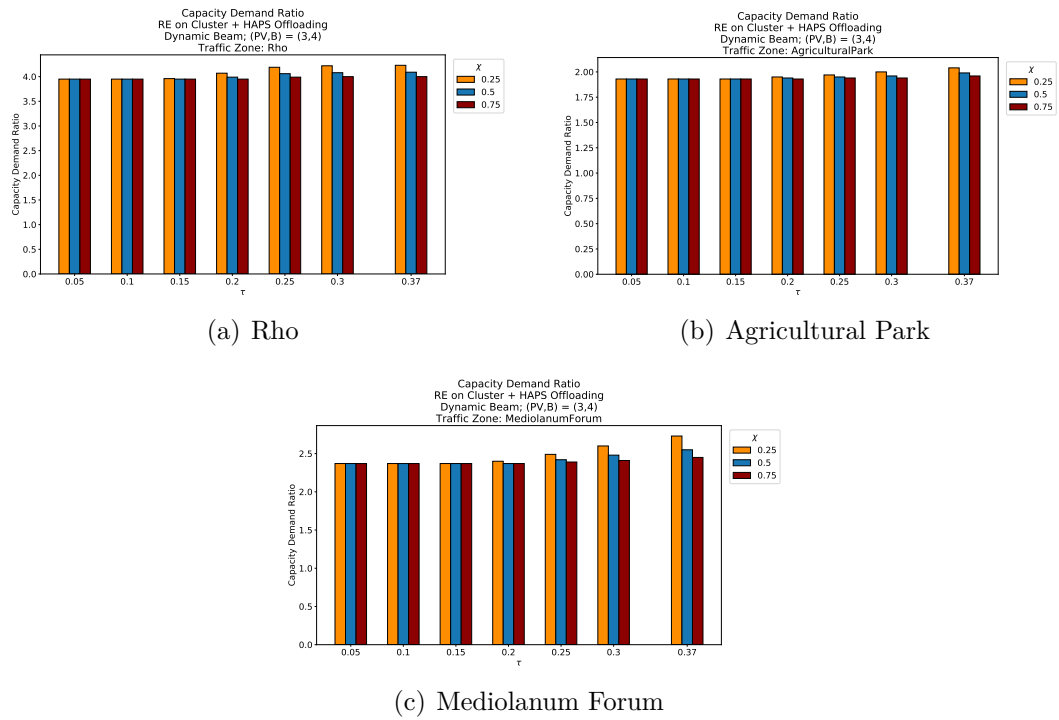


Figure 4.5: Variation of the capacity demand ratio as τ and χ parameters vary

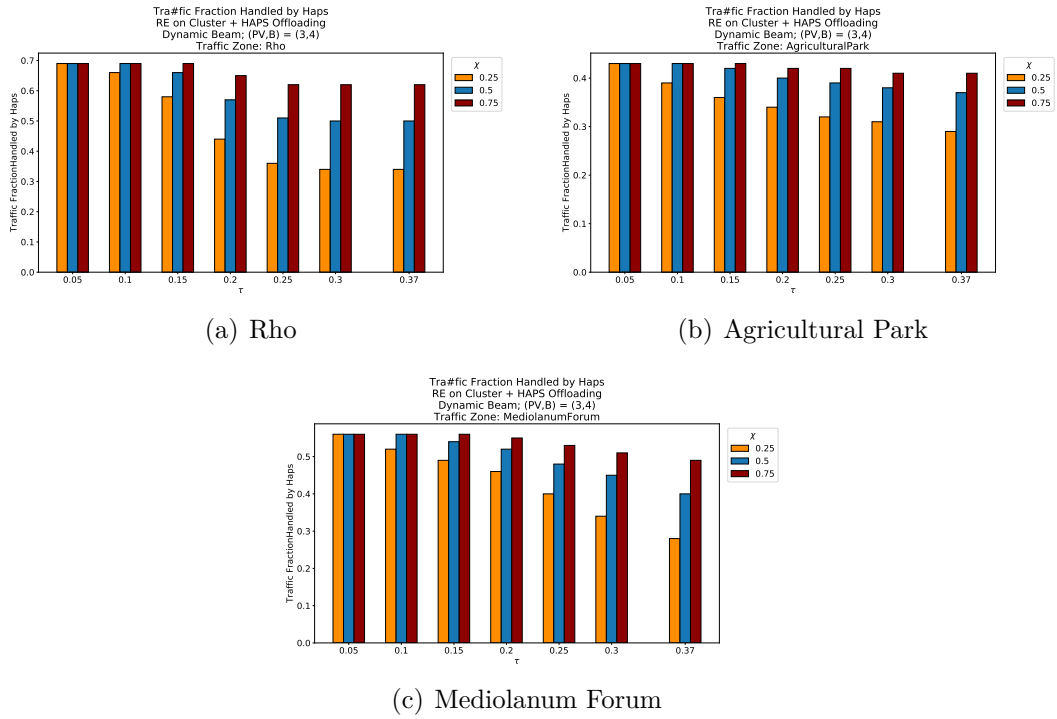


Figure 4.6: Variation of the traffic fraction handled by HAPS as τ and χ parameters vary

4.1.4 Selection of the sample traffic zones

To reduce the number of simulations to be performed without compromising the reliability of the analyzes, we decided to select 5 traffic zones out of 16. The analysis for the choice of these 5 sample zones was carried out on the traffic data pattern: more in detail, the traffic for each cluster was considered as the sum of the traffic managed by each micro BS and macro BS in each time step, that is, in each hour of the 1463 hours analyzed (i.e., the time horizon). Then the statistics of the traffic time series were calculated to select heterogeneous traffic zones, that is, in such a way that each of the sample zones had its own peculiarities and different from the other zones.

After this analysis, we selected the following five sample areas: (i) Rho; (ii) Business; (iii) Residential; (iv) Industrial; and (v) Tourism Attraction. The traffic time series for each of the 5 sample zones are plotted in Figure 4.7. Simply through a visual inspection it is possible to observe how the traffic trend differs from area to area: areas such as Residential, Business and Industrial tend to have a cyclical behavior, as they are closely linked to working hours. In turn, they have almost complementary traffic peaks: in the Business and Industrial area the traffic peaks are observed in the central hours of the day, while in the Residential area the traffic increases in the evening hours as it follows the typical behavior of people in everyday life. The traffic of the Tourism Attraction zone maintains a very high level throughout the observation time, due to the fact that being a tourist area it is visited by a considerable number of people during all hours of the day. Vice versa, the traffic of Rho has a relatively low average traffic but presents some spikes on some specific days, probably due to the fact that in those days the area hosted a major event. To have a more detailed view of the accumulated statistics, a summary of the most relevant statistical traffic indices for each of the 5 sample traffic zones is shown in Table 4.4.

Table 4.4: Summary of the statistical index for the five sample traffic zones

Statistical Index	Sample Traffic Zones				
	Rho	Business	Residential	Industrial	Tourisme
Mean [Mbps]	123,16	222,61	202,63	226,47	285,69
Std [Mbps]	88,33	149,02	97,96	138,06	153,81
Min [Mbps]	2,74	4,98	13,51	10,27	12,95
25% [Mbps]	60,50	89,22	119,57	96,83	139,80
50% [Mbps]	120,67	208,63	226,56	231,53	332,63
75% [Mbps]	158,23	345,47	273,84	344,03	411,75
Max [Mbps]	556,03	586,72	451,30	615,23	573,77

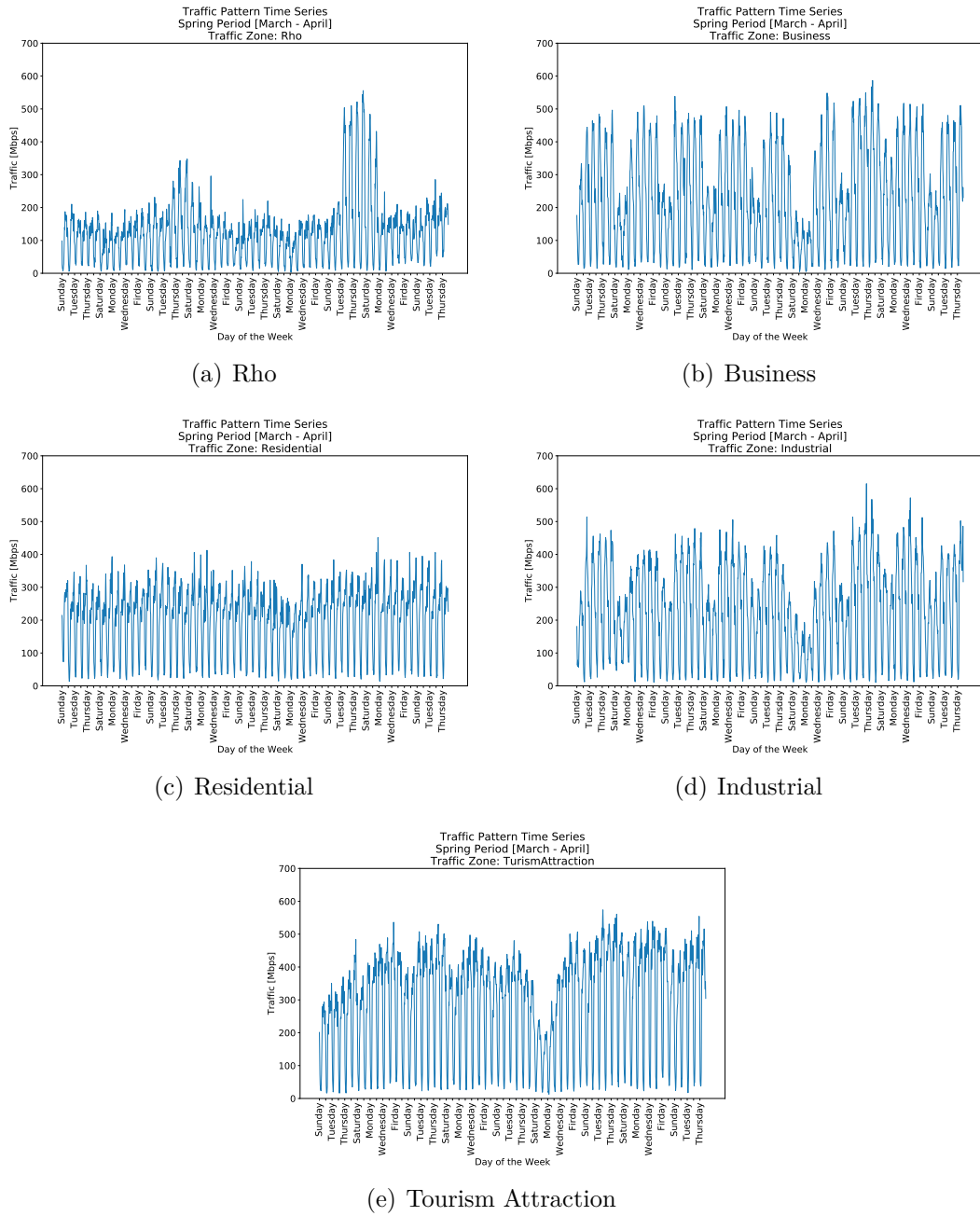


Figure 4.7: Traffic time series in the five sample traffic zones

Finally, in order to have a graphical answer relating to the statistics calculated in Table 4.4 for each of the five traffic zones, it was decided to report in Figure 4.8 the histogram and the density plot of the traffic data. Figure 4.8(a) shows the normalized histogram for traffic data: it shows the proportion of cases in which traffic falls within each range of traffic quantities, with the sum of the heights equal to 1. While, Figure 4.8(b) shows the density plot, which is a representation of the distribution of the traffic variable: it is a smoothed version of the histogram and is used in the same concept.

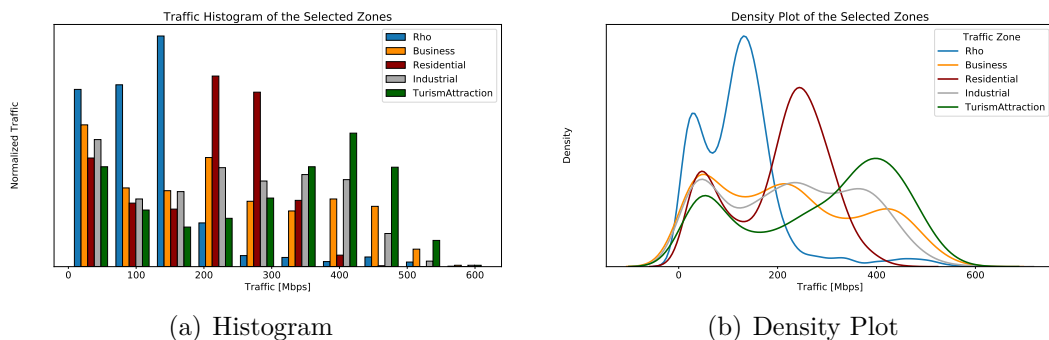


Figure 4.8: Visualization of the traffic statistics of the five sample areas

The plots of Figure 4.8 show that each of the five traffic zones has a different traffic profile than each other: this justifies the choice made and confirms the reliability of the simulations performed.

4.2 Simulation Phase

In this section, we analyze the performance indicators deriving from the simulation of different configurations. In detail, we start with the analysis of the simulations of the basic scenarios, in which, where necessary, we have used the parameter values deriving from the previous sizing phase. Moreover, among the simulations carried out, we have developed an analysis on the costs of the basic scenarios in three different periods of time and we have also analyzed how a variation in the dimensions of the PV panels and batteries leads to a variation in terms of energy and economic savings.

Then, we analyze the analysis of the performance indicators using more complex scenarios. Firstly, we evaluate the distribution of HAPS capacities among the various HAPS cells in proportion to the surface of the traffic area. Secondly, thanks to the results obtained from the previous simulations, we carry out a more

complex simulation taking into account the energy demand, the availability of RE and the price of the energy: thanks to these information, we produce a dynamic strategy for the selection of the threshold (τ) and of the reduction fraction of the maximum HAPS cell capacity (χ), to trade off the data traffic with respect to the actual situation of the cells, without wasting capacities and maintaining a high QoS.

Finally, we propose our solution for a realistic scenario in which we imagine to work with two clusters together: in this case, differently from what done in the previous analyzes, we envision to use the HAPS in a more dynamic manner, that is adapting the HAPS cell capacities depending on the instantaneous traffic of each cluster.

4.2.1 Analysis of basic scenarios

The first analysis concerns the study of the energy grid reduction for each cluster in the city of Milan and suburbs, in order to have an idea of the impact of the presence of RE or the application of the HAPS Offloading strategy. These simulations were performed using the base scenario configurations, namely: (i) NO RE; (ii) RE on Cluster; (iii) HAPS Offloading with Constant Beam and (iv) with Dynamic Beam; and (v) RE on Cluster + HAPS Offloading with Constant Beam and (vi) with Dynamic Beam. As a consequence of the sizing phase, for the scenarios with RE on the ground we set the dimensions $(PV, B) = (3, 4)$ [kWp, kWh], while for the scenarios with the HAPS Offloading with Dynamic Beam strategy applied we set the threshold $\tau = 0.15$ and the fraction of reduction of the maximum beam capacity $\chi = 0.5$.

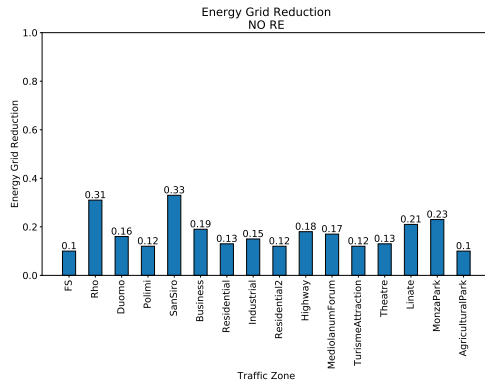
A general overview of the results obtained for each of the clusters of the 16 traffic zones is shown in Figure 4.9: for simplicity we have decided to number the configurations from I to VI and for each plot in the figure we have chosen to include the specifications of the parameters used in the title, as they are useful for the analyzes carried out in the following chapters. Moreover, to make more specific comments, we have chosen to collect in Table 4.5 the results of the energy grid reduction for each of the six configurations, considering only the five sample traffic zones selected in Section 4.1.4.

Table 4.5: Summary of the energy grid reduction for the five sample traffic zones in the basic scenarios

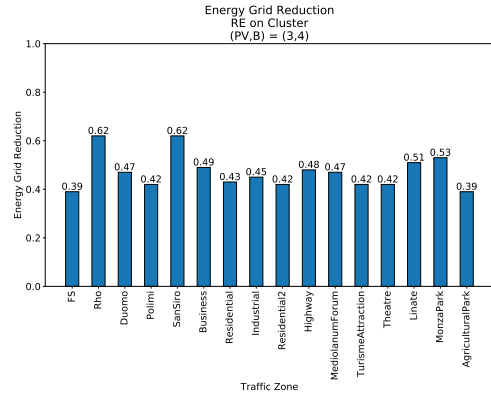
Configuration	Sample Traffic Zones				
	Rho	Business	Residential	Industrial	Tourism
I	31%	19%	13%	15%	12%
II	62%	49%	43%	45%	42%
III	51%	40%	36%	34%	32%
IV	44%	34%	31%	32%	29%
V	78%	69%	64%	67%	61%
VI	73%	64%	59%	61%	58%

From Table 4.5 it is possible to observe how the best configuration for all the five sample zones is the configuration V, i.e. RE on Cluster + HAPS Offloading with Constant Beam. This result is fully expected because with the presence of RE on the ground we limit the withdrawal of energy from the grid favoring the use of green energy, while with HAPS Offloading we make more use of HAPS, leaving less load on the ground to manage. Moreover, the use of the Constant Beam algorithm allows to associate a fixed capacity of 150 Mbps to each HAPS cell, so that each cluster has the possibility to have 150 Mbps of additional capacity even if the instant traffic is not high.

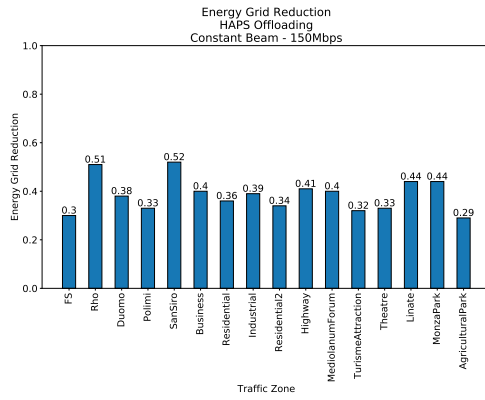
It is equally clear that configuration I is the one that has the lowest energy grid reduction for each of the six sample zones: despite the presence of only the applied RoD strategy, it results in an energy saving of 31% in the Rho zone, this result is clearly lower in the remaining areas. The reason lies in the fact that the Rho area on average has a low traffic, therefore the switching off of the micro BSs with relative shift and traffic management to the macro BS is frequent, while in the remaining areas the traffic is high and therefore the application of the RoD strategy will be less frequent. For this reason, the presence of RE on the ground allows an energy saving of 30 percentage points more: in configuration II, the presence of RE is able to compensate for the waste due to the withdrawal of energy from the grid. Finally, we notice that the presence of HAPS Offloading strategy (configurations III and IV) without the presence of RE on the Cluster, worsens the performance compared to configuration II, although providing a relevant grid energy reduction. Despite this, an average improvement of 20 percentage points is observed compared to configuration I: this is an excellent result obtained, because it suggests that the HAPS Offloading strategy applied in traffic areas with little surface available for mounting PV panels, improves significantly the performance in terms of energy saving.



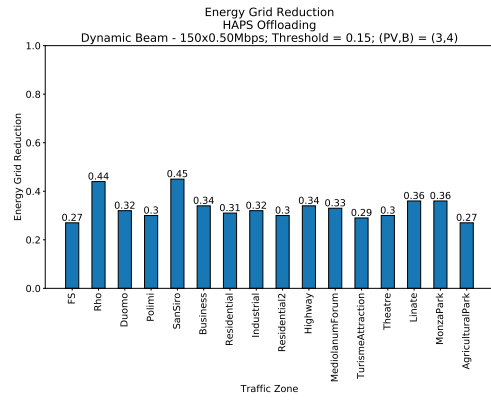
(a) Configuration I: NO RE



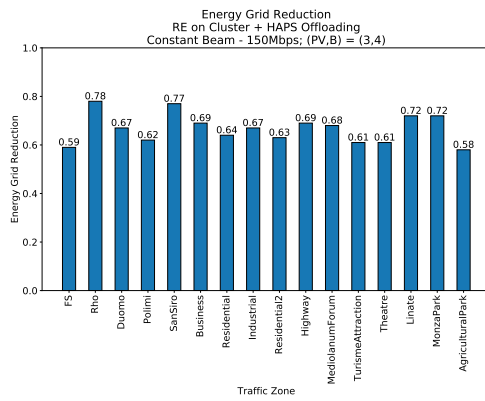
(b) Configuration II: RE on Cluster



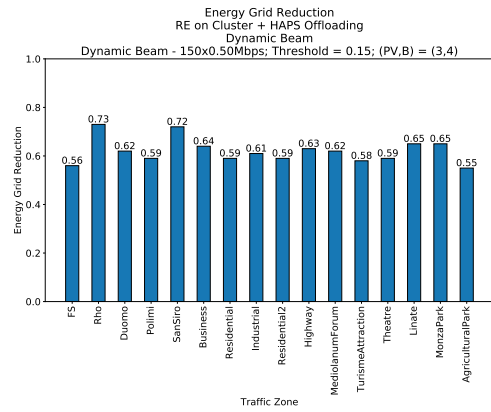
(c) Configuration III: HAPS Offloading with Constant Beam



(d) Configuration IV: HAPS Offloading with Dynamic Beam



(e) Configuration V: RE on Cluster + HAPS Offloading with Constant Beam



(f) Configuration VI: RE on Cluster + HAPS Offloading with Dynamic Beam

Figure 4.9: Analysis of the energy grid reduction for the basic scenarios

4.2.2 Cost analysis of the basic scenarios

In order to have an idea of the monetary savings by means of the presence of sophisticated strategies like the RoD or the HAPS Offloading, we have performed a cost analysis for the six configurations presented in the previous section. Moreover, in order to have an overview of the variability of the energy price all over the years, we decide to apply the cost analysis over three different periods: (i) winter 2021, from 00.00 on Sunday 3rd January to 11.00 pm on Thursday 4th March 2021; (ii) spring 2021, from 00.00 on Sunday 28th February to 11.00 pm on Thursday 29th April 2021; and (iii) spring 2015, from 00.00 on 1st March to 11.00 pm on 30th April 2015.

As already mentioned in Section 3.6.1, energy grid price data have been retrieved from the GME website [103] and they are expressed in €/MWh.

In order to have an idea of how the energy grid price has changed over the considered periods, we have decided to show the plot of the time series of the price in Figure 4.10.

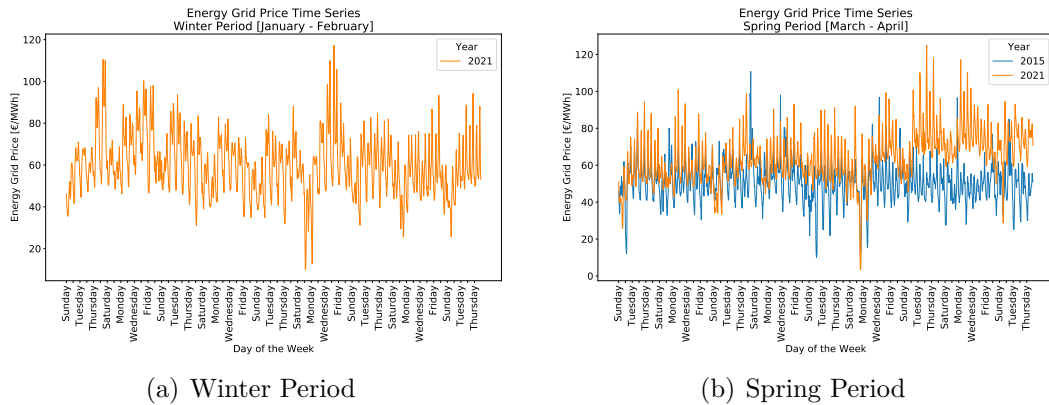


Figure 4.10: Energy grid price time series

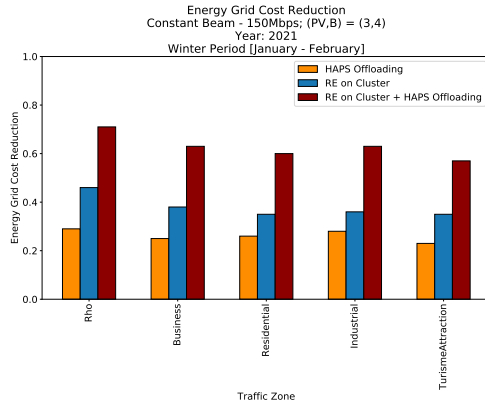
As can be seen from Figure 4.10(b), it is evident that passing from 2015 to 2021 the price of energy has increased. It is also noted that there is a minimal difference between the orange curve in Figure 4.10(a) and the orange one in Figure 4.10(b). Therefore, to have a better understanding of the cost in terms of energy provided by the grid in each cluster, we have aggregated the results over the entire time frame and for all three periods. The results are shown in Table 4.6.

Table 4.6: Summary of the energy grid cost for each traffic zone in the three selected periods

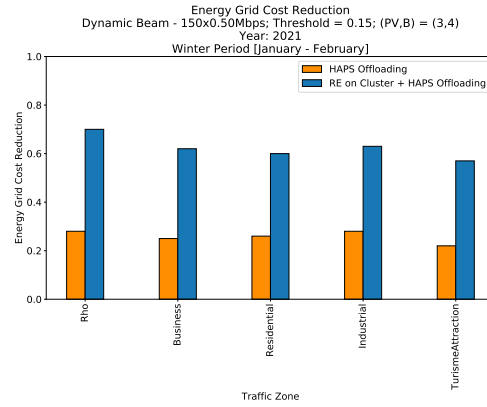
Traffic Zone	Energy Grid Cost [€]		
	Winter 21	Spring 21	Spring 15
FS	114.60	120.66	95.86
Rho	79.20	83.93	66.39
Duomo	101.79	106.49	84.84
Polimi	108.72	114.40	91.14
San Siro	78.45	82.82	66.07
Business	97.90	102.54	81.55
Residential	107.41	113.18	90.17
Industrial	103.08	108.68	86.50
Residential 2	108.39	113.90	90.70
Highway	100.52	105.69	84.26
Mediolanum Forum	98.72	104.24	83.17
Tourism Attraction	108.22	113.94	90.35
Theatre	109.93	115.53	91.99
Linate	94.74	99.53	79.20
Monza Park	92.96	98.00	78.09
Agricultural Park	114.47	120.43	95.95

It is useful to underline that the costs presented in Table 4.6 were calculated on configuration I (i.e., the NO RE scenario), as this configuration was used for the calculation of the basic cost. Therefore, from this result it was possible to calculate two KPIs: (i) the energy grid cost reduction; and (ii) energy cost savings. More specifically, the energy grid cost reduction is calculated as the ratio between two factors a and b, where: (a) is the difference between the reference cost of the cluster, i.e. the cost shown on Table 4.6, and the actual cost of the cluster, considering certain strategies applied; and (b) is the reference cost of the cluster. It is measured as a percentage of economic savings. Instead energy cost savings is simply the difference between the reference cost of the cluster and the actual cost of the cluster. It is measured as energy savings in monetary terms, therefore in euros.

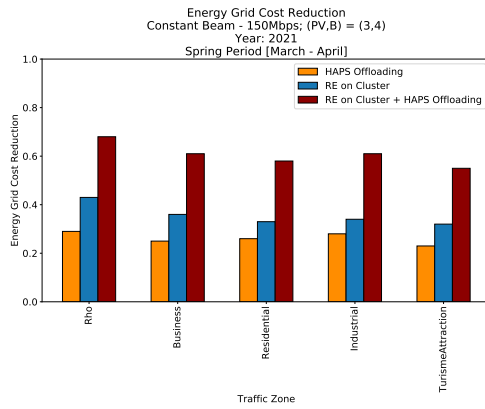
The cost analysis was carried out by analyzing the two KPIs described previously for the five sample traffic areas selected in Section 4.1.4. To present the results obtained we have chosen to divide the scenarios into configurations with Constant Beam and Dynamic Beam, that is configurations II, III and V, and configurations IV and VI respectively. The results are shown in Figure 4.11 and Figure 4.12.



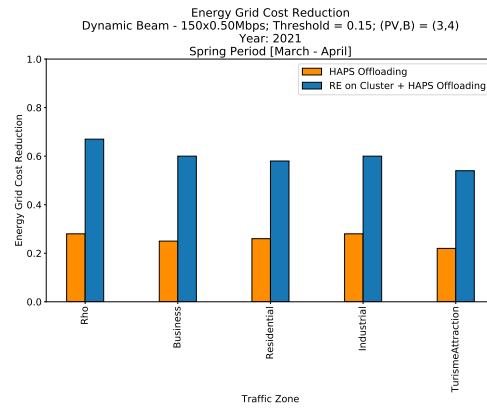
(a) Constant Beam - Winter 2021



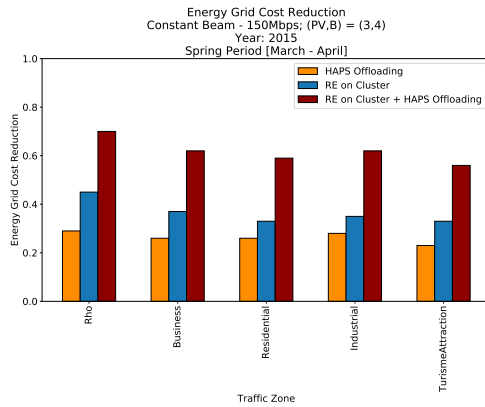
(b) Dynamic Beam - Winter 2021



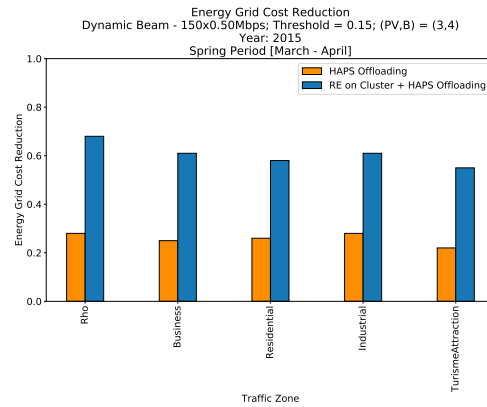
(c) Constant Beam - Spring 2021



(d) Dynamic Beam - Spring 2021

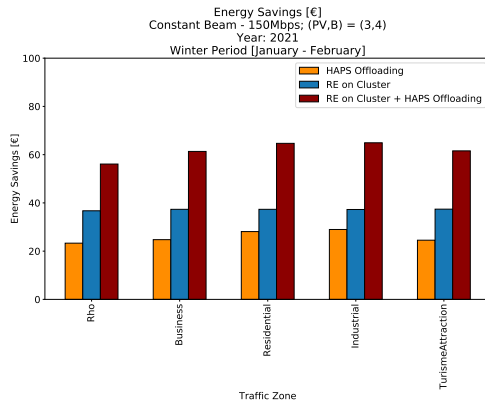


(e) Constant Beam - Spring 2015

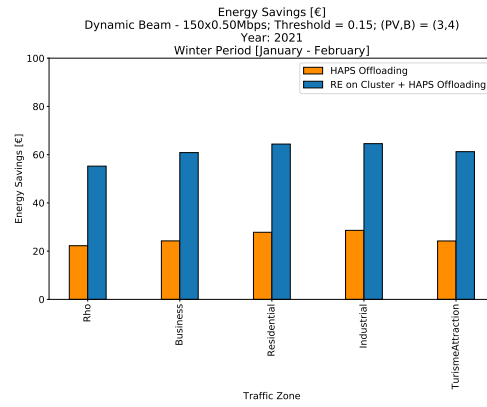


(f) Dynamic Beam - Spring 2015

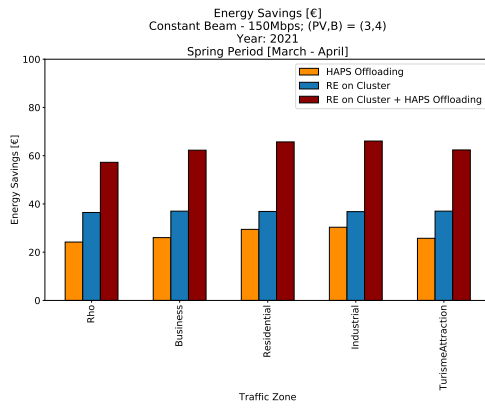
Figure 4.11: Energy Grid Cost Reduction



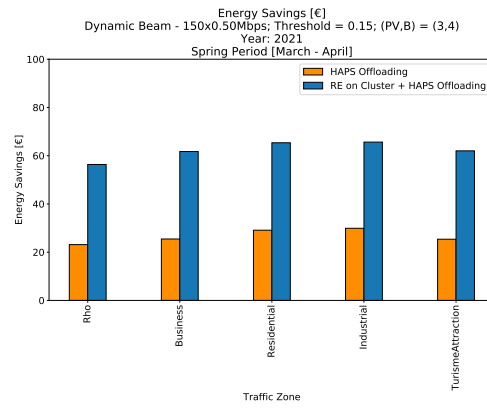
(a) Constant Beam - Winter 2021



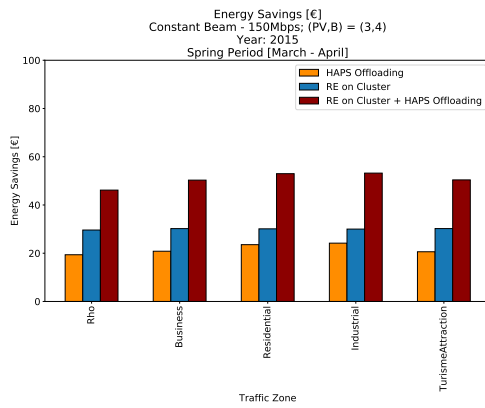
(b) Dynamic Beam - Winter 2021



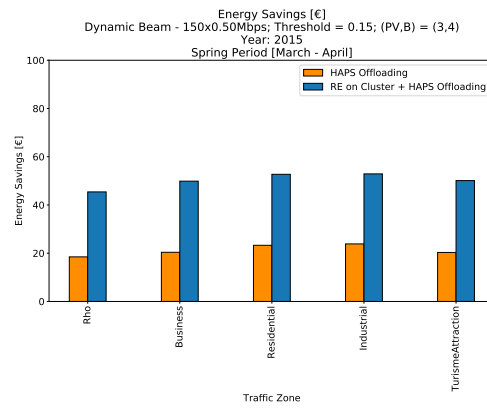
(c) Constant Beam - Spring 2021



(d) Dynamic Beam - Spring 2021



(e) Constant Beam - Spring 2015



(f) Dynamic Beam - Spring 2015

Figure 4.12: Energy Cost Savings

Looking at the graphs it is possible to see how, even in economic terms, the best configuration for all five sample zones is the configuration V, i.e. RE on Cluster + HAPS Offloading with Constant Beam.

Then, taking into consideration the plots of Figure 4.11, it can be seen how the energy grid cost reduction worsens slightly in the case in which the Dynamic Beam algorithm is applied: this behavior is understandable since through the application of the Dynamic Beam we want to reduce the capacity of the HAPS cell, in such a way as to be able to exploit the remaining capacity on other areas that require a higher bit rate. Therefore, it is inevitable that there will be a greater consumption by the BSs on the ground. However, a percentage reduction of only 1% of the energy grid cost reduction in the Dynamic Beam case is to be considered a positive result.

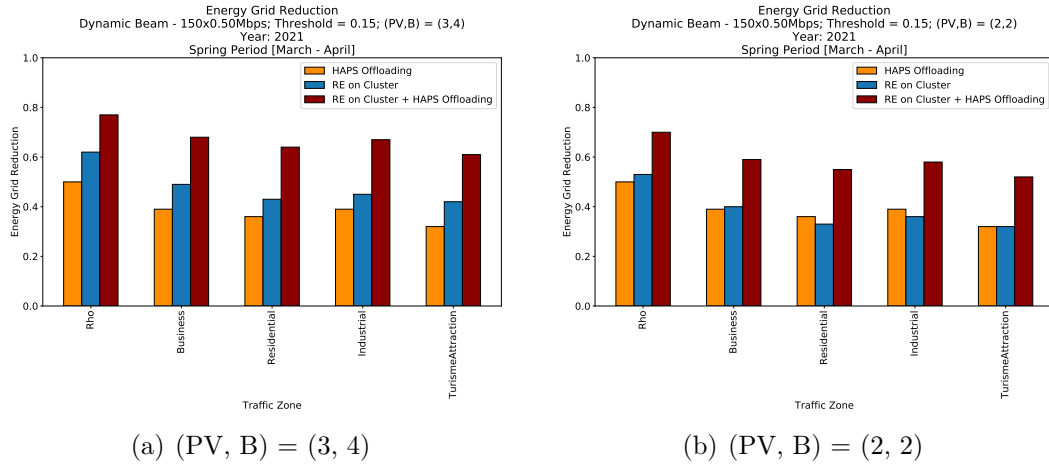
Furthermore, from the charts it can be seen that the behavior is almost the same, as the period considered varies: even if the percentage value of energy grid cost reduction in Figure 4.11 tends to remain almost unchanged, the absolute amount of euros saved, shown in Figure 4.12, has obvious differences. For example, taking into consideration the Rho cluster, we have that in the three periods the configuration III (i.e., HAPS Offloading with Constant Beam) has an energy grid cost reduction always equal to 29%. However, this percentage reduction translates into three different economic savings values, namely: (i) €23.31 in Winter 202; (ii) €24.20 in Spring 2021; and (iii) €19.37 in Spring 2015.

Finally, it is noted that the value of economic savings tends to be higher in the Spring 2021 period and that, in general, the configurations V and VI, i.e. the RE on Cluster + HAPS Offloading with Constant and Dynamic Beam scenario respectively, have savings much higher than the others.

4.2.3 Analysis of basic scenarios with other (PV, B) configurations

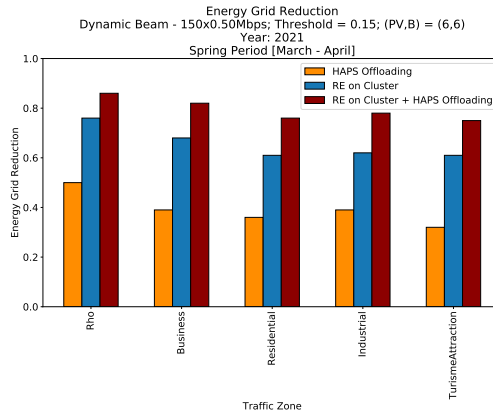
In this analysis we have chosen to evaluate the effect of two different configurations of the dimensions of (PV, B) in terms of energy savings and monetary savings. In order to reduce the number of simulations, we have chosen to consider only the configurations with the Dynamic Beam algorithm active, i.e., RE on Cluster, HAPS Offloading with Dynamic Beams, and RE on Cluster + HAPS Offloading with Dynamic Beams, for each of the five sample traffic zones. The parameters τ and χ have been set equal to 0.15 and 0.5 respectively. We have chosen to carry out the simulation only for the Spring 2021 period.

Since the basic configuration of (PV, B) was chosen to be equal to 3 kWp and 4 kWh, as explained in Section 4.1.2, in order to observe the effects of different sizes of PV panels and batteries, we have chosen to use (PV, B) = (2, 2) [kWp, kWh] and (PV, B) = (6, 6) [kWp, kWh].



(a) $(PV, B) = (3, 4)$

(b) $(PV, B) = (2, 2)$



(c) $(PV, B) = (6, 6)$

Figure 4.13: Analysis of the energy grid reduction with different dimensions of (PV, B)

The charts in Figure 4.13 show a plausible behavior: as the size of the PV panels and batteries increases, there is a significant increase in energy grid reduction. Furthermore, it is noted that using only the HAPS Offloading strategy, without considering the presence of RE on the ground, the energy grid cost reduction remains unchanged, since the dimension of (PV, B) remains in any case equal to $(0, 0)$ [kWp, kWh]. However, the choice to also plot the HAPS Offloading scenario is not trivial. As can be seen from Figure 4.13(b), in the Residential and Industrial traffic areas it is observed that the energy grid reduction is greater in the HAPS Offloading scenario than in the RE on Cluster scenario. This result is very relevant, because it allows us to state that in a traffic area where there is no space to install large PV panels, it is much more convenient to use HAPS.

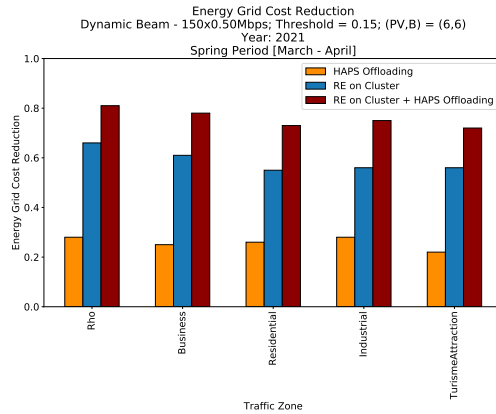
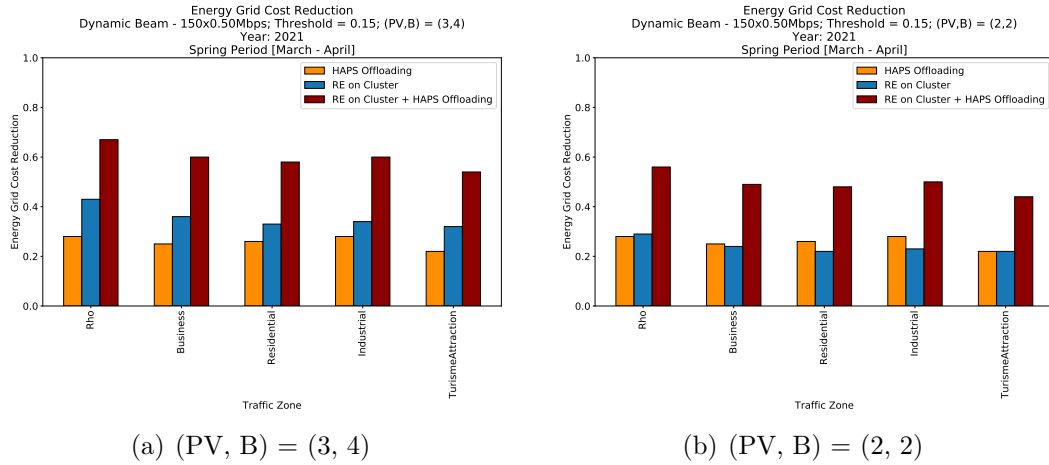


Figure 4.14: Analysis of the energy grid cost reduction with different dimensions of (PV, B)

Also in the case of energy grid cost reduction, we are witnessing a behavior similar to that analyzed for energy grid reduction. It is important to note that in Figure 4.14(b) we see the same performance seen for energy grid reduction. In this case, in addition to the Residential and Industrial traffic areas, there is an increase in monetary savings also in the Business traffic area, further demonstrating the fact that in traffic areas where we do not have space for the installation of PV panels, it is also economically convenient to make greater use of HAPS.

4.2.4 Analysis of the interaction of HAPS beams with traffic zones surfaces

For the first analysis of a more complex scenario, we have chosen to distribute the HAPS capacity among the various cells proportionally to the surface of the traffic zone. The advantage of having the additional capabilities from HAPS over larger areas is that through a single HAPS cell we are able to cover a very large area and therefore we can make more use of the RoD strategy, more easily turning off the unused micro BSs. On the other hand, we can decide to appropriately reduce the infrastructure to the ground by choosing to exploit HAPS more: just think that some initial implementations of NTN were born precisely to provide access to the network in very large remote areas where land were not available.

Knowing that in the basic scenarios we have associated a maximum bit rate for each HAPS cell of 150 Mbps, in this analysis we have decided to adapt the maximum capacity of the cell proportionally to the surface of the traffic area. In this way, the surface of the traffic zone becomes the proportionality factor that scales the maximum bit rate value based on the area of the zone. More in detail, we calculated the value of the bit rate per square kilometer (k) equal to 67 Mbps/km² and we multiplied this value by the surface of the traffic zone (S_{zone}), in order to obtain the maximum bit rate scaled value for each HAPS cell. Furthermore, in order not to allocate too high a bit rate for very large traffic areas, we have decided to insert an upper limit equal to 500 Mbps. By the same principle, in order not to allocate an extremely low bit rate for small traffic areas, we have decided to insert a lower limit equal to 150 Mbps, i.e., the same maximum bit rate for each cell in the basic scenario. For the sake of simplicity, we have called this algorithm adaptive HAPS max bit rate method, while the maximum fixed bit rate algorithm has been called constant HAPS max bit rate method.

In practice, the adaptive HAPS max bit rate method algorithm can be summarized through the following pseudocode.

²Assuming a single cell capacity $C_{cell} = 1.8 - 2$ Gbps and and the surface covered by one single cell $S_{cell} = 30$ km², we have that the bit rate per square kilometer is

$$k = \frac{C_{cell}}{S_{cell}} \approx 67 \text{ Mbps/km}^2$$

Algorithm 3 : Adaptive HAPS max bit rate

```

1: for  $n = 1, N$  do ▷ for each cell
2:    $C_n \leftarrow k \cdot S_n$  ▷ adapt the cell capacity
3:   if  $C_n > C_{MAX}$  then
4:      $C_n = C_{MAX}$  ▷ set the cell capacity equal to 500 Mbps
5:   end if
6:   if  $C_n < C_{min}$  then
7:      $C_n = C_{min}$  ▷ set the cell capacity equal to 150 Mbps
8:   end if
9: end for

```

The analysis was performed on the RE scenario on Cluster + HAPS Offloading with Dynamic Beam, since it is the target scenario of our thesis work. Furthermore, the parameters have been set as for the basic scenarios, that is: $(PV, B) = (3, 4)$ [kWp, kWh], $\tau = 0.15$ and $\chi = 0.5$. The summary of the scenario configuration is presented in Table 4.7.

Table 4.7: Summary of the configuration of the simulations for the analysis of the interaction of HAPS beams with traffic zones surfaces

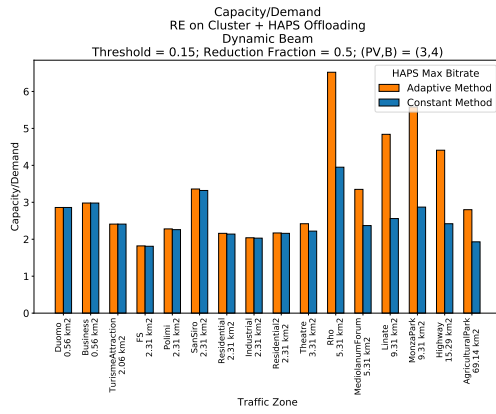
Scenario Beam Algorithm (PV, B)	RE on Cluster + HAPS Offloading Dynamic (3, 4)
τ	0.15
χ	0.5

The simulation has been performed for each traffic zone with both the HAPS max bit rate methods applied. Then, the analyzed performance indicators have been: (i) the capacity demand ratio; (ii) the energy grid reduction in relative and (iii) absolute values³; (iv) the grid energy⁴; and (v) the traffic fraction handled by HAPS.

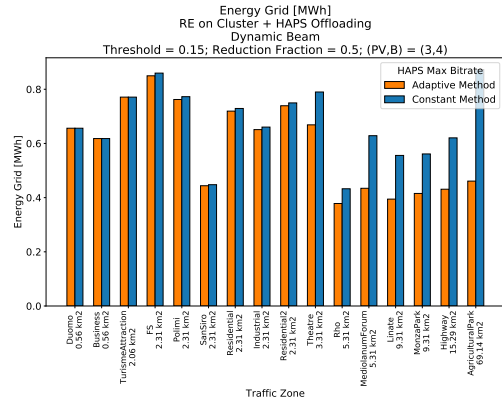
The results obtained for each of the clusters of the 16 traffic zones and for both the HAPS max bit rate methods applied is shown in Figure 1.9.

³It is measured as the difference between the reference consumption of the cluster, i.e. the consumption that the cluster would have considering the RoD strategy not applied and the BSs powered only by energy taken from the grid, and the actual consumption of the cluster, considering certain strategies applied. It is expressed in Wh.

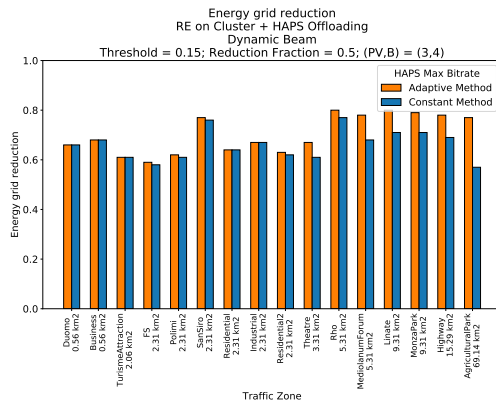
⁴It is the actual quantity of power taken from the grid. It is expressed in Wh.



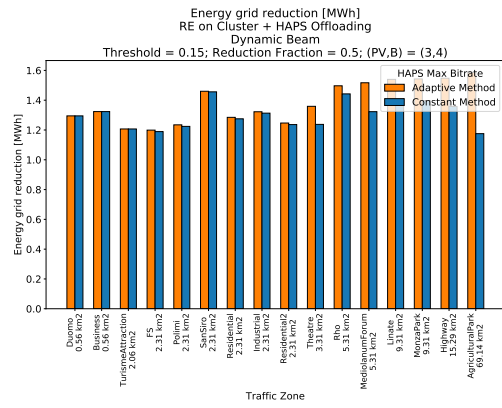
(a) Capacity Demand Ratio



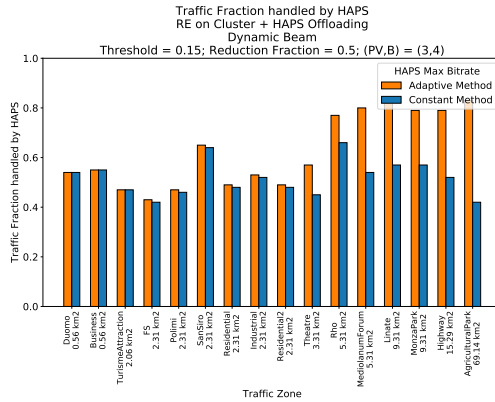
(b) Grid Energy



(c) Relative Energy Grid Reduction



(d) Absolute Energy Grid Reduction



(e) Traffic Fraction Handled by HAPS

Figure 4.15: Analysis of the interaction of HAPS beams with traffic zones surfaces

It is useful to underline that in Figure 1.9 the traffic zones have been positioned on the x-axis in increasing surface order and that the value of the relative surface is labelled in the figure. Furthermore, to get an idea of how the maximum capacities of the cells have been adapted, we decided to collect the simulation results in Table 4.8: for each traffic zone the surface in km^2 and the maximum bit rate of the cell of the HAPS in Mbps.

Table 4.8: Result of adapting the maximum cell capacity using the Adaptive Method algorithm.

Traffic Zone	Surface [km^2]	Capacity [Mbps]
FS	2.31	154
Rho	5.31	355
Duomo	0.56	150
Polimi	2.31	154
San Siro	2.31	154
Business	0.56	150
Residential	2.31	154
Industrial	2.31	154
Residential 2	2.31	154
Highway	15.29	500
Mediolanum Forum	5.31	355
Tourism Attraction	2.06	150
Theatre	3.31	221
Linate	9.31	500
Monza Park	9.31	500
Agricultural Park	69.14	500

From Figure 1.9(a), it is clearly seen that in traffic areas with an area greater than 3 km^2 , the capacity demand ratio is very high, which means that the system capacity is overdimensioned. In traffic areas such as Rho it is a waste to have too much capacity available, also because the further increase in the relative reduction of the energy network is very limited, as can be seen in Figure 1.9(c). In addition, traffic areas such as Rho, Mediolanum Forum, Linate, Monza Park, Highway and Agricultural Park, probably have lower basic consumption than other areas. In fact, the relative increase of a few percentage points of reduction in the energy grid demand corresponds to a slight increase in the reduction of the energy grid demand in absolute terms, as can be seen in Figure 1.9(d), despite the fact that there is a consistent reduction of the energy taken by the grid, as can be seen in Figure 1.9(b). Finally, Figure 1.9(e) clearly shows that the greater the capacity reserved

for a cell, the greater the amount of traffic handled by the HAPS, confirming the fact that the HAPS Offloading strategy is functional.

In conclusion, we can say that through this simulation it is clear that the advantage of allocating a certain amount of capacity based only on the extension of the surface is not relevant. In very large areas but not very loaded with data traffic, it is a waste to allocate a large amount of capacity and there is the risk of oversizing the system, as happens in the case of the Rho traffic area. Therefore, it is better to reserve the available capacity for the areas that have the most traffic and which would therefore benefit more in terms of saving of grid energy in absolute quantities.

4.2.5 Analysis of the strategy for the dynamic choice of τ and χ

Among the more complex strategies, we have developed a strategy of dynamic selection of the threshold τ and the reduction fraction of the maximum capacity of the HAPS cell χ . We have chosen to develop this strategy to try to further improve the performance of the system, making it adaptive to traffic conditions and responsive to the smart grid.

More specifically, we have chosen to vary τ within four discrete values: [0.05, 0.15, 0.25, 0.35]; and to vary χ within four discrete values: [0.25, 0.50, 0.75, 1]. For the selection of the optimal instantaneous value of τ , we considered: (i) the instantaneous energy demand of each cluster, that is the reference consume of each cluster assuming all BSs active and no applied strategies; and (ii) the price of instantaneous energy, which is the same for all clusters. Instead, for the selection of the optimal value of χ per time step, we considered the energy available per time step, which is calculated as the difference between the energy demand of each cluster per time step and the RE available for each cluster per time step, i.e. the amount of RE generated instantaneously from PV panels.

For the selection of τ with respect to the instantaneous energy demand (d^t), we have selected a minimum (d_{min}) and a maximum of the energy demand (d_{max}), taken as the minimum and maximum of the energy demand among all the clusters of the city of Milan and suburbs, throughout the period considered. After that, we divided the range between the minimum and maximum of the energy demand by four, i.e. equal to the number of discrete values of τ , thus defining the granularity of the energy demand (μ). Therefore, for each time step, we have associated to the cluster the optimal value of threshold with respect to the energy demand (τ_{demand}), as defined by the following algorithm.

Algorithm 4 : Selection of τ_{demand}

```

1: for  $t = 1, T$  do ▷ for each time step
2:   if  $d_{min} < d^t < d_{min} + \mu$  then
3:      $\tau_{demand}^t \leftarrow 0.35$ 
4:   else if  $d_{min} + \mu < d^t < d_{min} + 2\mu$  then
5:      $\tau_{demand}^t \leftarrow 0.25$ 
6:   else if  $d_{min} + 2\mu < d^t < d_{min} + 3\mu$  then
7:      $\tau_{demand}^t \leftarrow 0.15$ 
8:   else if  $d^t > d_{min} + 3\mu$  then
9:      $\tau_{demand}^t \leftarrow 0.05$ 
10:  end if
11: end for

```

It should be emphasized that the algorithm for choosing τ_{demand} is repeated for each of the 16 traffic zones.

An example of the result of assigning the value of τ_{demand} following the application of the algorithm is shown in Figure 4.16.

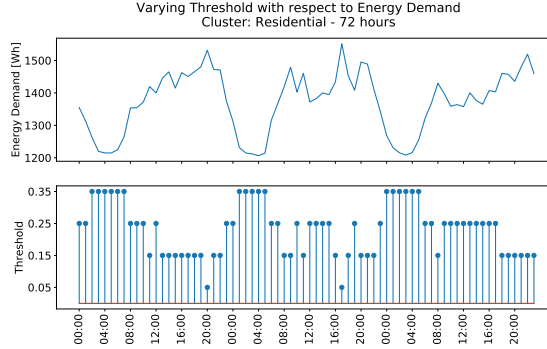


Figure 4.16: Selection of the optimal τ_{demand} values for the Residential cluster over a 72 hour period

The reason why we made these choices for the value of τ_{demand} is given by the fact that when the energy demand is low, we increase the value of the threshold. This means that with much more probability we will reduce the capacity of the HAPS beam by a fraction linked to the value of χ . As can be seen from Figure 4.16, during the night hours (i.e., between 2 am and 7 am) in a residential area, the energy demand is very low. For this, we are going to increase the threshold value, so that we increase the probability of reduction of the capacity of the HAPS cell and we can allocate the saved capacity for another cluster that perhaps requires

more energy.

After this analysis, we carried out a search for the selection of τ with respect to the instantaneous energy price (p^t). We have selected a minimum (p_{min}) and a maximum of the energy price (p_{max}), taken as the minimum and maximum of the energy price for the city of Milan and suburbs, considering historical data on the price of energy in the period considered. After that, we divided the range between the minimum and maximum of the energy price by four, i.e., equal to the number of discrete values of τ , thus defining the granularity of the energy price (ϕ). Therefore, for each time step, we have associated to the cluster the optimal instantaneous value of threshold with respect to the energy price (τ_{price}), as defined by the following algorithm.

Algorithm 5 : Selection of τ_{price}

```

1: for  $t = 1, T$  do ▷ for each time step
2:   if  $p_{min} < p^t < p_{min} + \phi$  then
3:      $\tau_{price}^t \leftarrow 0.35$ 
4:   else if  $p_{min} + \phi < p^t < p_{min} + 2\phi$  then
5:      $\tau_{price}^t \leftarrow 0.25$ 
6:   else if  $p_{min} + 2\phi < p^t < p_{min} + 3\phi$  then
7:      $\tau_{price}^t \leftarrow 0.15$ 
8:   else if  $p^t > p_{min} + 3\phi$  then
9:      $\tau_{price}^t \leftarrow 0.05$ 
10:  end if
11: end for

```

It should be emphasized that the algorithm for choosing τ_{price} is repeated for each of the 16 traffic zones.

An example of the result of assigning the value of τ_{price} following the application of the algorithm is shown in Figure 4.17.

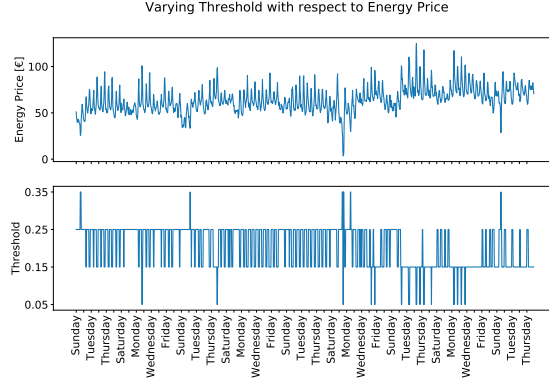


Figure 4.17: Selection of the optimal τ_{price} values for the Residential cluster over a two months period

The reason why we made these choices for the value of τ_{price} is given by the fact that when the energy price is low, we increase the value of the threshold. This means that with much more probability we will reduce the capacity of the HAPS cell by a fraction linked to the value of χ , because it is more convenient to take energy from the grid or in any case manage the traffic from the ground infrastructure.

After these two analyzes, we assign the optimal instantaneous threshold value by means of the following weighted average:

$$\tau^t = 0.65 \cdot \tau_{demand}^t + 0.35 \cdot \tau_{price}^t \quad (4.1)$$

We have chosen to assign more weight to τ_{demand} because the energy demand value is more linked to the cluster, while the value of the energy price is the same for all clusters, therefore less characteristic.

At the end of this process, we have obtained the optimal τ values per time step: this implies that for each time step (i.e., for each hour) each cluster will have assigned a τ value adapted to the cluster conditions.

After that, for the selection of the optimal value of χ per time step, we considered the energy available per time step (E^t), which is calculated as the difference between the energy demand of each cluster per time step (d^t) and the RE available for each cluster per time step (RE^t), i.e., the amount of RE generated from PV panels per time step. More specifically, the energy available per time step, is calculated as follow:

$$|E^t| = |RE^t - d^t| \quad (4.2)$$

Therefore, we assign $\chi = 0$ in the event that the instantaneous energy produced by the cluster exceeds the energy demand of the cluster: this means that we decide

to completely switch off the HAPS cell for the period of time considered because the ground infrastructure has a quantity of renewable energy such as to manage all the energy demand. Then, for the assignment of the other instantaneous values of χ , we selected the maximum of the energy demand (d_{max}) and the minimum of the RE generated (RE_{min}), taken as the maximum and minimum among all the clusters of the city of Milan and suburbs, throughout the period considered. So, we divided the range between the minimum of the RE generated and maximum of the energy demand by four, i.e., equal to the remaining number of discrete values of χ , thus defining the granularity of the energy available (ϵ). Therefore, for each time step, we have associated to the cluster the optimal instantaneous value of reduction fraction of the maximum HAPS cell capacity (χ), as defined by the following algorithm.

Algorithm 6 : Selection of χ

```

1: for  $t = 1, T$  do ▷ for each time step
2:   if  $RE^t > d^t$  then
3:      $\chi^t \leftarrow 0$ 
4:   else
5:     if  $|E^t| < \epsilon$  then
6:        $\chi^t \leftarrow 0.25$ 
7:     else if  $|E^t| < 2\epsilon$  then
8:        $\chi^t \leftarrow 0.5$ 
9:     else if  $|E^t| < 3\epsilon$  then
10:       $\chi^t \leftarrow 0.75$ 
11:    else if  $|E^t| < 3\epsilon$  then
12:       $\chi^t \leftarrow 1$ 
13:    end if
14:  end if
15: end for

```

It should be emphasized that the algorithm for choosing χ is repeated for each of the 16 traffic zones.

An example of the result of assigning the value of χ following the application of the algorithm is shown in Figure 4.18.

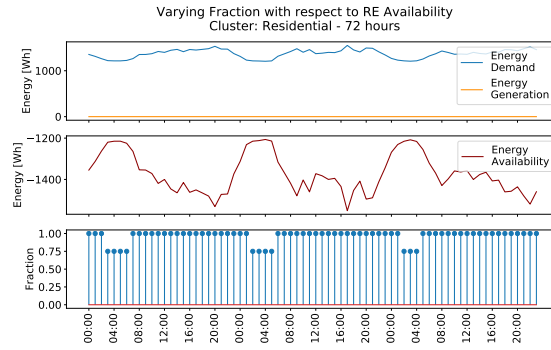


Figure 4.18: Selection of the optimal χ values for the Residential cluster over a 72 hours period

The reason why we made this choice for the value of χ is that when the RE produced by the cluster is in a sufficient quantity to supply energy we decrease the value of the reduction fraction. This means that we reserve HAPS capabilities for other clusters that need a greater supply of energy. From Figure 4.18, it can be seen that when the energy availability curve (red curve) is greater than zero, the value of χ is equal to 0. This means that the HAPS beam directed towards the Residential cluster will be turned off from 12 pm to 15 pm, to then increase its range until the RE produced by the cluster is close to zero.

For completeness, we decided to verify the correctness of the algorithm for selecting the optimal χ values even in a scenario where there is no RE production on the ground. For this, we analyzed the results obtained on the HAPS Offloading with Dynamic Beam configuration. The results for the Residential cluster are shown in Figure 4.19.

As can be seen from Figure 4.19, the values of χ tend to be at least equal to 0.75. This behavior is fully expected because as it can be seen from the trend of the energy generation curve (orange curve), there is no energy production so we tend to exploit HAPS more. For this reason, we choose to reduce the capacity of the HAPS cell only if the energy demand (blue curve) is low, i.e. at night, between 3 am and 6 am.

So at the end of these processes, we got a combination of optimal τ and χ values for each cluster, thus making HAPS adaptable to real cluster conditions. Consequently, we verified the effect of these changes by analyzing the KPIs for the five sample areas.

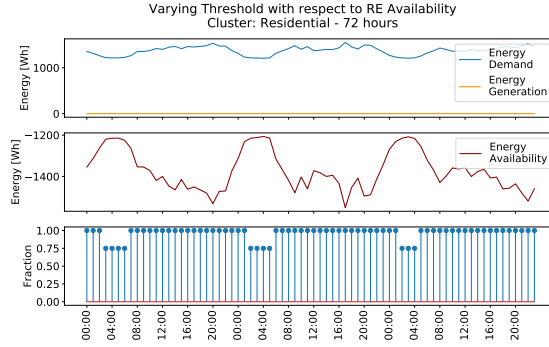


Figure 4.19: Selection of the optimal χ values for the Residential cluster over a 72 hours period - Configuration: HAPS Offloading with Dynamic Beam

We have analyzed two different scenario configurations: (i) HAPS Offloading with Dynamic Beam; and (ii) RE on Cluster + HAPS Offloading with Dynamic Beam. For each of the two configurations we compared the scenario with application of the dynamic strategy of selection of τ and χ (called for simplicity Dynamic Threshold Strategy), and the scenario without application of this strategy (called Fixed Threshold Strategy for simplicity). Furthermore, where necessary, the parameters have been as follows: (PV, B) = (3, 4) [kWp, kWh], $\tau = 0.37$, and $\chi = 0.5$.

The results obtained for the simulation of scenarios with HAPS Offloading with Dynamic Threshold configuration are shown in Figure 4.20.

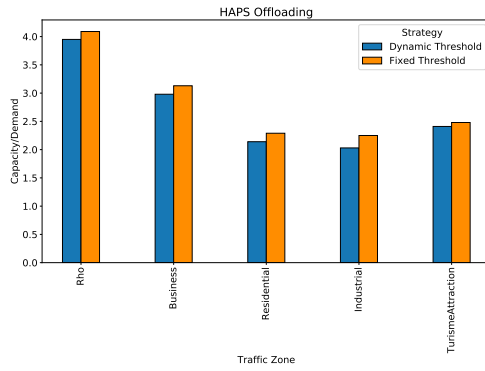
The plots show that through the adoption of the dynamic choice strategy of τ and χ there is an improvement in the results of the KPIs. In particular, it can be seen from the graph in Figure 4.20(a) that in all five sample areas we have a reduction in the value of the capacity demand ratio. This result is closely linked to the trend of Figure 4.20(e), which shows us that HAPS manages on average 30% more traffic in the case of the Dynamic Threshold strategy applied. Therefore, these two results suggest that the capacity provided by HAPS is exploited in a better way than when the Dynamic Threshold strategy is not applied, because despite the capacity demand ratio is almost identical, the HAPS is exploited more, keeping stable the QoS. By moving more traffic to the HAPS, there is inevitably a conspicuous reduction in the energy taken from the grid, as can be seen in Figure 4.20(b). This reduction involves an interesting increase in energy grid reduction both in relative and absolute value, as shown in Figure 4.20(c) and (d). A final consideration must be made on the energy grid cost reduction. As can be seen from Figure 4.20(f), we are witnessing a significant increase in cost reduction. The result

obtained on Rho is particularly interesting: there is an increase of approximately 53% in cost savings. This saving is remarkably high and allows us to establish that in traffic areas such as that of Rho, where the traffic is very variable and does not have a cyclic pattern, it is very convenient to use a strategy like the one we propose that adapts the use of the HAPS to the dynamically varying real time conditions of the area.

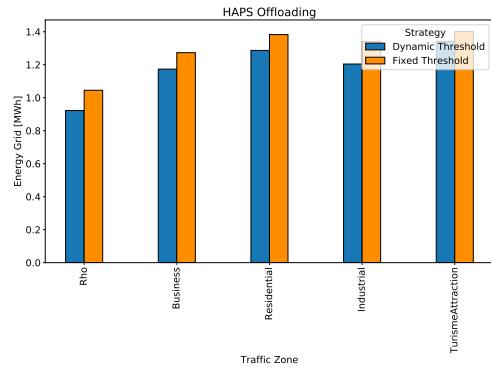
Finally, the results obtained for the simulation of scenarios with RE on Cluster + HAPS Offloading with Dynamic Threshold configuration are shown in Figure 4.21.

Looking at the graphs in Figure 4.21, we note that generally the behavior is very similar to what is obtained in the HAPS Offloading with Dynamic Beam configuration. Quantitatively, the results are better thanks to the presence of the RE supply on the ground, while the difference between the two strategies is smaller than in the previous configuration.

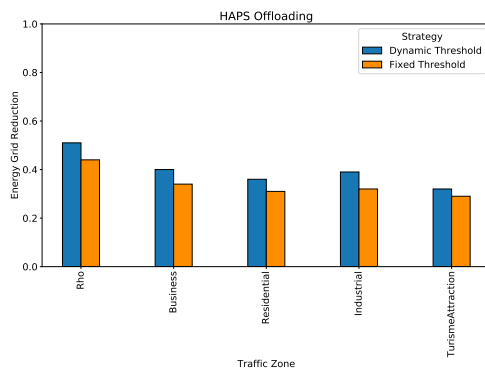
In conclusion, we can confirm that the adoption of the strategy based on the dynamic choice strategy of τ and χ has significantly improved the performance of the considered clusters. The use of the proposed algorithms has made it possible to develop a strategy capable of adapting the capacity of the HAPS to the traffic conditions of the cluster, to the trend in the price of energy and the quantity of RE produced automatically and in real time.



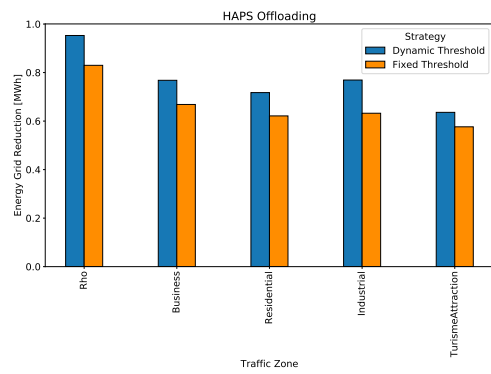
(a) Capacity Demand Ratio



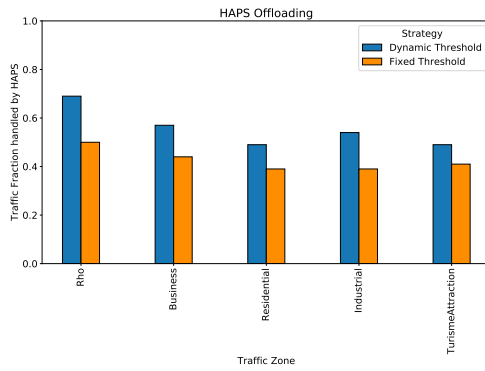
(b) Energy Grid



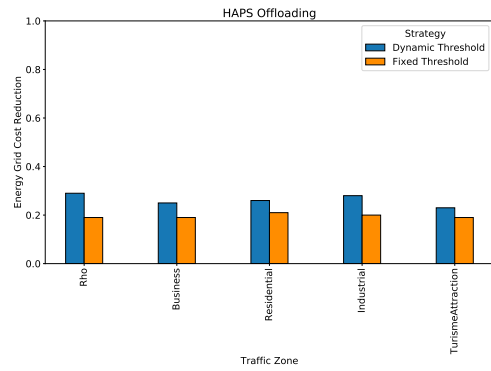
(c) Relative Energy Grid Reduction



(d) Absolute Energy Grid Reduction

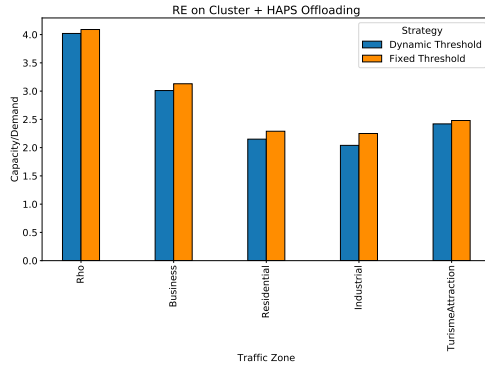


(e) Traffic Fraction Handled by HAPS

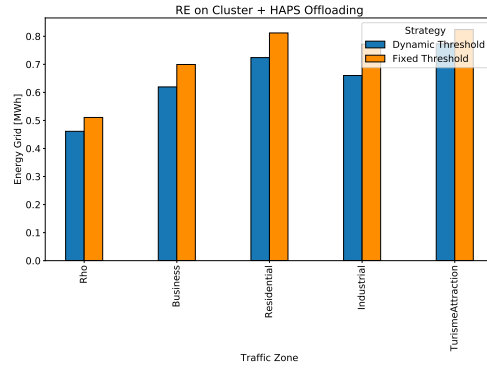


(f) Energy Grid Cost Reduction

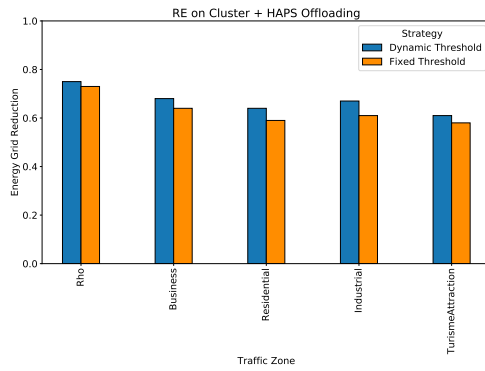
Figure 4.20: Analysis of the strategy for the dynamic choice of τ and χ with the HAPS Offloading with Dynamic Beam strategy applied



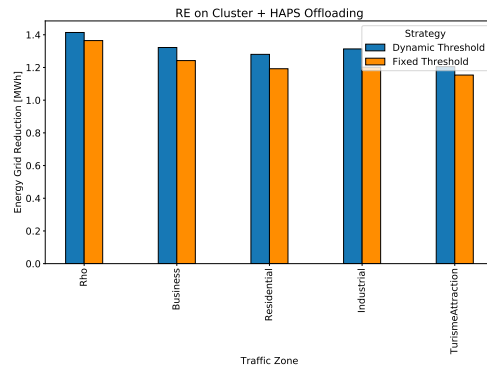
(a) Capacity Demand Ratio



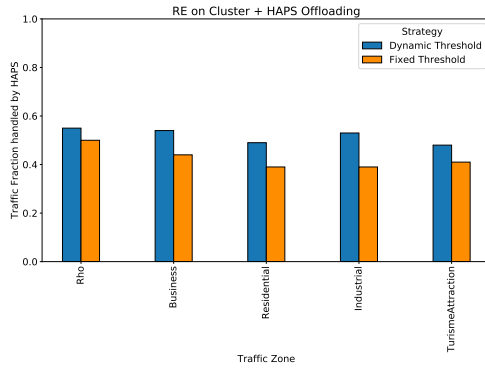
(b) Energy Grid



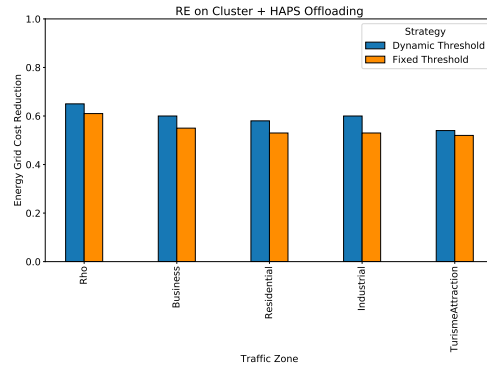
(c) Relative Energy Grid Reduction



(d) Absolute Energy Grid Reduction



(e) Traffic Fraction Handled by HAPS



(f) Energy Grid Cost Reduction

Figure 4.21: Analysis of the strategy for the dynamic choice of τ and χ with the RE on Cluster + HAPS Offloading with Dynamic Beam strategy applied

4.2.6 Analysis of a realistic scenario: interaction between two clusters

In this last analysis we suppose to simulate a realistic scenario, in which we imagine to offer coverage to two distinct clusters, having different characteristics, through the same HAPS. Unlike the analyzes carried out so far, in which we have not imagined cooperation between the clusters and therefore each cluster had its own directed HAPS beam, in this study we assume that the capacity provided to each of the two clusters depends on the traffic conditions of the cluster itself and the other cluster. To have a clearer view of the scenario we have simulated, it is useful to observe the diagram in Figure 4.22.

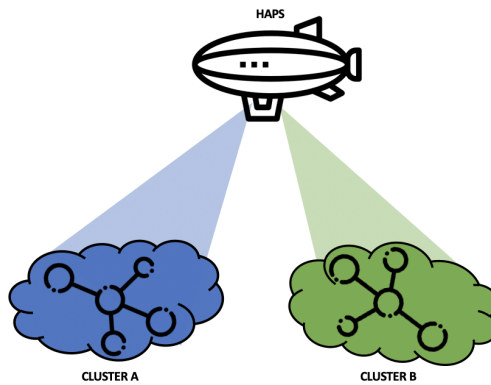


Figure 4.22: Schematic of the scenario for the analysis of the interaction between two clusters at the same time

The diagram in Figure 4.22 shows that a single HAPS offers additional capacities for two clusters, called for simplicity cluster A and cluster B, simultaneously through two distinct HAPS beams. The purpose of this simulation is to study the behavior of the HAPS in a realistic situation, i.e. in which the HAPS is able to instantly adapt the capacity of the cells based on certain variables, such as data traffic, energy availability and others.

In the case in question, having two clusters at the same time, we assumed the maximum available capacity equal to 300 Mbps, which is double the capacity assumed for a single cluster in the first part of this work, as demonstrated in Section 3.4. The total available capacity is not necessarily uniformly distributed among the clusters, but a cluster can be assigned a higher amount of capacity than the other.

To determine the effectiveness of the proposed algorithm, we choose to simulate

two distinct scenarios: (i) scenario S1, in which the Business and Residential clusters are considered; and (ii) scenario S2, in which the Business and Rho clusters are considered. In the S1 scenario we perform two further configurations: (i) configuration A, in which we assign RE on Cluster + HAPS Offloading with Dynamic Beam configuration for both clusters; and (ii) configuration B, in which we both assign the HAPS Offloading configuration with Dynamic Beam configuration. In the S2 scenario, on the other hand, we assigned the HAPS Offloading configuration with Dynamic Beam to the Business cluster and RE on Cluster + HAPS Offloading with Dynamic Beam to the Rho cluster. We made this choice to observe how the system reacts when the two clusters have two different configurations, due to possible physical or bureaucracy constraints that may limit the free PV panel installation in some areas, and how much this scenario produces different results than the one in which the two clusters have the same configuration. Furthermore, the S2 scenario was developed to analyze the system performance in areas with spatial constraints (e.g. Business), where it is difficult to install PV panels, compared to areas without any restrictions (e.g. Rho).

It should be emphasized that in both simulations we used the algorithm for the dynamic choice of the instantaneous values of τ presented in Section 4.2.5, while for the selection of the instantaneous values of χ we have developed another algorithm. Moreover, it should be emphasized that we have chosen to compare the results obtained in the analysis with the interaction of two clusters, with the results obtained in the analysis in which the clusters are treated individually.

The first part of the algorithm for the selection of the instantaneous values of χ , concerns the definition of the state of the clusters. Suppose it is the n^{th} cluster and we check the amount of instant traffic present in the cluster (λ_n^t). If λ_n^t is less than the total capacity of the cluster (C_n) times the instantaneous threshold (τ_n^t), determined a priori through the dynamic selection algorithm of the threshold, then we define that cluster n is below threshold, otherwise we define that cluster n it is above the threshold. Assuming we have N clusters, at the end of the algorithm a vector (X) of zeros and ones is generated, which determines whether a cluster is above or below the threshold.

In practice, the cluster state selection algorithm can be summarized through the following pseudocode.

Algorithm 7 : Cluster state

```

1: for  $t = 1, T$  do                                ▷ for each time step
2:    $X \leftarrow 0 \times N$                           ▷ cluster state vector initialized to zero
3:   for  $n = 1, N$  do                                ▷ for each cluster
4:     if  $\lambda_n^t \leq \tau_n^t \cdot C_n$  then
5:        $X_n \leftarrow 1$                             ▷ cluster n is below the threshold
6:     else
7:        $X_n \leftarrow 0$                             ▷ cluster n is above the threshold
8:     end if
9:   end for
10: end for

```

The presented algorithm is scalable for any number of clusters. In our case, having only two clusters at the same time, we have three cases at the end of the process:

- (i) both clusters are below the threshold, so we adopt the reduction strategy for both, considering τ and χ initialized through the dynamic choice strategy of the threshold;
- (ii) one cluster is below the threshold and the other is above the threshold, which means the cluster above the threshold will need more capacity from the HAPS, so we allocate to that cell χ equal to 2 minus χ of the sub-threshold cluster, the latter obtained using the dynamic selection method presented in Section 4.2.5;
- (iii) both clusters are above the threshold, so have chosen to allocate all the available capacity in proportion to the amount of traffic of each cluster, so as not to have unused HAPS capacity.

Below, we report the results obtained for the analyzes on the Business and Residential clusters, and on the Business and Rho clusters.

A. Scenario S1: Business and Residential clusters

To make the two clusters impartial, we have decided to associate the dimensions of (PV, B) to each cluster, which allow for the same percentage of energy grid reduction in both. Taking up the results obtained in Figure 4.1, we have chosen to associate 3 kWp with Business for PV panels and 3 kWh for batteries, while with Residential 4 kWp for PV panels and 3 kWh for batteries, because both guarantee the same percentage of energy grid reduction, i.e., around 70%.

The result of applying the dynamic choice strategy of the threshold τ and the fraction χ , based on the state of the clusters, is shown in Figure 4.23.

The charts in Figure 4.23 show the variation of the beams capacity in a specific week for the two clusters considered. Observing the profile of the residential area, it is noted that in some hours on Sunday all the available capacity is allocated, i.e. 300 Mbps, while, in the same hours, the beam directed to the business area is turned off: this behaviour is optimal, because on Sundays people stay at home and therefore workplaces are presumably empty.

We have chosen to collect the results obtained on the KPIs in tables, in order to quantitatively observe the variations obtained. In particular, we defined configuration A, the RE on Cluster + HAPS Offloading with Dynamic Beam configuration, and configuration B, the HAPS Offloading with Dynamic Beam configuration. Furthermore, for the results obtained from the analysis in which the clusters are treated individually we used the strategy with fixed τ and χ , in which we used the following parameters: $(PV, B) = (3,4)$ [kWp, kWh] (only for configuration A), $\tau = 0.37$, and $\chi = 0.5$.

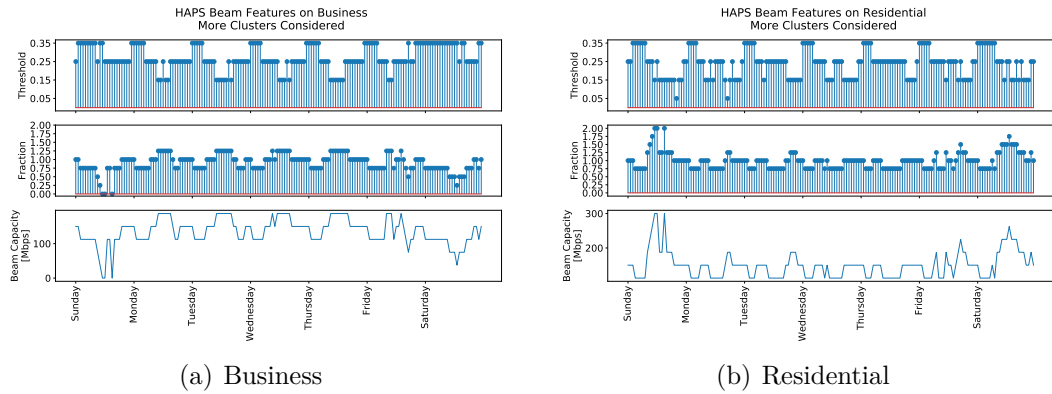


Figure 4.23: Allocation of HAPS capacity for the two Business and Residential clusters

Table 4.9: Result of the interaction between two cluster in the Business cluster with the RE on Cluster + HAPS Offloading with Dynamic Beam configuration

KPI	Configuration A	
	Cluster: Business	
	Single Cluster	Scenario S1
Capacity Demand Ratio	3.13	3.03
Energy Grid Reduction [%]	64	65
Traffic Fraction Handled by HAPS [%]	44	53
Energy Grid Cost Reduction [%]	55	55

Table 4.10: Result of the interaction between two cluster in the Residential cluster with the RE on Cluster + HAPS Offloading with Dynamic Beam configuration

KPI	Configuration A	
	Cluster: Residential	
	Single Cluster	Scenario S1
Capacity Demand Ratio	2.29	2.13
Energy Grid Reduction [%]	59	64
Traffic Fraction Handled by HAPS [%]	39	50
Energy Grid Cost Reduction [%]	53	57

Regarding the configuration RE on Cluster + HAPS Offloading with Dynamic Beams, as can be seen from Tables 4.9 and 4.10, in both clusters there is a decrease of about 15% in the capacity demand ratio, while we have an increase in the traffic fraction handled by HAPS of 20% on Business and 28% on Residential. These results show us that in the case of cluster interaction, the distribution of traffic changes, as HAPS manages more traffic, but the capacity demand ratio undergoes an acceptable variation and still remains in high values. This implies that the QoS is not affected: on the contrary, the available capacity is better exploited. Instead, as far as savings are concerned, we observe a different behavior in the two clusters. In detail, we see that in Business there is no variation in the energy grid cost reduction and an increase of only 1.5% in the energy grid reduction. In the Residential zone we have 8% increases in the energy grid cost reduction and 9% in the energy grid reduction. This situation is plausible, because as can be seen from Figure 4.23, in the Residential area more capacity is allocated by HAPS while in the Business area only in some central working hours of the week, χ reaches 1.25,

i.e., more capacity is allocated than to Residential.

In general, we observe that the results obtained through the interaction of two clusters simultaneously are better than the results obtained in the case of analyzing the clusters individually, demonstrating that the application of properly designed algorithms for the management and dynamic allocation of capacities improves the performance in the case of a more realistic scenario.

Table 4.11: Result of the interaction between two cluster in the Business cluster with the HAPS Offloading with Dynamic Beam configuration

KPI	Configuration B	
	Cluster: Business	
	Single Cluster	Scenario S1
Capacity Demand Ratio	3.13	3.01
Energy Grid Reduction [%]	34	40
Traffic Fraction Handled by HAPS [%]	44	56
Energy Grid Cost Reduction [%]	19	25

Table 4.12: Result of the interaction between two cluster in the Residential cluster with the HAPS Offloading with Dynamic Beam configuration

KPI	Configuration B	
	Cluster: Residential	
	Single Cluster	Scenario S1
Capacity Demand Ratio	2.29	2.15
Energy Grid Reduction [%]	31	35
Traffic Fraction Handled by HAPS [%]	39	48
Energy Grid Cost Reduction [%]	21	26

Regarding the configuration HAPS Offloading with Dynamic Beam, as can be seen from Tables 4.11 and 4.12, for the capacity demand ratio and for the traffic fraction handled by HAPS the same considerations made for configuration A apply. However, as regards the savings, it is noted that the benefit of using the Multi-cluster strategy is more evident than the RE on Cluster + HAPS Offloading scenario. The advantage both in terms of energy saved and costs is also evident in the cluster of the Business zone: in this configuration, we have an increase of 32% of the energy grid cost reduction and of 18% of the energy grid reduction, while in

the configuration A these increases have been null or only of 1.5% . Furthermore, focusing on Residential, in the case of HAPS Offloading we have a cost reduction that has an increase of 24%, while in the case of RE on Cluster + HAPS Offloading we have had a cost reduction increased by only 8%.

Finally, we can confirm that the results obtained, especially in the case of applying the HAPS Offloading configuration, are satisfactory. These results in fact show us that in traffic areas where it is not possible to have PV panels available, the use of the HAPS Offloading strategy with dynamic capacity management results in very high economic and energy benefits. Furthermore, observing also the KPI related to the system capacity, it is observed that the QoS is not affected, on the contrary there is a better exploitation of the available resources.

B. Scenario S2: Business and Rho clusters

In this simulation we have chosen to reproduce an even more realistic scenario. In fact, we thought of observing how the system reacts in the case in which the two clusters have different intrinsic configurations. For this reason, we have chosen to apply the RE on Cluster + HAPS with Dynamic Beam configuration to Rho: being a peripheral area with an area of 5.31 km² available, we have decided to use PV panels with size 6 kWp and batteries with size 6 kWh. Instead, being Business a central area with little space available, as it has an extension of 560 m², we have chosen to apply the HAPS Offloading with Dynamic Beam configuration, i.e. without the presence of RE on the ground.

The result of applying the dynamic choice strategy of τ and χ , based on the state of the clusters, is shown in Figure 4.24.

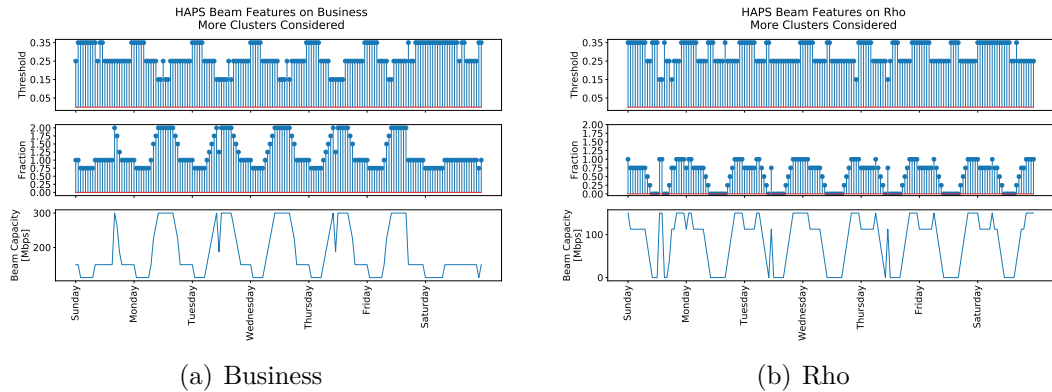


Figure 4.24: Allocation of HAPS capacity for the two Business and Rho clusters

The results shown in Figure 4.24 show us that on Rho χ is at most equal to 1, that is, the strategy of reducing the percentage of beam of the active HAPS is always applied, precisely due to the fact that (PV, B) larger. On the contrary, on Business, since there is no RE on the ground, HAPS is exploited more often with χ which is more often greater than 1, i.e., more capacity is provided. These results are very positive, because they show us that the applied strategy is able to correctly manage the amount of HAPS capacity to be allocated to each cell, based on the cluster configuration.

Also in this case it was decided to collect the results obtained on the KPIs in tables, in order to quantitatively observe the variations obtained. The tables compare the results obtained for each cluster, in the case of clusters treated together and individually. More precisely, for the results obtained from the analysis in which the clusters are treated individually we used the strategy with fixed τ and χ , set equal to 0.37 and 0.5 respectively. For Rho, in the case of cluster treated individually, we have selected (PV, B) = (3, 4) [kWp, kWh].

Table 4.13: Result of the interaction between two cluster in the Business cluster with the HAPS Offloading with Dynamic Beam configuration

KPI	Cluster: Business	
	Single Cluster	Scenario S2
Capacity Demand Ratio	3.13	2.87
Energy Grid Reduction [%]	34	44
Traffic Fraction Handled by HAPS [%]	44	64
Energy Grid Cost Reduction [%]	19	31

Table 4.14: Result of the interaction between two cluster in the Rho cluster with the RE on Cluster + HAPS Offloading with Dynamic Beam configuration

KPI	Cluster: Rho	
	Single Cluster	Scenario S2
Capacity Demand Ratio	4.09	4.02
Energy Grid Reduction [%]	73	74
Traffic Fraction Handled by HAPS [%]	50	48
Energy Grid Cost Reduction [%]	61	63

The results obtained and reported in Tables 4.13 and 4.14 show that the system

reacts very well even in situations where we have two clusters configured differently from each other. Starting from the Business cluster, it can be seen that with an 8% reduction in the capacity demand ratio, the traffic managed by HAPS goes from 44% to 64%. By moving more traffic to the aerial platform, energy savings of 44% are achieved, which is about 30% more than if the Business cluster is managed individually. This energy saving translates into an economic saving of over 63% if the cluster is managed individually. Furthermore, the positive aspect lies in the fact that the Rho district also obtains better results if treated simultaneously with the business district. Although Rho's data traffic is mainly managed on the ground, there is still a slight increase in energy and monetary savings. Once again we can confirm that the use of the HAPS Offloading strategy implies relevant benefits affecting energy, economic and QoS performances, not only for those clusters that have more capacity reserved, but consequently also for the clusters that are covered by the same HAPS.

Chapter 5

Conclusions

In this thesis work, we simulated to integrate a mobile network with a ground infrastructure with an air network formed by a HAPS acting as HAPS-SMBS. We plan to offer coverage for 16 traffic zones which include urban and suburban areas of the city of Milan (Italy). For each traffic zone, we consider a sample cluster of 7 BSs (i.e. 1 macro BS and 6 micro BSs) powered by PV panels, equipped with energy storage units and connection to the electricity grid. We have studied the effectiveness of resource management strategies, such as RoD and HAPS Offloading, modifying the parameters and analyzing increasingly complex scenarios, in order to reduce the energy consumption from the grid and limiting the operational cost, without significantly impairing the QoS.

With our analysis, we have shown that in areas with a low traffic load, such as rural areas or remote areas, it is better to take advantage of HAPS instead of putting a more expensive infrastructure on the ground. Furthermore, we have shown that in high-density urban areas, where it is not possible to install large PV panels, it is possible to exploit more HAPS to have excellent results, obtaining an energy saving greater than about 30% compared to that obtainable with a small supply of RE and achieving excellent levels of QoS.

Finally, through the analysis of a realistic scenario, in which we have dynamically adapted the HAPS capacity on two clusters, it was possible to evaluate the correctness and the efficiency of the dynamic algorithm for the choice of the threshold values and the fraction of reduction of the maximum capacity of the HAPS beam, within the type of traffic zone. The results highlight the potential of HAPS in terms of flexibility in the dynamic distribution of capacity in space and time, in order to effectively adapt to changes in external factors. Furthermore, the results focus the importance of developing appropriately designed resource and energy management

strategies and fine-tuning the setting parameters, in order to optimize the effectiveness of the presence of a HAPS-SMBS and the green energy produced on the ground.

As a future work, it could be planned to simulate the behavior of this new type of mobile network with more than two clusters considered together. This may require the development of a more complex algorithm, which tends to simulate an increasingly realistic scenario to furthermore enhance the benefits introduced by the presence of HAPSs as complementary aerial network nodes in future mobile networks.

Bibliography

- [1] *Wireless Connectivity Market by Connectivity Technology, Type, End-use And Region - Global Forecast to 2025*. White Paper. MarketsandMarkets, Oct. 2020. URL: <https://www.marketsandmarkets.com/Market-Reports/wireless-connectivity-market-192605963.html> (cit. on p. 2).
- [2] Chin-Lung Hsu and Judy Chuan-Chuan Lin. «Exploring Factors Affecting the Adoption of Internet of Things Services». In: *Journal of Computer Information Systems* 58.1 (2018), pp. 49–57. DOI: [10.1080/08874417.2016.1186524](https://doi.org/10.1080/08874417.2016.1186524) (cit. on p. 2).
- [3] IEEE Transmitter. *Why the Development of Wireless Networks Is Important for Global IoT Growth*. <https://transmitter.ieee.org/why-the-development-of-wireless-networks-is-important-for-global-iot-growth/>. Accessed: 2021-06-24 (cit. on p. 2).
- [4] D. van Welsum, W. Overmeer, van Ark, European Commission. Directorate-General for the Information Society, Media, and Conference Board. *Unlocking the ICT Growth Potential in Europe: Enabling People and Businesses : Using Scenarios to Build a New Narrative for the Role of ICT in Growth in Europe. Final Background Report*. Publications Office, 2013. ISBN: 9789279347047. URL: <https://books.google.it/books?id=Dm3onQAACAAJ> (cit. on p. 2).
- [5] Department of Economic United Nations and Social Affairs. *World Urbanization Prospects: The 2018 Revision (ST/ESA/SER.A/420)*. Population Division, August 2019. ISBN: 9789210043144. DOI: <https://doi.org/10.18356/b9e995fe-en> (cit. on p. 2).
- [6] Mirjam Johannes. *Smart City and Urbanization Challenges*. <https://www.e-zigurat.com/blog/en/smart-cities-urbanization-challenges/>. Accessed: 2021-06-24. Zigurat, Global Institute of Technology, May 2019 (cit. on p. 2).
- [7] Adnan Akhunzada, Saif ul Islam, and Sherali Zeadally. «Securing Cyberspace of Future Smart Cities with 5G Technologies». In: *IEEE Network* 34.4 (2020), pp. 336–342. DOI: [10.1109/MNET.001.1900559](https://doi.org/10.1109/MNET.001.1900559) (cit. on p. 2).

- [8] Sam Musa. «Smart Cities - A Roadmap for Development». In: *Journal of Telecommunications System Management* 05 (Jan. 2016). DOI: [10.4172/2167-0919.1000144](https://doi.org/10.4172/2167-0919.1000144) (cit. on p. 3).
- [9] Reply. *5G and Smart Cities: smarter solutions for a hyperconnected future*. <https://www.reply.com/en/industries/telco-and-media/5g-smart-cities>. Accessed: 2021-06-24 (cit. on p. 3).
- [10] Mitsuru Kodama. «The World's First 3G Mobile Phone Service: A Case Study of Innovation». In: *Journal of General Management* 28 (2002), pp. 43–57. DOI: [10.1177/030630700202800203](https://doi.org/10.1177/030630700202800203) (cit. on p. 4).
- [11] *Global Mobile Trends 2021 - Navigating Covid-19 and beyond*. Report. GSMA Intelligence, Dec. 2020. URL: <https://data.gsmaintelligence.com/api-web/v2/research-file-download?id=58621970&file=141220-Global-Mobile-Trends.pdf> (cit. on pp. 5–7).
- [12] *This is 5G*. Report. Ericsson, 2020. URL: https://www.ericsson.com/49df43/assets/local/newsroom/%20media-kits/5g/doc/ericsson_this-is-5g_pdf_2019.pdf (cit. on p. 6).
- [13] *5G Spectrum - GSMA Public Policy Position*. Report. GSMA, Mar. 2021. URL: <https://www.gsma.com/spectrum/wp-content/uploads/2021/04/5G-Spectrum-Positions.pdf> (cit. on p. 7).
- [14] Sacha Kavanagh. *What is 5G New Radio (5G NR)*. <https://5g.co.uk/guides/what-is-5g-new-radio/>. Accessed: 2021-06-27. 5G.co.uk, March 2020 (cit. on p. 7).
- [15] Lei Wan, Zhiheng Guo, and Xiang Chen. «Enabling Efficient 5G NR and 4G LTE Coexistence». eng. In: *IEEE wireless communications* 26.1 (2019), pp. 6–8. DOI: [10.1109/MWC.2019.8641417](https://doi.org/10.1109/MWC.2019.8641417) (cit. on p. 7).
- [16] *Recommendation ITU-R M.2083-0 - IMT Vision – Framework and overall objectives of the future development of IMT for 2020 and beyond*. Report. Geneva, Switzerland: ITU-R, 2015. URL: https://www.itu.int/dms_pubrec/itu-r/rec/m/R-REC-M.2083-0-201509-I!!PDF-E.pdf (cit. on pp. 7, 8, 16).
- [17] *CISCO Annual Internet Report (2018-2023)*. White Paper. CISCO, Mar. 2020. URL: <https://www.cisco.com/c/en/us/solutions/collateral/executive-perspectives/annual-internet-report/white-paper-c11-741490.html> (cit. on p. 9).
- [18] ITU. *5G - Fifth generation of mobile technologies*. <https://www.itu.int/en/mediacentre/backgrounders/Pages/5G-fifth-generation-of-mobile-technologies.aspx>. Accessed: 2021-06-27. December 2019 (cit. on p. 9).

- [19] M. Fiore L. Chiaraviglio and E. Rossi. «5G Technology: Which Risks From the Health Perspective?» In: *The 5G Italy Book 2019: a Multiperspective View of 5G*. Rome, Italy, 2019, pp. 37–48 (cit. on p. 9).
- [20] Ta-Hao Ting, Tsung-Nan Lin, Shan-Hsiang Shen, and Yu-Wei Chang. «Guidelines for 5G End to End Architecture and Security Issues». In: *CoRR* abs/1912.10318 (2019). URL: <http://arxiv.org/abs/1912.10318> (cit. on p. 10).
- [21] *5G Network Architecture - A High-Level Perspective*. White Paper. Huawei Technologies Co., Ltd., 2016. URL: <https://www.huawei.com/minisite/hwmbbf16/insights/5G-Nework-Architecture-Whitepaper-en.pdf> (cit. on pp. 10, 11).
- [22] Behnaam Aazhang et al. *Key drivers and research challenges for 6G ubiquitous wireless intelligence (white paper)*. Sept. 2019. ISBN: 978-952-62-2353-7 (cit. on p. 11).
- [23] Sofie Lambert, Ward Heddeghem, Willem Vereecken, Bart Lannoo, Didier Colle, and Mario Pickavet. «Worldwide electricity consumption of communication networks». In: *Optics express* 20 (Dec. 2012), B513–24. DOI: [10.1364/OE.20.00B513](https://doi.org/10.1364/OE.20.00B513) (cit. on p. 12).
- [24] Mohammed H. Alsharif, Anabi Hilary Kelechi, Mahmoud A. Albreem, Shehzad Ashraf Chaudhry, M. Sultan Zia, and Sunghwan Kim. «Sixth Generation (6G) Wireless Networks: Vision, Research Activities, Challenges and Potential Solutions». In: *Symmetry* 12.4 (2020). ISSN: 2073-8994. DOI: [10.3390/sym12040676](https://doi.org/10.3390/sym12040676). URL: <https://www.mdpi.com/2073-8994/12/4/676> (cit. on p. 12).
- [25] Khaled B Letaief, Wei Chen, Yuanming Shi, Jun Zhang, and Ying-Jun Angela Zhang. «The Roadmap to 6G – AI Empowered Wireless Networks». eng. In: (2019) (cit. on p. 12).
- [26] *6G - The Next Hyper Connected Experience for All*. White Paper. Samsung, July 2021. URL: <https://cdn.codeground.org/nsr/downloads/researchareas/6G%5C%20Vision.pdf> (cit. on pp. 13–15, 17, 18).
- [27] Benjamin Sliwa, R. Falkenberg, and C. Wietfeld. «Towards Cooperative Data Rate Prediction for Future Mobile and Vehicular 6G Networks». In: *2020 2nd 6G Wireless Summit (6G SUMMIT)* (2020), pp. 1–5 (cit. on p. 16).
- [28] Muhammad Waseem Akhtar, Syed Hassan, Rizwan Ghaffar, Haejoon Jung, Sahil Garg, and M. Shamim Hossain. «The shift to 6G communications: vision and requirements». In: *Human-centric Computing and Information Sciences* 10 (Dec. 2020). DOI: [10.1186/s13673-020-00258-2](https://doi.org/10.1186/s13673-020-00258-2) (cit. on p. 16).

- [29] FCC Docket 18-21. *FCC Opens Spectrum Horizons for New Services and Technologies*. <https://docs.fcc.gov/public/attachments/DOC-356588A1.pdf>. March 15, 2019 (cit. on p. 16).
- [30] 3GPP. *Study on requirements for NR beyond 52.6 GHz*. Technical report (TR) 38.807. Version 16. 3rd Generation Partnership Project (3GPP), Mar. 2021. URL: <https://portal.3gpp.org/desktopmodules/Specifications/SpecificationDetails.aspx?specificationId=3522> (cit. on p. 17).
- [31] Marco Giordani and Michele Zorzi. «Non-Terrestrial Networks in the 6G Era: Challenges and Opportunities». In: *IEEE Network* 35.2 (2021), pp. 244–251. DOI: [10.1109/MNET.011.2000493](https://doi.org/10.1109/MNET.011.2000493) (cit. on pp. 18, 25).
- [32] Mohammad Mozaffari, Ali Taleb Zadeh Kasgari, Walid Saad, Mehdi Bennis, and Mérouane Debbah. «Beyond 5G With UAVs: Foundations of a 3D Wireless Cellular Network». In: *IEEE Transactions on Wireless Communications* 18.1 (2019), pp. 357–372. DOI: [10.1109/TWC.2018.2879940](https://doi.org/10.1109/TWC.2018.2879940) (cit. on p. 18).
- [33] Marco Giordani and Michele Zorzi. «Satellite Communication at Millimeter Waves: a Key Enabler of the 6G Era». In: *2020 International Conference on Computing, Networking and Communications (ICNC)*. 2020, pp. 383–388. DOI: [10.1109/ICNC47757.2020.9049651](https://doi.org/10.1109/ICNC47757.2020.9049651) (cit. on pp. 18, 24).
- [34] Federica Rinaldi, Helka-Liina Maattanen, Johan Torsner, Sara Pizzi, Sergey Andreev, Antonio Iera, Yevgeni Koucheryavy, and Giuseppe Araniti. «Non-Terrestrial Networks in 5G Beyond: A Survey». In: *IEEE Access* 8 (2020), pp. 165178–165200. DOI: [10.1109/ACCESS.2020.3022981](https://doi.org/10.1109/ACCESS.2020.3022981) (cit. on pp. 20–22).
- [35] 3GPP. *Solutions for NR to support Non-Terrestrial Networks (NTN)*. Technical report (TR) 38.821. Version 16.1. 3rd Generation Partnership Project (3GPP), June 2021. URL: <https://portal.3gpp.org/desktopmodules/Specifications/SpecificationDetails.aspx?specificationId=3525> (cit. on pp. 20, 21).
- [36] 3GPP. *Study on New Radio (NR) to support non-terrestrial networks*. Technical report (TR) 38.811. Version 15.4. 3rd Generation Partnership Project (3GPP), Oct. 2020. URL: <https://portal.3gpp.org/desktopmodules/Specifications/SpecificationDetails.aspx?specificationId=3234> (cit. on p. 21).
- [37] Oltjon Kodheli et al. «Satellite Communications in the New Space Era: A Survey and Future Challenges». In: *IEEE Communications Surveys Tutorials* 23.1 (2021), pp. 70–109. DOI: [10.1109/COMST.2020.3028247](https://doi.org/10.1109/COMST.2020.3028247) (cit. on pp. 22, 24).

- [38] Jean-Luc Muraro, Guillaume Nicolas, Do Nhut, Stephane Forestier, Stéphane Rochette, O. Vendier, Dominique Langrez, Jean-Louis Cazaux, and Marziale Feudale. «GaN for space application: Almost ready for flight». In: *International Journal of Microwave and Wireless Technologies* 2 (Apr. 2010). DOI: [10.1017/S1759078710000206](https://doi.org/10.1017/S1759078710000206) (cit. on p. 22).
- [39] Jonathan’s Space Pages. *Starlink Statistics*. <https://planet4589.org/space/stats/star/starstats.html>. Accessed: 2021-07-16 (cit. on p. 22).
- [40] Fulvio Babich, Massimiliano Comisso, Alessandro Cuttin, Mario Marchese, and Fabio Patrone. «Nanosatellite-5G Integration in the Millimeter Wave Domain: A Full Top-Down Approach». In: *IEEE Transactions on Mobile Computing* 19.2 (2020), pp. 390–404. DOI: [10.1109/TMC.2019.2897091](https://doi.org/10.1109/TMC.2019.2897091) (cit. on p. 24).
- [41] Matilde Boschiero, Marco Giordani, Michele Polese, and Michele Zorzi. «Coverage Analysis of UAVs in Millimeter Wave Networks: A Stochastic Geometry Approach». In: *2020 International Wireless Communications and Mobile Computing (IWCMC)*. 2020, pp. 351–357. DOI: [10.1109/IWCMC48107.2020.9148550](https://doi.org/10.1109/IWCMC48107.2020.9148550) (cit. on p. 24).
- [42] Gunes Karabulut Kurt, Mohammad G. Khoshkholgh, Safwan Alfattani, Ahmed Ibrahim, Tasneem Darwish, Md Sahabul Alam, and Abbas Yongacoglu. *A Vision and Framework for the High Altitude Platform Station (HAPS) Networks of the Future*. July 2020 (cit. on pp. 25, 26, 29, 31–33).
- [43] 3GPP. *Study on using satellite access in 5G*. Technical report (TR) 22.822. Version 16. 3rd Generation Partnership Project (3GPP), July 2018. URL: <https://portal.3gpp.org/desktopmodules/Specifications/SpecificationDetails.aspx?specificationId=3372> (cit. on p. 26).
- [44] Alexandru Budianu, Teodoro J. Willink Castro, Arjan Meijerink, and Mark J. Bentum. «Inter-satellite links for cubesats». In: *2013 IEEE Aerospace Conference*. 2013, pp. 1–10. DOI: [10.1109/AERO.2013.6496947](https://doi.org/10.1109/AERO.2013.6496947) (cit. on p. 26).
- [45] *ITU Radio Regulations, Section IV*. Radio Stations and Systems – Article 1.66A. ITU, 2016. URL: <https://search.itu.int/history/HistoryDigitalCollectionDocLibrary/1.43.48.en.101.pdf> (cit. on p. 26).
- [46] HAPSMobile Inc. *HAPS MOBILE*. <https://www.hapsmobile.com/en/>. Accessed: 2021-07-19 (cit. on p. 27).
- [47] Vince Matinde. *Why high altitude platforms are still a good bet for African connectivity*. <https://www.cio.com/article/3612734/why-high-altitude-platforms-are-still-a-good-bet-for-african-connectivity.html>. Accessed: 2021-07-19. CIO from IDG, March 2021 (cit. on p. 28).

- [48] ITU. *HAPS – High-altitude platform systems*. <https://www.itu.int/en/mediacentre/backgrounders/Pages/High-altitude-platform-systems.aspx>. Accessed: 2021-07-19. December 2019 (cit. on p. 28).
- [49] Monroe Conner. *Where Are They Now: Pathfinder Plus*. https://www.nasa.gov/centers/armstrong/history/where_are_they_now/Pathfinder_Plus.html. Accessed: 2021-07-19. NASA, August 2017 (cit. on p. 29).
- [50] Junfei Qiu, David Grace, Guoru Ding, Muhammad D. Zakaria, and Qihui Wu. «Air-Ground Heterogeneous Networks for 5G and Beyond via Integrating High and Low Altitude Platforms». In: *IEEE Wireless Communications* 26.6 (2019), pp. 140–148. DOI: [10.1109/MWC.0001.1800575](https://doi.org/10.1109/MWC.0001.1800575) (cit. on p. 29).
- [51] *Recommendation ITU-R F.1500 - Preferred characteristics of systems in the fixed service using high altitude platforms operating in the bands 47.2-47.5 GHz and 47.9-48.2 GHz*. Report. Geneva, Switzerland: ITU-R, 2010. URL: https://www.itu.int/dms_pubrec/itu-r/rec/f/R-REC-F.1500-0-200005-I!!PDF-E.pdf (cit. on p. 30).
- [52] Vasilis Milas, Maria Koletta, and Philip Constantinou. «Interference and Compatibility Studies Between Satellite Service Systems and Systems Using High Altitude Platform Stations». In: *ESA Special Publication*. Ed. by H. Lacoste. Vol. 541. ESA Special Publication. July 2003, p. 34 (cit. on p. 30).
- [53] Ryu Miura and Masayuki Oodo. «Wireless Communications System Using Stratospheric Platforms: R and D Program on Telecom and Broadcasting System Using High Altitude Platform Stations». In: *Journal of the Communication Research Laboratory*, vol. 48, iss. No. 4, p. 33-48 (Dec. 2001) (cit. on p. 30).
- [54] *Recommendation ITU-R F.2438-0 - Spectrum needs of high-altitude platform stations broadband links operating in the fixed service*. Report. Geneva, Switzerland: ITU-R, 2018. URL: https://www.itu.int/dms_pub/itu-r/opb/rep/R-REP-F.2438-2018-PDF-E.pdf (cit. on pp. 30, 52).
- [55] D. Grace and Mihael Mohorcic. «Broadband Communications via High Altitude Platforms». In: *Broadband Communications via High Altitude Platforms* (Aug. 2010). DOI: [10.1002/9780470971840](https://doi.org/10.1002/9780470971840) (cit. on p. 31).
- [56] Jesús Gonzalo. *Stratospheric platforms HAPPIEST*. <http://uleia.unileon.es/index.php/en/research-projects/aerospace-system-engineering1/unconventional-unmanned-aircrafts/16-research-projects/aerospace-engineering/high-altitude-pseudo-satellites-haps/52-stratospheric-platforms-happiest>. Accessed: 2021-07-20. Aerospace Engineering Area of University of León/Spain, February 2021 (cit. on p. 31).

- [57] Mark Handley. «Using Ground Relays for Low-Latency Wide-Area Routing in Megaconstellations». In: *Proceedings of the 18th ACM Workshop on Hot Topics in Networks*. HotNets '19. Princeton, NJ, USA: Association for Computing Machinery, 2019, pp. 125–132. DOI: [10.1145/3365609.3365859](https://doi.org/10.1145/3365609.3365859) (cit. on p. 32).
- [58] Markku Kojo and Jukka Manner. *Mobility Related Terminology*. RFC 3753. June 2004. DOI: [10.17487/RFC3753](https://doi.org/10.17487/RFC3753). URL: <https://rfc-editor.org/rfc/rfc3753.txt> (cit. on p. 32).
- [59] *What is Intelligent Edge?* https://www.hpe.com/emea_europe/en/what-is/intelligent-edge.html. Accessed: 2021-07-21. Hewlett Packard Enterprise Development LP (cit. on p. 32).
- [60] Panfeng He, Naiping Cheng, and Jianhua Cui. «Handover performance analysis of cellular communication system from high altitude platform in the swing state». In: *2016 IEEE International Conference on Signal and Image Processing (ICSIP)*. 2016, pp. 407–411. DOI: [10.1109/SIPROCESS.2016.7888294](https://doi.org/10.1109/SIPROCESS.2016.7888294) (cit. on p. 33).
- [61] Ogonnaya Anicho, Philip B Charlesworth, Gurvinder S Baicher, Atulya Nagar, and Neil Buckley. «Comparative Study for Coordinating Multiple Unmanned HAPS for Communications Area Coverage». In: *2019 International Conference on Unmanned Aircraft Systems (ICUAS)*. 2019, pp. 467–474. DOI: [10.1109/ICUAS.2019.8797881](https://doi.org/10.1109/ICUAS.2019.8797881) (cit. on p. 33).
- [62] Kuljeet Kaur, Sahil Garg, Gagangeet Singh Aujla, Neeraj Kumar, Joel J. P. C. Rodrigues, and Mohsen Guizani. «Edge Computing in the Industrial Internet of Things Environment: Software-Defined-Networks-Based Edge-Cloud Interplay». In: *IEEE Communications Magazine* 56.2 (2018), pp. 44–51. DOI: [10.1109/MCOM.2018.1700622](https://doi.org/10.1109/MCOM.2018.1700622) (cit. on p. 34).
- [63] Bo Han, Vijay Gopalakrishnan, Lusheng Ji, and Seungjoon Lee. «Network function virtualization: Challenges and opportunities for innovations». In: *IEEE Communications Magazine* 53.2 (2015), pp. 90–97. DOI: [10.1109/MCOM.2015.7045396](https://doi.org/10.1109/MCOM.2015.7045396) (cit. on p. 34).
- [64] Md Sahabul Alam, Gunes Karabulut Kurt, Peiying Zhu, and Ngoc Đào. «High Altitude Platform Station based Super Macro Base Station (HAPS-SMBS) Constellations». In: (July 2020) (cit. on pp. 34, 35, 47).
- [65] Rakesh Taori and Arun Sridharan. «Point-to-multipoint in-band mmwave backhaul for 5G networks». In: *IEEE Communications Magazine* 53.1 (2015), pp. 195–201. DOI: [10.1109/MCOM.2015.7010534](https://doi.org/10.1109/MCOM.2015.7010534) (cit. on p. 36).
- [66] Aditi Malik and Preeti Singh. «Free Space Optics: Current Applications and Future Challenges». In: *International Journal of Optics* 2015 (Nov. 2015), pp. 1–7. DOI: [10.1155/2015/945483](https://doi.org/10.1155/2015/945483) (cit. on p. 36).

- [67] Mohamed Alzenad, Muhammad Z. Shakir, Halim Yanikomeroglu, and Mohamed-Slim Alouini. «FSO-Based Vertical Backhaul/Fronthaul Framework for 5G+ Wireless Networks». In: *IEEE Communications Magazine* 56.1 (2018), pp. 218–224. DOI: [10.1109/MCOM.2017.1600735](https://doi.org/10.1109/MCOM.2017.1600735) (cit. on p. 36).
- [68] Tianyang Bai, Rahul Vaze, and Robert W. Heath. «Analysis of Blockage Effects on Urban Cellular Networks». In: *IEEE Transactions on Wireless Communications* 13.9 (2014), pp. 5070–5083. DOI: [10.1109/TWC.2014.2331971](https://doi.org/10.1109/TWC.2014.2331971) (cit. on p. 37).
- [69] Christian Quadri, Vincenzo Mancuso, Marco Ajmone Marsan, and Gian Paolo Rossi. «Platooning on the Edge». In: *Proceedings of the 23rd International ACM Conference on Modeling, Analysis and Simulation of Wireless and Mobile Systems. MSWiM '20*. Alicante, Spain: Association for Computing Machinery, 2020, pp. 1–10. ISBN: 9781450381178. DOI: [10.1145/3416010.3423220](https://doi.org/10.1145/3416010.3423220). URL: <https://doi.org/10.1145/3416010.3423220> (cit. on p. 38).
- [70] Flavio D'Oliveira, Francisco Melo, and Tessaleno Devezas. «High-Altitude Platforms - Present Situation and Technology Trends». In: *Journal of Aerospace Technology and Management* 8 (Aug. 2016), pp. 249–262. DOI: [10.5028/jatm.v8i3.699](https://doi.org/10.5028/jatm.v8i3.699) (cit. on pp. 38, 39).
- [71] Anggoro Widiawan and Rahim Tafazolli. «High Altitude Platform Station (HAPS): A Review of New Infrastructure Development for Future Wireless Communications». In: *Wireless Personal Communications* 42 (Aug. 2007), pp. 387–404. DOI: [10.1007/s11277-006-9184-9](https://doi.org/10.1007/s11277-006-9184-9) (cit. on p. 38).
- [72] *Report ITU-R F.2471-0 - Sharing and compatibility studies of HAPS systems in the fixed service in the 21.4-22 GHz frequency range for Region 2*. Report. Geneva, Switzerland: ITU-R, 2019. URL: https://www.itu.int/dms_pub/itu-r/opb/rep/R-REP-F.2471-2019-PDF-E.pdf (cit. on p. 38).
- [73] *Report ITU-R F.2472-0 - Sharing and compatibility studies of HAPS systems in the fixed service in the 24.25-27.5 GHz frequency range in Region 2*. Report. Geneva, Switzerland: ITU-R, 2019. URL: https://www.itu.int/dms_pub/itu-r/opb/rep/R-REP-F.2472-2019-PDF-E.pdf (cit. on p. 38).
- [74] *Report ITU-R F.2475-0 - Sharing and compatibility studies of High Altitude Platform Station systems in the fixed service in the 38-39.5 GHz frequency range*. Report. Geneva, Switzerland: ITU-R, 2019. URL: https://www.itu.int/dms_pub/itu-r/opb/rep/R-REP-F.2472-2019-PDF-E.pdf (cit. on p. 38).

- [75] Steve Chukwuebuka Arum, David Grace, and Paul Daniel Mitchell. «A review of wireless communication using high-altitude platforms for extended coverage and capacity». In: *Computer Communications* 157 (2020), pp. 232–256. ISSN: 0140-3664. DOI: <https://doi.org/10.1016/j.comcom.2020.04.020>. URL: <https://www.sciencedirect.com/science/article/pii/S0140366419313143> (cit. on p. 39).
- [76] Killian Fox. *Auguste Piccard: the physicist who went stratospheric*. <https://www.theguardian.com/science/2011/mar/27/auguste-piccard-will-gregory>. Accessed: 2021-07-25. Guardian News and Media Limited, March 2011 (cit. on p. 39).
- [77] Hao Liu and Fabio Tronchetti. «Regulating Near-Space Activities: Using the Precedent of the Exclusive Economic Zone as a Model?» In: *Ocean Development & International Law* 50.2-3 (2019), pp. 91–116. DOI: [10.1080/00908320.2018.1548452](https://doi.org/10.1080/00908320.2018.1548452) (cit. on p. 39).
- [78] Stu McCormick. *SHARP (Stationary High Altitude Relay Platform)*. <http://www.friendsofcrc.ca/Projects/SHARP/sharp.html>. Accessed: 2021-07-25. Friends of CRC, 1997, February 2001 (cit. on p. 40).
- [79] Thomas Noll, Stephen Ishmael, Bart Henwood, Marla Perez-Davis, Geary Tiffany, John Madura, Matthew Gaier, John Brown, and Ted Wierzbanski. «Technical Findings, Lessons Learned, and Recommendations Resulting from the Helios Prototype Vehicle Mishap». In: (Nov. 2007), p. 19 (cit. on pp. 40, 44).
- [80] Peter Lobner. «Japan’s Stratospheric Platform (SPF) & SkyNet». In: (Dec. 2020), p. 14 (cit. on p. 40).
- [81] StratoCat. *CAPANINA*. <http://stratocat.com.ar/fichas-e/2005/KRN-20050831.htm>. Accessed: 2021-07-26 (cit. on p. 41).
- [82] *The X-Station data sheet*. Hünenberg, Switzerland: StratXX Holding AG (cit. on p. 41).
- [83] Zero 2 Infinity S.L. *Elevate*. <https://www.zero2infinity.space/elevate/>. Accessed: 2021-07-26 (cit. on p. 41).
- [84] X Development LLC. *Loon*. <https://x.company/projects/loon/>. Accessed: 2021-07-26 (cit. on p. 42).
- [85] Airbus S.A.S. *Zephyr - Pioneering the Stratosphere*. <https://www.airbus.com/defence/uav/zephyr.html>. Accessed: 2021-07-26 (cit. on p. 42).

- [86] Facebook Engineering. *Flying Aquila: Early lessons from the first full-scale test flight and the path ahead*. <https://engineering.fb.com/2016/07/21/connectivity/flying-aquila-early-lessons-from-the-first-full-scale-test-flight-and-the-path-ahead/>. Accessed: 2021-07-26 (cit. on p. 42).
- [87] Facebook Engineering. *High altitude connectivity: The next chapter*. <https://engineering.fb.com/2018/06/27/connectivity/high-altitude-connectivity-the-next-chapter/>. Accessed: 2021-07-26 (cit. on p. 42).
- [88] Peter Lobner. «Thales Alenia Space Stratobus». In: (Apr. 2020), p. 11 (cit. on p. 43).
- [89] Garrett Reim. *HAPSMobile Sunlider reaches 63,000ft, demos broadband transmission*. <https://www.flightglobal.com/civil-uavs/hapsmobile-sunlider-reaches-63000ft-demos-broadband-transmission/140535.article>. Accessed: 2021-07-26. FlightGlobal, October 2020 (cit. on p. 43).
- [90] Aviation Week Network. *BAE Plans U.S. PHASA-35 Demonstrations*. <https://aviationweek.com/defense-space/space/bae-plans-us-phas-a-35-demonstrations>. Accessed: 2021-07-26. January 2021 (cit. on p. 43).
- [91] Leonardo S.p.A. *Leonardo invests in the world's first solar-powered drone capable of perpetual flight with heavy payloads*. <https://www.leonardocompany.com/en/press-release-detail/-/detail/11-11-leonardo-invests-in-the-world-s-first-solar-powered-drone-capable-of-perpetual-flight-with-heavy-payloads>. Accessed: 2021-07-26. November 2019 (cit. on p. 43).
- [92] CISION PR Newswire. *Skydweller Aero Inc. Validates Initial Flight Hardware and Autopilot Software*. <https://www.prnewswire.com/news-releases/skydweller-aero-inc-validates-initial-flight-hardware-and-autopilot-software-301271421.html>. Accessed: 2021-07-26. April 2021 (cit. on p. 44).
- [93] Honglian Zhai and Anthony Euler. «Material Challenges for Lighter-Than-Air Systems in High Altitude Applications». In: Sept. 2005. ISBN: 978-1-62410-067-3. DOI: [10.2514/6.2005-7488](https://doi.org/10.2514/6.2005-7488) (cit. on p. 44).
- [94] MathWorks. *What Is Massive MIMO?* <https://www.mathworks.com/discovery/massive-mimo.html>. Accessed: 2021-08-10 (cit. on p. 47).
- [95] *gmpplot*. <https://github.com/gmpplot/gmpplot>. Accessed: 2021-03-25. 2020 (cit. on p. 49).

- [96] Marco Ajmone Marsan, Giuseppina Bucalo, Alfonso Di Caro, Michela Meo, and Yi Zhang. «Towards zero grid electricity networking: Powering BSs with renewable energy sources». In: *2013 IEEE International Conference on Communications Workshops (ICC)*. 2013, pp. 596–601. DOI: [10.1109/ICCW.2013.6649303](https://doi.org/10.1109/ICCW.2013.6649303) (cit. on p. 50).
- [97] Mohammed H. Alsharif and Jeong Kim. «Optimal Solar Power System for Remote Telecommunication Base Stations: A Case Study Based on the Characteristics of South Korea’s Solar Radiation Exposure». In: *Sustainability* 8.9 (2016). URL: <https://www.mdpi.com/2071-1050/8/9/942> (cit. on p. 50).
- [98] Michela Meo, Yi Zhang, Raffaella Gerboni, and Marco Ajmone Marsan. «Dimensioning the power supply of a LTE macro BS connected to a PV panel and the power grid». In: *2015 IEEE International Conference on Communications (ICC)*. 2015, pp. 178–184. DOI: [10.1109/ICC.2015.7248318](https://doi.org/10.1109/ICC.2015.7248318) (cit. on p. 51).
- [99] Gunther Auer, Oliver Blume, and Vito Giannini. *Energy efficiency analysis of the reference systems, areas of improvements and target breakdown*. Dec. 2010 (cit. on p. 51).
- [100] Łukasz Budzisz et al. «Dynamic Resource Provisioning for Energy Efficiency in Wireless Access Networks: A Survey and an Outlook». In: *IEEE Communications Surveys Tutorials* 16.4 (2014), pp. 2259–2285. DOI: [10.1109/COMST.2014.2329505](https://doi.org/10.1109/COMST.2014.2329505) (cit. on p. 54).
- [101] Mattia Dalmaso, Michela Meo, and Daniela Renga. «Radio Resource Management for Improving Energy Self-Sufficiency of Green Mobile Networks». In: *SIGMETRICS Perform. Eval. Rev.* 44.2 (Sept. 2016), pp. 82–87. ISSN: 0163-5999. DOI: [10.1145/3003977.3004001](https://doi.org/10.1145/3003977.3004001). URL: <https://doi.org/10.1145/3003977.3004001> (cit. on p. 54).
- [102] NREL. *PVWatts Calculator*. <https://pvwatts.nrel.gov>. Accessed: 2018-05-21 (cit. on p. 58).
- [103] GME. *Dati storici MGP*. <http://www.mercatoelettrico.org/It/download/DatiStorici.aspx>. Accessed: 2021-05-21 (cit. on pp. 58, 76).
- [104] Mahshid Javidsharifi, Hamoun Pourroshanfekr, Tamas Kerekes, Dezso Sera, Sergiu Spataru, and Josep M. Guerrero. «Optimum Sizing of Photovoltaic and Energy Storage Systems for Powering Green Base Stations in Cellular Networks». In: *Energies* 14.7 (2021). ISSN: 1996-1073. DOI: [10.3390/en14071895](https://doi.org/10.3390/en14071895). URL: <https://www.mdpi.com/1996-1073/14/7/1895> (cit. on p. 61).